



Potential impacts of abrupt *in situ* CO₂ acidification on microbial abundance and community structure in deep-sea sediments

Master program: MSc Geobiology

Working place: Centre for Geobiology (CGB)/Institute of Biology University of Bergen **Supervisors:** Laila Johanne Reigstad (CGB/Department of Earth Science, UiB) and Andrew K Sweetman (CGB /Norwegian institute of Water Research/International Research Institute of Stavanger)

By: Camilla Marie Bøe

Date: 31.06.2013



UNIVERSITY OF BERGEN
Faculty of Mathematics and Natural Sciences

ABSTRACT

Studying the environmental impacts of CO₂ leakage is important to evaluate the risk of sub sea CO₂ storage. If there were possibilities that small amounts of CO₂ would leak out, what would the environmental impact be on the sedimentary microbial community? To be able to make this decision is important to know how to detect a leak and what to look for, a study on the microbial community can be an important biomarker for a CO₂ leak. The presented *in situ* experiments are designed to mimic a CO₂ leak from a CO₂ storage site, and cope with the complications of working on the seafloor. This is made possible by using a benthic lander with incubation chambers that are able to close. By having two chambers placed on the seafloor, the sediments in one of them was exposed to CO₂ acidified water of either 2 000 or 20 000 $\mu\text{atm pCO}_2$, while the other was a parallel or control to compare any differences that occurred between the treatments after 40 hours experiment time. This study is a pin pointer in how the microbial community reacts when the pH is lowered because of CO₂ acidification. Previous studies imply that a lowered ocean pH has a significant impact on the environment, and this study suggests that a decrease in one pH unit potentially could cause an increase in microbial activity are connected, which also leads to a increase in sediment oxygen consumption. Identification of the microbial community of the sediment using the 454 pyrosequencing method and by applying the mathematical tools Principal Component Analysis (PCA) in order to find the difference between a microbial community exposed to CO₂ acidified water and microbial communities exposed to normal seawater. The PCA picked up a pattern in the relative abundance data indicating a depth gradient and also a difference between the sediments exposed to 20 000 $\mu\text{atm CO}_2$ and the sediment that did not receive this treatment.

Acknowledgements:

First of all I would like to thank my supervisors Laila J. Reigstad and Andrew Sweetman for giving me a unique possibility of doing research on something so relevant to todays society as environmental impacts of elevated CO₂. I would also like to thank them for being patient with me, and giving me advice when I needed it. In addition I would like to thank NIVA, which is a lead partner in the EC projects RISCS (Research into Safe CO₂ Storage), which has funded much of the lander and equipment of this *in situ* CO₂ acidification experiments that this thesis is based on. And the SUCCESS project, which have funded all microbial analyses. I would like to thank Centre for Geobiology for letting me take a master here and the kind and helpful “colleagues” who works here, it has been a unique and educational two years. And most importantly, thank you for having a coffee machine!! And a special thanks to thank Laila J. Reigstad, Frida Lise Daae, and Vidar Stålesen for being very helpful in the lab, and Bjarte Hannisdal for helping with PCA.

I would also like to thank Maria Michelsen and my other fellow master students for mutual support and advice, this has been very important for motivation throughout the master period. I want to thank my “other” friends for bringing my mind onto something else than this project, when my mind needs a break (and hopefully they will still remember me after submitting this thesis!). And the most important person I would like to thank is my boyfriend, Tarald Eik Mong, for always being patient and giving me motivation in rough times. Last of all I would like to thank my family for being the ultimate reason for me reaching this far.

Table of Contents:

ABSTRACT	1
Acknowledgements	2
Table of Contents	3
Figures and Tables List	5
1.0 Introduction	8
1.1 Introduction to CO ₂ capture and storage	8
1.2 Potential environmental impacts of CO ₂ leakage and natural analogues	9
1.3 The deep-sea sediment as a habitat	11
1.4 Molecular methods for sediment community analysis	15
1.5 Projects involved in safety and storage of CO ₂	17
1.6 The benthic lander	17
2.0 Aims of study	19
3.0 Materials and Methods	20
3.1 The Lander experiment in Byfjorden, Bergen in August 2011	20
3.2 The Aquarious lander	21
3.3 The <i>in situ</i> treatments	21
3.4 Harvest of sediment; slicing of cores and treatment	22
3.5 Samples included in this thesis	23
3.6 Molecular methods in the laboratory	24
3.6.1 RNA isolation	25
3.6.2 cDNA synthesis	27
3.6.3 Amplification of microbial 16S rRNA gene using PCR	28
3.7 Quantification of 16S rRNA genes using qPCR	30
3.8 Statistical methods and analysis	32
3.9 16S rRNA gene Amplicon 454 Sequencing	35
3.9.1 Samples selected for 16S rRNA gene amplicon 454 sequencing	36
3.10 Bioinformatic tools and procedures for the 454 sequencing data	37
3.10.1 Removal of noise from 454 sequencing data	38
3.10.2 CREST	38
3.10.4 Principal Component Analysis of the microbial community structure	38
4.0 Results	40

4.1	Numbers of bacterial and archaeal 16S rRNA gene copies per gram sediment (RNA level)	40
4.1.1	RNA isolation and cDNA synthesis	40
4.1.2	Amplification of 16S rRNA genes using PCR	41
4.1.3	Quantification of bacterial and archaeal 16S rRNA genes using quantitative PCR	42
4.2	Statistical analyses on number of 16S rRNA per gram sediment	48
4.2.3	T-test analyses for significant difference between the three treatments	49
4.7.2	Interpreting pH and sediment oxygen consumption (SOC) data using regression analyses	51
4.3	Microbial community composition	56
4.3.1	Amplicon 454 Sequencing of 16S rRNA genes	57
4.3.2	Principal Component Analysis (PCA)	61
5.0	Discussion	66
5.1	Overview of Experiment	66
5.2	Sediment as a habitat	67
5.3	Number of copies of 16S rRNA genes measured by qPCR	68
5.4	pH and sediment oxygen consumption (SOC)	69
5.5	T-test and regression	70
5.6	Microbial communities	71
5.6.3	Principal Component Analysis (PCA)	75
6.0	Conclusions	77
7.0	Further studies	79
	References	81
	APPENDIX	86

Figures and Tables List:

- Figure 1:** The idealized vertical stratification of electron acceptor in marine sediments. From the top is the electron acceptor that yields most free energy, starting with O₂, NO₃, Mn, Fe, SO₄ and last methanogenesis. On the left-hand side is a list of the respiration pathways. Source: Canfield 2005.....14
- Figure 2:** The Aquarius lander used in this *in situ* mimic of a CO₂ leakage. A) The Aquarius lander floating in the water after recovery from the seafloor. B) Handling water sample syringes on one of the two lander chambers after lander is back on ship deck.....18
- Figure 3:** Location of the four lander dives in Bygjorden, Bergen. The pins mark the location of the different dives (RISCS1, 2, 3 and 4). Map source: Google Earth.....20
- Figure 4:** Schematic drawing of the three different treatments the sediment was exposed to. The lander only had two chambers, and the treatments were given in a random order on the seafloor. The white spots inside the CO₂ Experiment chamber resemble CO₂ acidified water (2 000 or 12 000 μ atm pCO₂), and the green spots resemble ¹³C labelled algae.....22
- Figure 5:** Chamber of the Aquarius lander filled with fine-grained clay sediment. A) Inside chamber and syringe outlets. B) Close-up of sediment inside chamber. C) Tubes are pushed into sediment for core sub-sampling, the cores can then be taken out and the sediment sliced.....23
- Figure 6:** Flowgram of the experimental design. First total RNA is extracted from the sediment samples, then cDNA synthesis is performed on the RNA, then these samples are either used in 16S rRNA Amplification or qPCR. The 16S rRNA amplification is then prepared for 454 sequencing, and the result will be analysed using bioinformatics, CREST and PCA. The qPCR data is further used in statistical analyses. n is number of samples.....26
- Figure 7:** cDNA synthesis of the first strand with Omniscript Revers Transcriptase (Source: Qiagen).....28
- Figure 8:** Real-time qPCR graph. Showing example of threshold line and Ct Value during the exponential phase.....31
- Figure 9:** Forward (primer A) and reverse (primer B) primer sequence designed for 454 sequence tagging (Source: www.my454.com, Guideline Protocol).....36
- Figure 10:** Examples of the total RNA isolated from sediment in the RISCS1 dive. Numbers at the bottom indicate the various sediment depths the RNA was isolated from. Left panel shows the total RNA from lander Chamber 1 in RISCS dive 1. Panel to the right shows the total RNA isolated from sediment in Chamber 2 of RISCS dive 1. Blue arrows indicate band of 23S and 16S rRNA. (Ladder 100 bp: MBI Fermentas).....41
- Figure 11:** Example of PCR-amplified bacterial 16S rRNA genes (primers Uni787F/1391R) from the sediment cDNA, from sediments of RISCS2 and RISCS3. The numbers on the bottom is the depth RNA was isolated from. The left panel is from RISCS2 Chamber 2 (Control), the panel in the middle is from RISCS2 Chamber 1 (CO₂ Experiment), and the right panel is from RISCS3 Chamber 2 (Baseline). (Ladder 100 bp: MBI Fermentes).....42
- Figure 12:** Number of bacterial 16S rRNA copies per gram sediment plotted logarithmically against sediment depth (cm). Each point represents triplicate qPCR analyses. A) Sediment exposed to 2 000 or 12 000 μ atm pCO₂ (dives: RISCS2 Chamber 1, RISCS4 Chamber 1 and 2), B) Control sediment exposed to ¹³C labelled algae (dives: RISCS1 Chamber 2 and RISCS2 chamber 2), C) Untreated Baseline sediment (dives: RISCS1 Chamber 1 and RISCS3 Chamber 2).....44
- Figure 13:** Number of 16S rRNA copies for archaea per gram sediment plotted logarithmically against sediment depth (cm). Each point represents the mean of the triplicate qPCR analyses. A) Sediment exposed to 2 000 or 12 000 μ atm pCO₂ (dives: RISCS2

Chamber 1, RISC4 Chamber 1 and 2), B) Control sediment exposed to ¹³ C labelled algae (dives: RISC1 Chamber 2 and RISC2 chamber 2), C) Untreated Baseline sediment (dives: RISC1 Chamber 1 and RISC3 Chamber2).....	47
Figure 14: Principal Component Analysis of number of bacterial and archaeal 16S rRNA plotted against depth. The data clustering at 0.5 cm depth is average number of 16S rRNA of depth 0-1 cm and 1-2 cm.....	48
Figure 15: Mean bacterial 16S rRNA numbers from different treatments. 16.A) 0-1 cm sediment depth, B) 1-2 cm sediment depth, C) 3-4 cm sediment depth, D) 6-7 cm sediment depth. Error bars denote ±1 SE for CO ₂ Experiment, ± SD for the Control and Baseline treatment (Note: exponential scale on y-axis).....	40
Figure 16: Mean Archaeal 16S rRNA numbers from different treatments. 16.A) 0-1 cm sediment depth, B) 1-2 cm sediment depth, C) 3-4 cm sediment depth, D) 6-7 cm sediment depth. Error bars denote ±1 SE for CO ₂ Experiment, ± SD for the Control and Baseline treatment (Note: exponential scale on y-axis).....	51
Figure 17: Regression of number of copies of bacterial 16S rRNA plotted against pH, A) 0-1 cm depth, B) 1-2 cm depth, C) 3-4 cm depth, D) 6-7 cm depth.....	53
Figure 18: Regression of number of copies of archaeal 16S rRNA plotted against pH, A) 0-1 cm depth, B) 1-2 cm depth, C) 3-4 cm depth, D) 6-7 cm depth.....	54
Figure 19: Regression of number of copies of bacterial 16S rRNA plotted against SOC, A) 0-1 cm depth, B) 1-2 cm depth, C) 3-4 cm depth, D) 6-7 cm depth.....	55
Figure 20: Regression of number of copies of archaeal 16S rRNA plotted against SOC, A) 0-1 cm depth, B) 1-2 cm depth, C) 3-4 cm depth, D) 6-7 cm depth.....	56
Figure 21: Overview of distributions of different phyla from 454 sequencing data that constitute more than 2% of total amplicon sequences. The sediment depths are indicated to the left. From the top going down: the first row is the CO ₂ Experiment community, second row is Control community and third row is Baseline community structure of the active population. The sector group “Other” is a collection of phylum that constitutes less than 2% of the total number of amplicon sequences. This group includes several candidate divisions, and known and unknown phyla of bacteria, which alone do not make up more than 2% of total number of amplicon sequences. The group “Unclassified” is sequences that could not be classified by CREST.....	59
Figure 22: Overview of distributions of different classes from the 454 sequencing data. The sediment depths are indicated to the left. From the top going down: the first row is the CO ₂ Experiment community, second row is Control community and third row is Baseline community structure of the active population. The sector group “Other” is a collection of phylum that constitutes less than 2% of the total number of amplicon sequences. This group includes several candidate divisions, and known and unknown phyla of bacteria, which alone do not make up more than 2% of total number of amplicon sequences. The group “Unclassified” is sequences that could not be classified by CREST.....	60
Figure 23: Scatter plot of the 454 sequencing samples on phylum level measured along the maximum variation axis, PC1 and PC2. The box on the right indicate the meaning of the colour and shape of the points in the plot.....	62
Figure 24: Scatter plot of the 454 sequencing samples on class level measured along the maximum variation axis, PC1 and PC2. The box on the right indicate the meaning of the colour and shape of the points in the plot.....	63
Figure 25: Scatter plot of the 454 sequencing samples on class level measured along the maximum variation axis, PC1 and PC3. The box in the upper right corner indicate the meaning of the colour and shape of the points in the plot.....	64

Figure 26: Scatter plot of the 454 sequencing samples on OTU level measured along the maximum variation axis, PC1 and PC2. The box on the right indicate the meaning of the colour and shape of the points in the plot.....**65**

Table I: Timeframe of actions during CO₂ experiment.....**22**
Table II: Overview of lander dives, which chamber was given what experimental treatment, and which samples were chosen for molecular analysis. From each chambers four horizons are used (0-1 cm, 1-2 cm, 3-4 cm and 6-7cm).....**24**
Table III: Overview of methods used in this thesis, and description.....**25**
Table IV: Components in cDNA synthesis.....**28**
Table V: Master mixture reaction components in 16S rRNA amplification.....**29**
Table VI: Overview of components in qPCR master mixture.....**32**
Table VII: pH and sediment oxygen consumption (SOC) with ±SD.....**52**

1.0 Introduction:

1.1 Introduction to CO₂ capture and storage

The oceans are a natural sink for CO₂ from the atmosphere and so far, have absorbed approximately half of all anthropogenic produced CO₂. When CO₂ mixes with seawater, it reacts with H₂O and forms a weak acid called carbonic acid (H₂CO₃), causing lowering of the pH of the seawater in a process termed ocean acidification, which leads to increasing carbonate dissolution (Konhauser, 2004). This is especially detrimental to certain marine fauna that possess calcareous shells and tests, as ocean acidification will lead to shell dissolution, and sometimes lowered rates of calcification. Different species vary in their ability to tolerate and counteract these effects and this has implications for biodiversity, eventual trophic structure and ecosystem functioning (Widdicombe and Needham, 2007). Although the ocean has a very good buffer system and responds when the pH is lowered causing bicarbonate (HCO₃⁻, a weak base) to form, but at a certain point the amount of dissolved CO₂ in the ocean water exceeds the buffer capacity of this system. Therefore, pressure to reduce CO₂ levels in the atmosphere and prevent ocean acidification has been put on politicians, and led governments to seek new strategies for dealing with rising atmospheric CO₂ levels (Widdicombe and Needham, 2007). CO₂ capture and storage (CCS) is, at present, one of the most promising measures for immediate regulation of CO₂ emissions, while non-petroleum energy sources are being sought. Norway has taken a leading role in developing and implementing CCS, whilst international conventions, such as London and OSPAR, and regulations (EU directives) are defining the regulatory framework for CCS, in particular, for CO₂ storage in geological structures including those under the seabed. However, CCS permits will require assessments of the effects of CO₂ leakage on the marine habitat before CCS is carried out at industrial scales.

Statoil has currently four projects on CO₂ capture and storage locations; Sleipner area in the North Sea, Snøhvit LNG development in the Barents Sea, In Salah in Algeria and test CO₂ capture at the Technology Centre Mongstad, Bergen. When natural gas is retrieved from the reservoirs it contains around 9% CO₂ (Kongsjorden et al., 1998), which makes the gas useless for burning, this is why the CO₂ must be removed from the gas by amine processes. In general, the best storage location for CO₂ sub-seafloor is at a depth of 800-4000 metres below the ocean floor where the CO₂ is in a liquefied state (Eiken *et al.*, 2010). The geology for the

storage site is very important and has to consist of a layer of porous sandstone (aquifer) enclosed by several thick, dense layers of cap-rock (Shale). The storage site can be an old/empty oil/gas/coal field, deep saline aquifers or structural closures (Eiken *et al.*, 2010). An example of CO₂ storage in an offshore saline aquifer is the Statoil-operated CO₂ storage in the Sleipner field in the North Sea. CO₂ has been extracted from the natural gas harvested from approximately 3000 m depth and further been reinjected into a saline aquifer below the seafloor since 1996. The CO₂ from the Sleipner field is injected into the Utsira formation, located at 800-1100 m depth. The CO₂ injection into the Utsira formation is continuous and today about 14 million tons (about 48 billion m³) are stored. The plume covers today about 4 x 2 km². The focus is on how the CO₂ plume moves within the reservoir based on seismic surveys and gravimetric data and wellhead pressure. By today, no leakage of CO₂ from the Utsira Formation has been observed, but the risk of leakage is still present.

1.2 Potential environmental impacts of CO₂ leakage and natural analogues

Until recent, very little research has been performed on the environmental effect of CO₂ leakage on the seafloor from a storage location in marine environments. But there has been substantial effort to look into ocean acidification effects the last 5-6 years, where different aspects of environmental impacts of elevated CO₂ levels have been investigated. These will be explained here. CO₂ leakage at the seafloor acidifies surrounding seawater, and the impact of a leakage depends on how powerful the leakage is, how long the leakage persists, how strong the current is at the site. Song *et al.*, (2005) demonstrate in their article that CO₂ in solution with seawater had a higher density than normal seawater, and the density increased with a higher content of CO₂ (Song *et al.*, 2005). In a natural CO₂ analogue site at the Okinawa Trough off Taiwan, it has been shown that a CO₂ leakage from the seafloor can form a dense plume of CO₂ rich seawater over the seafloor (Inagaki *et al.*, 2006). There have been a few incidents where CO₂ have accumulated in volcanic fresh-water lakes in tropical areas, and a sudden turnover in the lake has caused CO₂ gas to emerge from the deep and kill hundreds of people living around the lakes (Schmid *et al.*, 2002). An CO₂-rich layer on the seafloor will have a lower pH compared to the normal seawater and a leakage will therefore have a potential impact on the macro-, -meio and microorganisms present in the top layers of the seafloor. In addition, many organisms in the sediment top layers are making burrows and channels, this will in turn lead the acidified seawater downwards in the sediment so that it is not only the seabed surface that might be affected. There are a few natural analogues for CO₂-leakage where CO₂ leaks from the ocean floor. These areas are: Okinawa Trough off

Taiwan, the Juist Salt Dome in the North Sea, the Florina CO₂ gas field, outside Panarea Islands, Italy, and the Mohn-Ridge in the North Sea. The microbiology from these CO₂ sites are significantly different compared to background sites, but this is currently being studied by scientists and has not yet been published (ECO2 – Summary report 2013).

There are a few places where CO₂ leakage occurs naturally and accumulates in CO₂ rich “lakes” on the seafloor. Like in Okinawa Trough, there is a hydrothermal system where CO₂ leaks and is accumulating in a liquid phase on the seafloor and causes low-pH extremes at around 1400 m depth. The CO₂ accumulates because the physical properties of the location, makes the CO₂ denser than ocean water (Song *et al.*, 2005 and Nealson *et al.*, 2006). Inagaki, Yanagawa and co-workers (2006) have investigated the microbial activity and community structure in this area and confirm that the prokaryotic community in these sediments is very sensitive to low pH. They found that the microbial density ($>10^9$ - 10^7 cells per cm⁻³), diversity and metabolic activity significantly decreased in the sediments exposed to higher levels of liquid CO₂ (pH = 5.5), than those in low CO₂-zones (pH = 6.6). This appears to be a very rough environment for life and could indicate that microbes that are specially adapted to environments with a very low pH, can survive here. Such acidophilic prokaryotes can be the cause of low diversity in sediments in CO₂ rich zones (Ignaki *et al.*, 2006, Yanagawa *et al.*, 2012 and Nunoura *et al.*, 2012). Yanagawa and Inagaki *et al.*, studied the active microbial community structure in these CO₂ rich sediments, and found that sulphate reducing bacteria (belonging to the Deltaproteobacteria) and anaerobic methanotrophic archaea (ANME-2c) were most active at the top of the sediment and that these dominate this acidophilic environment (Inagaki *et al.*, 2006 and Yangawa *et al.*, 2012).

Coffin *et al.*, (2004) conducted a laboratory experiment to mimic a CO₂ depositing event on the seafloor by adding pressure to the sediment samples collected from 600 m depth outside Hawaii. The team exposed the sediment to different pH levels (pH 5.6 and 7.6) and temperatures (5, 10 and 15°C) to measure the effect on bacterial production. They found that metabolic rates of bacteria decreased with increased temperature and longer exposure time (up to 96 hr) at the lowest pH (pH = 5.6) (Coffin *et al.*, 2004). Huesemann *et al.*, demonstrates in a study on how the nitrification rate is affected by a potential CO₂ disposal in deep oceans. The result was that the nitrification rate decreased to 50% at only one pH unit drop, and the nitrification rate was inhibited by pH 6 (Huesemann *et al.*, 2002). Nitrification is when ammonium is converted to nitrite and then to nitrate. If the nitrification was inhibited

this would cause ammonium to accumulate and which could rise to the photic zone and cause a bloom in dinoflagellates, which may be hazardous to humans, but there can also be consequences that are yet unknown (Huesemann *et al.*, 2002).

At Ketzin, west of Berlin, Germany, there is a reservoir well suited for CO₂ storage at 600-700 m depth, and in 2008 the CO₂ injections started. The microbial community inside the reservoir has been carefully monitored prior and during CO₂ injections by FISH and DAPI staining. A high abundance (10⁶ cells ml⁻¹) and diversity of microorganisms was detected before CO₂ was injected, halophilic and sulphate-reducing bacteria dominated the microbial population. After injection the microbial community structure changed and the abundance decreased, and the sulfate reducing bacteria was out competed by the methanogenic archaea (Morozova *et al.*, 2010 and 2011).

Widdicombe and his co-workers conducted a study on the effects of a CO₂ leakage (pH 6.5-5.6) on faunal diversity and sediment nutrient fluxes. This low pH causes a shock-response by the organisms and significant loss of biodiversity, especially of juveniles, while some species could withstand the acidification for weeks, and that the effect of low pH was greater in sandy sediments than in muddy sediments for both faunal diversity and nutrients fluxes. There was a rise in in sandy and muddy sediments, and a decrease in nitrite, nitrate and silicate only in sandy sediments (Widdicomb *et al.*, 2009).

There have also been studies conducted on the effects of elevated CO₂ on the microbial soil communities. Lesaulnier *et al.*, did a study on how soil microbial diversity in trembling aspen woods was affected by elevated CO₂ levels (560 ppm). The abundance of microbes did not change, but the number of decomposers and fungi associated with tree roots increased, while bacteria and archaea involved in nitrification decreased (Lesaulnier *et al.*, 2007). He and coworkers also found significant alternations in the microbial soil community in a grassland system when exposed to elevated CO₂ levels (560 μmol⁻¹) over a ten-year period of time. They found that total microbial abundance increased, especially those involved in decomposing, and carbon and nitrogen fixation, but fungi abundance was unchanged (He *et al.*, 2010).

1.3 The deep-sea sediment as a habitat

The ocean is the largest habitat on Earth and covers around 70% of its surface. Most of the ocean floor is not in contact with sunlight and this is known as the deep-sea (Orcutt *et al.*, 2011). The deep seafloor is an extreme habitat for life, harbouring unique organisms, which must be adapted to absence of light, very little precipitating organic material and extremely high pressures. The microbes here cannot use light as an energy source, and they have developed different metabolic pathways for primary and secondary production, and are therefore quite distinct from those in habitats on land (Orcutt *et al.*, 2011). There has been some effort to study the enumeration of prokaryotes in the seafloor sediments, and it is discovered that these are extremely abundant, with 3.5×10^{30} cells (Whitman *et al.*, 1998). More than 99% of the archaea and bacteria of deep-sea sediments are uncultivated and most only have distantly related cultured members, these are therefore difficult to identify (Orcutt *et al.*, 2011). Because of the tight link between geochemistry and microbiology, it is this microscopic life, which is largely in control of the geochemical cycling and diagenesis on Earth and regulate the geochemical species that accumulate (Jørgensen *et al.*, 2012). The number of microorganisms in the ocean floor is estimated to 10^6 - 10^7 cells per cm^{-3} in the top layer of the sediment, which decrease with increased depth (Parkes *et al.*, 1994, 2000). Archaeal species that dominate the sediments are identified to belong to the lineages Marine Group I(1a), Deep-sea Archaeal Group (DSAG), Terrestrial Miscellaneous Euryarchaeotal Group (TMEG), Miscellaneous Crenarchaeotic Group (MCG) and South African Goldmine Chrenarchaeotic Groups (SAGCG) (Orcutt *et al.*, 2011, Jørgensen *et al.*, 2012). While the bacterial lineages with representatives in the deep sediments belong to the groups Chloroflexi, Bacteroidetes, Planctomycetes, Acidobacteria, Proteobacteria and candidate divisions. These phyla are all very diverse, and some of these may not be present at all locations, and the ratio between them can differ a lot (Fry *et al.*, 2008, Orcutt *et al.*, 2011, Jørgensen *et al.*, 2012).

1.2.1 Sediment components

The deep-sea sediment is deposited of particles that have sedimented out from the above water column. In the open ocean the sediment constitutes of fine-grained clay particles, and in coastal areas terrigenous coarse-grained sand particles dominate. The deep-sea sediments are composed of materials, which are divided by where they come from; lithogenous (from land), biogenous (plankton sink), autogenic (ocean precipitation) and cosmogenic (from space). The composition of these types of sediment materials can vary from location to location (Jørgensen *et al.*, 2012). The top layer of the sediment on the seafloor is a heterogeneous

environment very rich in biomass, and sometimes covered in patches of biofilms or thick microbial mats from a few millimetres to centimetres thick. These have unique complex community structures, and are mostly self-sufficient ecosystems, including their own primary producers (e.g., chemolithoautotrophs; colorless sulphur bacteria, methanotrophs) (Konhauser, 2007). Often these mats exist in harsh environments, where nutrients are scarce and grazing macrofauna is inhibited (e.g. high temperatures and salinity, anoxic). The number of cells in the sediment tends to decrease with increased depth, but this can vary due to local change in geochemical compositions (Parkes *et al.*, 2000, Kallmeyer *et al.*, 2012). The decrease in number of cells at increased depth is caused by increased distance to land, sedimentation rate and availability of essential elements needed for metabolic activity, like electron donors and acceptors and a carbon source (D'Hondt *et al.*, 2004, Jørgensen *et al.*, 2012).

1.3.2 Sediment stratification:

In theory, the sediment is highly stratified because of intense competition of electron acceptors, where the redox of elements that yield the most free energy is used first in the top layer, and the elements that yields the second most free energy is used second, and so on (Fig.1). The energy is then stored or used in form of ATP (adenosine triphosphate) in the cell (Madsen *et al.*, 2011). The stratification can be detected by identifying the microbes and their metabolism, and chemical components of porewater profiles. The stratification can sometimes be visible where different layers have different colours; this is because of the geochemical residuals from biological processes in the sediments (Fig.1). But in many sediments it is much more complicated than this, because many substances can be used in several different reactions and cycles, and different microbes in the sediment are dependant on waste from other types of microbes in the sediment community (Konhauser , 2007, Madsen *et al.*, 2011).

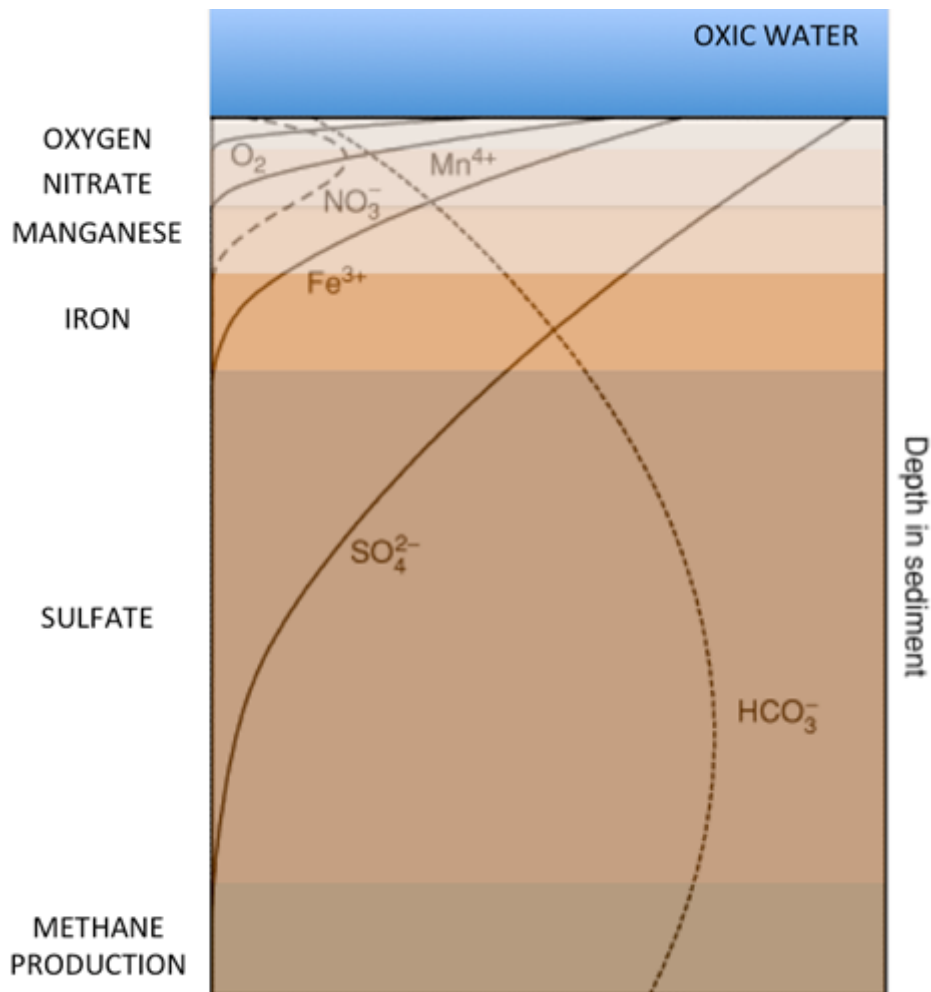


Figure 1: The idealized vertical stratification of electron acceptor in marine sediments. From the top is the electron acceptor that yields most free energy, starting with O₂, NO₃, Mn, Fe, SO₄ and last methanogenesis. On the left-hand side is a list of the respiration pathways. Source: Canfield 2005.

1.3.3 Geochemical aspects

The most favourable electron acceptor thermodynamically is O₂ (aerobic respiration), and is used up in the top millimetre or centimetre of the sediment (Glud *et al.*, 2008). After depletion of oxygen, other reducing agents like nitrate (NO₃), manganese (Mn⁴⁺), iron (Fe³⁺) and sulphate (SO₄²⁻) are used, though these can overlap (Van Der Loeff *et al.*, 1990, D'Hondt *et al.*, 2004) (Fig.1). Carbon sources (mainly particulate organic carbon converted to CO₂ and CH₄) are the most preferred electron donor and is a limiting factor for the microorganisms in the sediment. When there is sufficiently organic carbon available, oxygen is used up rapidly.

1.3.4 Nitrogen cycle

The nitrogen cycle in the sediments is highly complex reactions, which depend on degradation of organic material to ammonium. Ammonium and oxygen is used to make nitrate (NO₃) in a process known as nitrification. This reaction occurs mostly in the top layer

of the sediment. NO_3 is then involved in denitrification, where nitrate is reduced to N_2 . Several other metabolic reactions are known that use reduced or oxidized forms of nitrogen and manganese or sulphide, which make the nitrogen cycle complicated (Konhauser, 2007). Deeper into the sediment manganese reduction, iron reduction, sulphate reduction and methanogenesis are common metabolic pathways.

1.3.5 pH

The pH profile in the sediment is affected by biotic and abiotic reactions, especially CO_2 and H_2S , which derive from metabolic activity and cause a decrease in pH (Fisher *et al.*, 1981). The pH can change very quickly in a very short distance, where the pH of the ocean water above the sediment is around 8,0 and quickly decreases to pH 7,0 in the top cm/mm and is stable around pH 7 deeper in the sediment (Fischer *et al.*, 1981).

1.3.6 Bioturbation

The deep-sea sediments contain a large and highly diverse population of macrofauna. Several invertebrates have been identified, like polychaete worms, molluscs and crustaceans as well as bottom dwelling fish, which can alter the seafloor with their activity (Grassle, 1989). Dead fish/animals or bottom dwelling macrofauna (via bioturbation or burrowing) can alter the profile of pH, O_2 and nutrients in the sediment. These physical fluctuations can also have an impact on the number of microbes and their activity. Decaying animals can cause the pH and oxygen levels to decrease significantly, while bottom dwelling macrofauna stir oxygen and sea level pH deeper into the marine sediments.

1.4 Molecular methods for sediment community analysis

Molecular methods can be used to study the genetic pool in environmental samples, without using cultivation and microscopy methods for identification. With molecular methods, like quantification PCR (polymerase chain reaction) and DAPI fluorescent staining (4',6-diamidino-2-phenylimndole) on DNA, it is possible to count number of cells in a sample, but many of the cells in the sediment can lay dormant (as spores), and are not active. These cells do not have an impact on the environment, and can create a false impression of the microbial community structure and diversity. By studying the RNA pool in a sample, we can learn more about who is active and what they are doing. Because RNA is continuously produced in a cell when there is a need for cell repair, growth or enzymes and proteins in metabolic processes, it

can thus be an indirect measurement of activity (Poulsen *et al.*, 1993, Bremer *et al.*, 1996, Lanzen *et al.*, 2010).

The ribosome is responsible for making proteins in a cell and it consists of RNA and proteins working as one. The ribosome is unstable and in a constant state of turnover in a cell. Active cells have more ribosomes, than less active cells. Phylogenetic analyses on the ribosome are therefore suitable to study the active population in a microbial community (Poulsen *et al.*, 1993, Bremer *et al.*, 1996, Lanzen *et al.*, 2010). The 16S rRNA is a RNA molecule in the ribosome and is around 1500 base pairs long, and commonly used for identification and taxonomical analysis, because of its sequence properties (Muyzer *et al.*, 1993). It is distinct for prokaryotes, it has specific regions that are specific to some microbial lineages and non-specific regions that are general for all bacteria and archaea, these regions are used for primer binding. Sequencing the 16S rRNA molecule can thus be used for identification (Case *et al.*, 2006). Commonly used methods to study the microbial community is by quantification PCR and sequencing methods on total isolated RNA from a sample, even though there is some bias associated with PCR, like mismatch of primers binding to templates (Ishii *et al.*, 2001). When applied to RNA level, these methods are very well suited for quantifying and identifying the bacteria and archaea who dominate the active community and diversity (degree of variation of species in a chosen ecosystem).

To find out what happens if CO₂ from a storage site leaks, it is necessary to study the microorganisms in the sediments. They are suitable for studying because of their properties; they can have short life spans and are mostly immobile. By studying the gene pool directly from environmental samples, we can find out what microbial taxa exist and what these organisms need to survive. Using molecular methods to study the community is more effective than cultivation methods and identification by microscopy, because only a few species are cultivatable and possible to identify and these may not be representative for the community. On the other hand molecular methods using DNA and RNA can be isolated directly from the environmental sample and analysed (Muyzer *et al.*, 1993, D'Hondt *et al.*, 2004). As stated before, very few species from deep-sea environments are described, and therefore identification is difficult in these environments when only distantly related species are known. This is still a major research area, and little is yet known because accessing the seafloor in deep oceans is difficult and expensive (Fry *et al.*, 2008).

1.4 Projects involved in safety and storage of CO₂

In terms of CCS, several institutes in Norway are working together to find out how marine organisms are affected by abrupt CO₂ acidification in the oceans from CO₂ leakage as well as how to access the seafloor. Researchers from the Centre of Geobiology (CGB) and the Norwegian Institute for Water Research (NIVA) are involved in major national and European projects, which are assessing the risks and impacts of leakage and the development and testing of a variety of monitoring aspects for sub seafloor CO₂ storage sites. CGB and NIVA are currently involved in three projects together, namely SUCCESS (Subsurface CO₂ storage – Critical Elements and Superior Strategy) funded by the Norwegian Research Council, CO₂ Base founded by CLIMIT and Gassnova, and ECO2 (Sub-seabed CO₂ storage: Impacts on Marine Ecosystems) funded by the EC. In addition, NIVA is a lead partner in the EC projects RISCs (Research into Safe CO₂ Storage), which has funded much of the *in situ* CO₂ acidification experiments that this thesis is based on.

1.5 The Benthic Lander:

To be able to characterize ecosystem changes on the seafloor resulting from CO₂ leakage, investigations should preferentially be carried out *in-* rather than *ex-situ*. This is because standard coring techniques and later laboratory-based mesocosm experiments are limited by the poor control one has on the disturbances imposed on sediment structure and the community when bringing seafloor sediments to the surface (e.g. porewater loss, changes in bio-irrigation by macrofauna, decompression and heating artifacts), and the exclusion of fauna when using small coring devices. ROVs and submersibles can be used to overcome a number of these limitations, but they are limited in the amount of time they can operate on the seafloor, the types of studies that they can perform (simple coring, basic experimental manipulations) and the fact that they are demanding on ship-time (needs to be controlled and repaired by specialized staff). Autonomous benthic landers overcome almost all of the above-mentioned limitations as they provide a powerful platform for carrying out short- (hrs) to long-term (weeks) *in situ* benthic studies and are also capable of being deployed in very deep water (up to 6000m depth). When used in conjunction with benthic chambers, they can be used to experimentally manipulate large volumes of seafloor-sediment (up to 10000 cm³) and quantify a variety of important physical/chemical properties and functions over time-scales of days to weeks. Biodiversity, nutrient fluxes, biogeochemical cycling by microbes and meio- and macrofauna can be studied on sediment samples where the experiments were carried out

without significantly disturbing the sediment fabric or introducing significant experimental artifacts during the experimental time frame (Fig. 2).



Figure 2: The Aquarius lander used in this *in situ* mimick of a CO₂ leakage.. A) The Aquarius lander floating in he water after recovery from the seafloor. B) Handling water sample syringes on one of the two lander chambers after lander is back on ship deck.

Experimentally manipulated sediments can also be brought to the surface for sampling at the end of an experiment because the chambers are closeable. Experiments for this thesis were carried out using a benthic chamber lander named Aquarius (Fig. 2) operated by Dr. Andrew Sweetman at the International Research Institute of Stavanger (IRIS) (formerly at the Norwegian Institute for Water Research).

2.0 Aims of study:

The goal of this thesis was to examine the microbial abundance and community structure in the seafloor sediments of Byfjorden, Bergen, after *in situ* exposure to CO₂ acidified water for 40 hours and compare with seafloor sediments exposed to normal seawater. This is to represent what could happen during a potential leak of CO₂ from a sub-seafloor CO₂ storage site. The molecular methods used focused on the 16S rRNA gene pool in the sediment samples, and the goal is to answer:

- Does the exposure to CO₂ acidified water have any effect on the activity (16S rRNA genes) of bacteria and archaea (RNA-level)?
- Does the exposure have any effects on the microbial community composition?
- And if so, what groups of microorganisms does the CO₂ Experiment affect?

Hypotheses:

- 1) Bacteria and Archaea: «*Acidification from CO₂ has no effect on activity in deep-sea upper seafloor sediments*»
- 2) Bacteria and Archaea: «*Acidification from CO₂ has no effect on microbial community structure in deep-sea upper seafloor sediments*»

3.0 Materials and Methods:

3.1 The Lander experiment in Byfjorden, Bergen

The project was carried out in August/September 2011, and the Aquarius lander (Fig. 2) was deployed on the seafloor four times. Each dive was named RISCs, the short name for the Research Into Impacts and Safety of CO₂ project, plus the given dive number hence; RISCs1, -2, -3 and -4, and the chambers are named 1 and 2, for each dive. All dives lasted 40 hours on the seafloor, at a depth of 350 meters in Byfjorden, outside Bergen, with 25 to 100 meters distance between each dive (Fig. 3). The lander was lowered from the ship into the water and sank to the seafloor because of heavy weights attached to the three feet of the lander. Byfjorden is reckoned as a near-shore deep-sea environment.

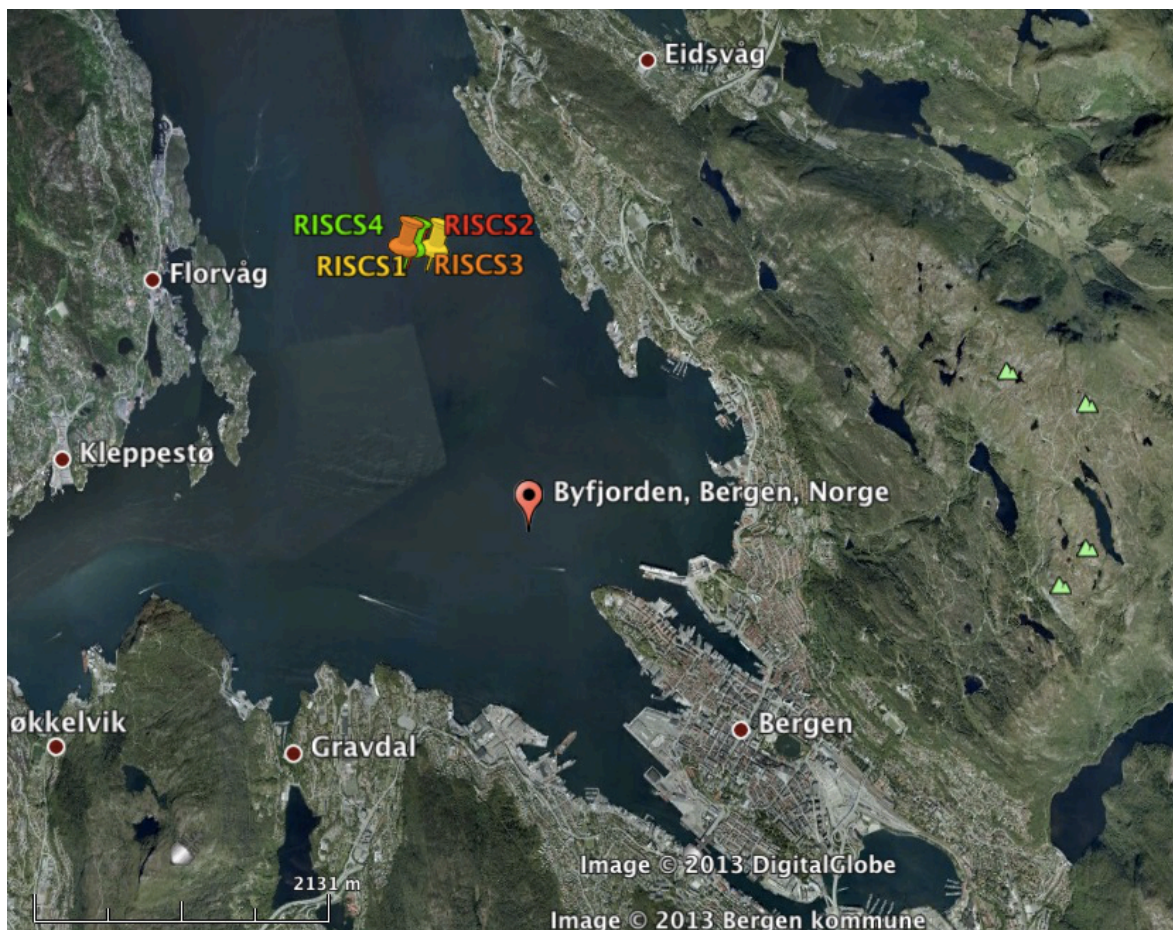


Figure 3: Location of the four lander dives in Byfjorden, Bergen. The pins mark the location of the different dives (RISCs1, 2, 3 and 4). Map source: Google Earth.

3.2 The Aquarious lander

This lander was equipped with two incubation chambers, which upon reaching the seafloor were driven into the sediment by motors to a pre-programmed sediment depth. The chambers were installed with sensors for oxygen (Aanderaa oxygen optode 3975A with 5% accuracy), pH (AMT pH shallow water sensor with pH 0,05 accuracy), conductivity (Aanderaa conductivity sensor 3919A with accuracy $\pm 0,05$ mS/cm) and temperature (Aanderaa temperature sensor 4050 with accuracy $\pm 0,03$ °C). These data were measured throughout the experiment. A syringe sampler with eight syringes of 50 mL each was attached to each chamber. The sampler could withdraw seven liquid samples from the chambers and inject one via an on-board computer. Inside each chamber there was a stirrer to create a steady diffusive flux of solutes into the sediment.

3.3 The *in situ* treatments

Once on the seafloor, each chamber was exposed to one out of three treatments (Fig.4). The three different treatments are referred to as “CO₂ Experiment”, “Control”, and “Baseline”. In the CO₂ Experiment treatment 100 ml of CO₂ acidified seawater was injected into one of the chambers. This seawater had been kept at seawater temp (7°C) and further sterile filtered through a 0.2 um pore-sized filter in order to avoid introducing new organisms to the experiment. After filtration the water bubbled with clean CO₂ gas until the pH was pH 5.1 corresponding to 20 000 μatm pCO₂. This number was estimated by the program CO2calc, which uses the physical parameters measured from field data to find all carbonate parameters (e.g. total alkalinity, total CO₂, pH, fCO₂ or pCO₂) (Robbins et al., 2012). The pCO₂ calculation was done by Tamara Baumberger with CO2calc. Additionally, labeled ¹³C-algae were added to the chamber (Fig.4). *Skeletonema costatum*, a diatom, was freeze-dried, and used to simulate particulate organic material (POM) sinking from the euphotic zone to the deep-sea sediments, at a rate like in natural open waters (though this can vary with seasons) (Sweetman *et al.*, 2007 and Sweetman *et al.*, 2008). The labeled algae are consumed by micro and macrofauna, and can later be traced to study the food web of the ecosystem by measuring stable isotopes. It is possible to study which organisms feed and which do not when exposed to CO₂ acidified water using this approach. The part of the experiment involving the data from ¹³C labeled algae is not included in this thesis. The Control treatment was normal sterile filtered seawater with the ¹³C labeled algae, except that the water added was seawater of a normal pH (pH = 7.9). The Baseline treatment comprised incubation with no added seawater. Seven water samples were withdrawn from each chamber during the experiment at set times

to measure of water chemistry (incl. pH and alkalinity) (Figs. 2 and 4).

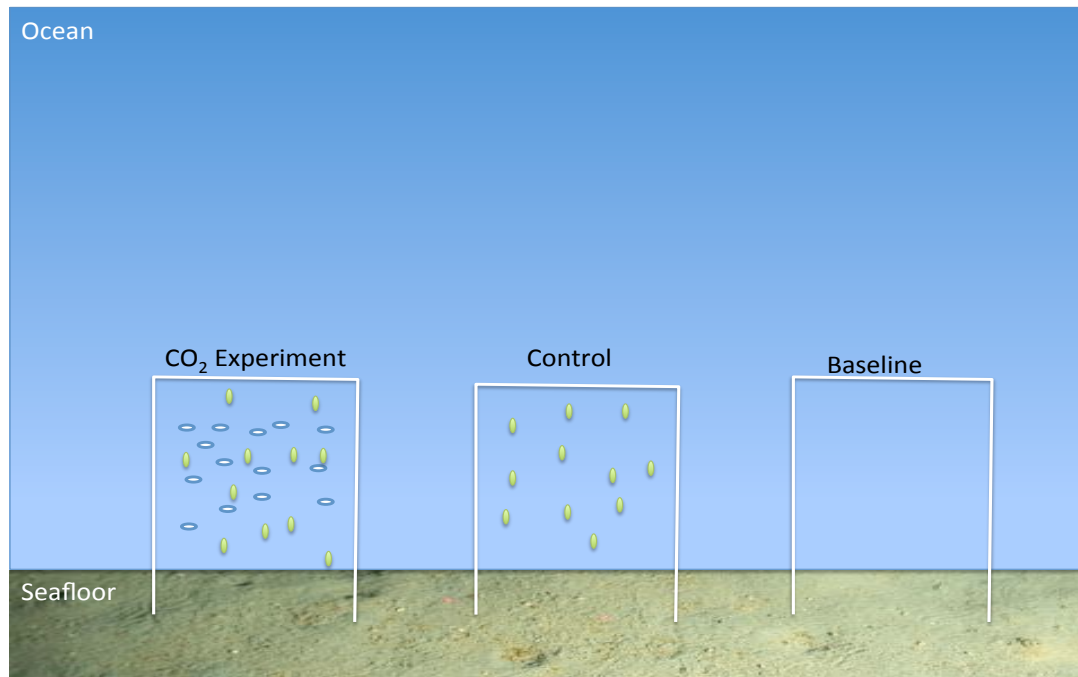


Figure 4: Schematic drawing of the three different treatments the sediment was exposed to. The lander only had two chambers, and the treatments were given in a random order on the seafloor. The white spots inside the CO₂ Experiment chamber resemble CO₂ acidified water (2 000 or 20 000 μ atm pCO₂), and the green spots resemble ¹³C labelled algae.

Once placed on the seafloor, the movement of the chambers, lids and syringes on the lander was programmed before deployment to the sea as described in Table 1.

Table I Timeframe of actions during CO₂ experiment

Action	Time
15:00 Lander deployed from the ship	
17:00:00 Push chambers down	
18:20 Start stirrer	
20:00 First syringe sample taken (Background)	
20:25:00 Stop stirrer before injection	
20:30 Injection CO ₂ -acidifiedwater/sea water	0
20:35 Stirrer starts after injection	
20:40 Second syringe sample taken	40 min
03:55 Third syringe sample taken	7t 25 min
09:00 Opening Lid for service on	
11:10 Fourth syringe sample taken	15t 35 min
18:25 Fifth syringe sample taken	22t 50 min
01:40 Sixth syringe samples taken	30t 5 min
08:00 Seventh syringe sample taken	36t 25min

08:58 Stirrer stops	
09:00 Get chamber up	
11:00 Lander weights released by acoustics and lander floats to the surface	
11:30 Sampling and analyses begin	

After 40 hours of exposure to 20 000 uatm pCO₂, the lander was recalled from the seafloor by acoustic release of the weights. Once back on deck, the seven syringes was collected and sub-cores was taken of the sediments. The pore water was withdrawn from the sediment cores by Rhizon samplers (Rhizonspere Research Products), for easy and safe sampling. Samples for faunal and microbial studies were also prepared by making sub sediment cores from the sediment inside the chambers. pH and other geochemical parameters (e.g. alkalinity) was measured of the liquid withdrawn from the chambers by the seven syringes (performed by Dr Laila Reigstad, CGB).

3.4 Harvest of sediment; slicing of cores and treatment:

Six different cores were taken of the sediment inside the chambers (see Fig. 5). The tubes for core sampling were manually pushed into the sediment (Fig. 5c) and the core was then removed and sliced every centimeter and the different layers were divided into separate containers for storage. The sediment samples for DNA analysis were frozen instantly at -20 °C, and the samples for RNA analysis was added RNALater solution (Ambion) and then frozen to -20 °C. The RNALater Solution stabilizes and protects cellular RNA from degradation and RNA can also be stored for months without affecting its quality (Life Technologies Corporation).

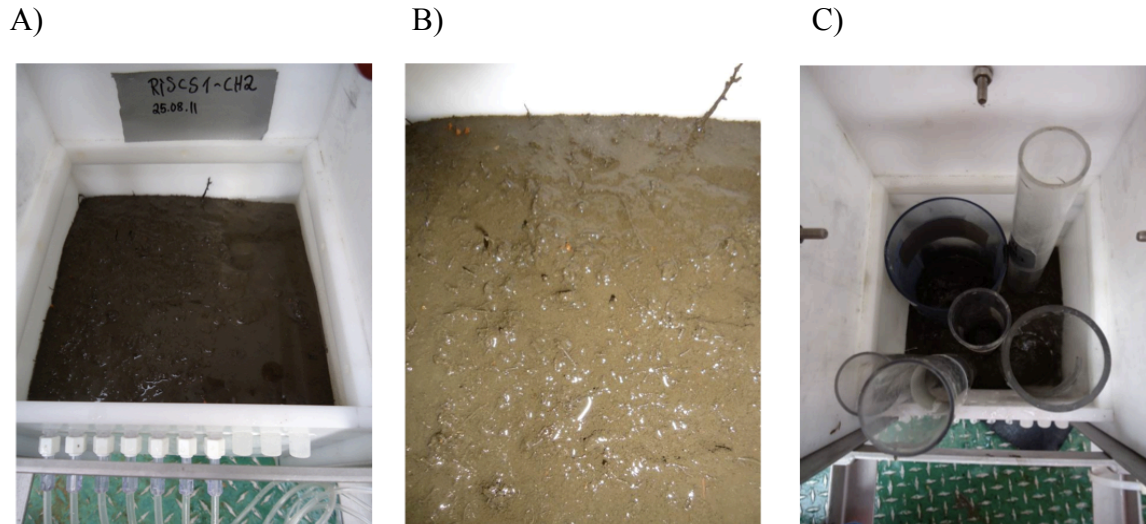


Figure 5: Chamber of the Aquarius lander filled with fine-grained clay sediment. A) Inside chamber and syringe outlets. B) Close-up of sediment inside chamber. C) Tubes are pushed into sediment for core subsampling, the cores can then be taken out and the sediment sliced.

3.5 Samples included in this thesis

The samples selected for analyses were (Table II):

1. CO₂ Experiment: samples from 3 chambers
2. Control: samples from 2 chambers
3. Baseline: samples from 2 chambers

The following sediment horizons chosen for molecular analysis were:

0-1 cm, 1-2 cm, 3-4 cm, 6-7 cm.

These specific horizons have been chosen to make it possible to detect any differences as a function of depth resulting from exposure to CO₂ acidified seawater. DNA and RNA extractions were performed at these depths. Samples chosen for 454 sequencing were selected based on treatment, and will be explained later.

Table II: Overview of dives, which chamber was given what experimental treatment, and which samples were chosen for molecular analysis. From each chambers four horizons are used (0-1 cm, 1-2 cm, 3-4 cm and 6-7 cm.

Dive	Chamber	Treatments	454sequencing	16S rRNA qPCR, bacteria and archaea
RISCS1	1	Baseline		Yes
RISCS1	2	Control		Yes
RISCS2	1	CO ₂ Experiment	Yes	Yes
RISCS2	2	Control	Yes	Yes

RISCS3	1	Baseline		
RISCS3	2	Baseline	Yes	Yes
RISCS4	1	CO ₂ Experiment		Yes
RISCS4	2	CO ₂ Experiment		Yes

Samples from three different chambers with the three sediment horizons per chamber gave a total of nine samples for 454 sequencing analysis. For qPCR analyses RNA isolation was done from seven chambers with the four selected sediment horizons per chamber, and gave a total of 56 samples.

3.6 Molecular methods in the laboratory:

The methods used in this thesis are listed in Table III.

Table III: Overview of methods used in this thesis, and description.

Methods:	Description:
Total RNA isolation	RNA will be used further
cDNA synthesis	Performed on RNA
16S rRNA Amplification	PCR amplification on the 16S rRNA gene, for bacteria and archaea
Quantification PCR	Quantify number of bacterial and archaeal 16S rRNA genes
454 sequencing	Identify prokaryotic community structure

The analyses performed on RNA is presented in the flowgram below and will be thoroughly presented in the following sections (Fig. 6).

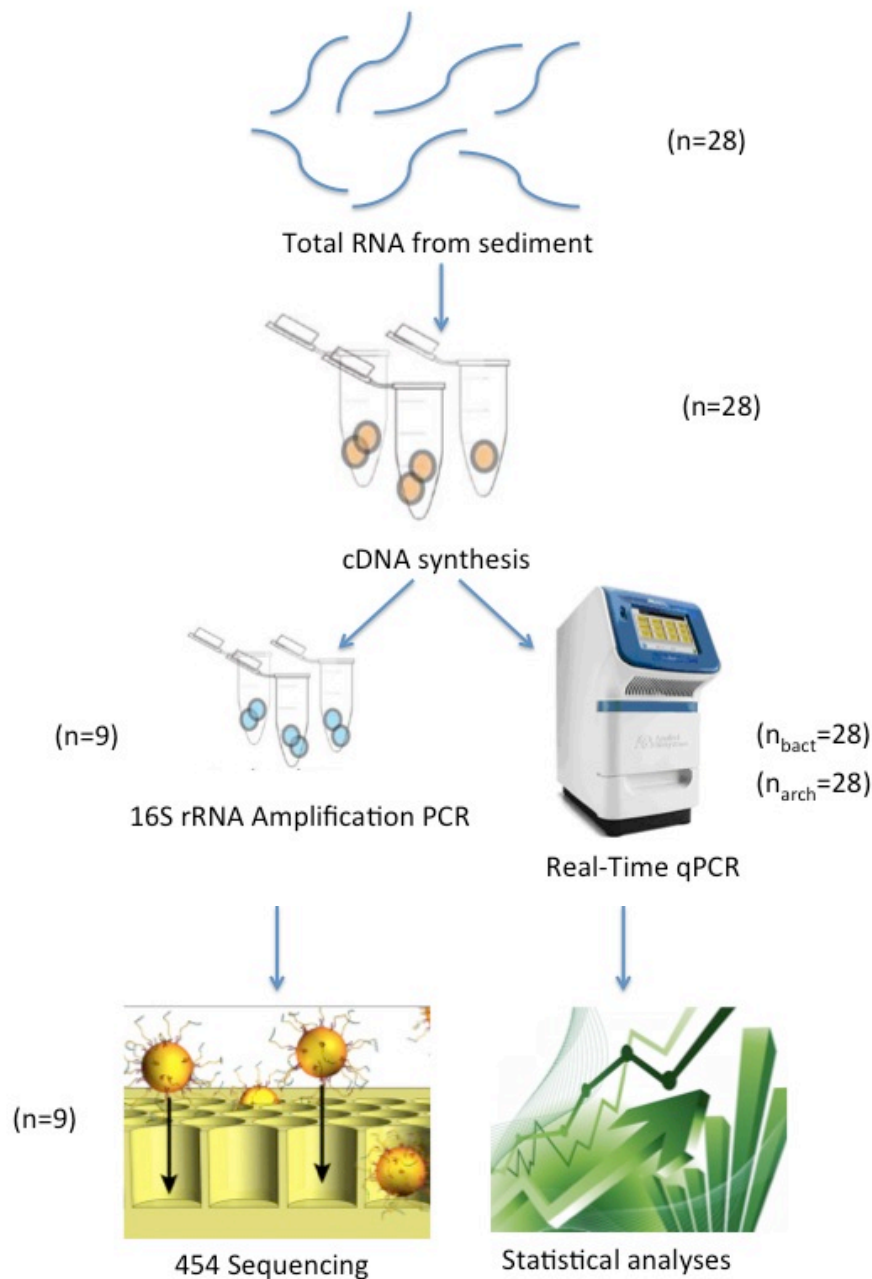


Figure 6: Flowgram of the experimental design. First total RNA is extracted from the sediment samples, then cDNA synthesis is performed on the RNA, then these samples are either used in 16S rRNA Amplification or qPCR. The 16S rRNA amplification is then prepared for 454 sequencing, and the result will be analysed using bioinformatics, CREST and PCA. The qPCR data is further used in statistical analyses. n is number of samples.

3.6.2 RNA isolation:

RNA is very important to investigate because RNA is used to assess which microbes are currently growing and active (Kramer *et al.*, 1993). The study on RNA can provide information on which microbial taxa are still active and what they are doing after CO₂ is injected by comparing the control and the CO₂ acidified samples. RNA can be difficult to

isolate from sediment samples, and often only the DNA level is analyzed. The sediment sample for RNA was transferred to a Falcontube and RNALater solution was added immediately on site. Total RNA was isolated from sediment fixed RNALater-solution with the Qiagen RNAEasy Kit (Qiagen) by following a protocol by Laila J. Reigstad (Sept. 2011). Only a few samples were analysed simultaneously, as RNA degrades quickly when removed from the RNALater solution. The sediment for RNA extraction (in RNALater) was thawed on ice; and meanwhile several solutions used for the isolation were prepared. One of them is a lysozyme solution with a concentration of 3mg/ml TE buffer. The lysozyme is from egg white and is used to break down the cell walls (SIGMA, cat.: L-7651). The second is an RLT buffer solution, which is also prepared. To make this solution 10 μ L 2-mercaptoethanol (B-ME) is used per mL RLT buffer (1% B-ME), and needs to be applied in the hood because it is toxic. 2-Mercaptoethanol has the ability to break disulphide bonds in ribonuclease an enzyme that degrades RNA (Nelson *et al.*, 2005) DNase I stock solution (freshly made at every use) added to Buffer RDD. DNase I removes genomic DNA from the RNA pool. When the RNALater-fixed sediment was thawed, around 1 mL sediment was transferred to two 2 mL Eppendorf tubes, and centrifuged at 16,000 x g for 10 minutes in a pre-cooled centrifuge (+7 °C) to remove the RNALater solution and to pellet microbial cells in solution. After the supernatant was removed, the sediment was weighed into a new 2 mL eppendorf tube. Afterwards 200 μ L lysozyme solution (3mg/mL) was added to the sample, and incubated for 10 minutes, and then RLT buffer with B-ME was added and mixed thoroughly followed by centrifuging 16,000 x g for 2 minutes. The RNA-containing supernatant was added to 250 μ L absolute ethanol and mixed, which makes DNA and RNA precipitate. The mixture was then transferred to a RNeasy spin column and centrifuged at 9000 x g for 15 seconds. This makes RNA stick to the filter. Next, 350 μ L RW1 buffer was added to the spin column and centrifuged again at 9000 x g for 15 seconds, and the flow-through was discarded. Afterwards, the DNase I incubation mix (80 μ L) was added to the spin column membrane to break down DNA, and this was incubated at room temperature for 15 minutes. Then, 350 μ L RW1 buffer was added and centrifuged at 9000 x g for 15 seconds. The flow-through was discarded. The 500 μ L RPE buffer (with ethanol) was then added and centrifuged twice. The last centrifugation step and without addition of liquid, was centrifuged for 1 minute at 13,000 x g to completely remove all ethanol in RPE buffer. At last, the spin column was transferred to a clean, 1.75 mL eppendorf tube, 40 μ L elution water (RNAse free H₂O) was added and the tube was then centrifuged at 1 minute at 13,000 x g to catch the total RNA. The RNA was aliquoted into two batches, and frozen at -20 °C consecutively. Five μ L of each RNA sample was taken out for

quality and quantity evaluation using gel electrophoresis as described for DNA samples. The electrophoresis program was as follows: 50 V for 30 min.

3.6.3 cDNA synthesis:

Complementary DNA (cDNA) is a single-stranded DNA molecule transcribed of mRNA by using reverse transcriptase isolated from retro viruses. This is done because DNA is more stable than RNA, and is easier to do further analyses on. A complementary DNA (cDNA) synthesis was performed on the RNA to make single-stranded DNA (Fig.7). For the procedure, the Omniscript® Reverse Transcription Kit and following protocol was used (Qiagen).

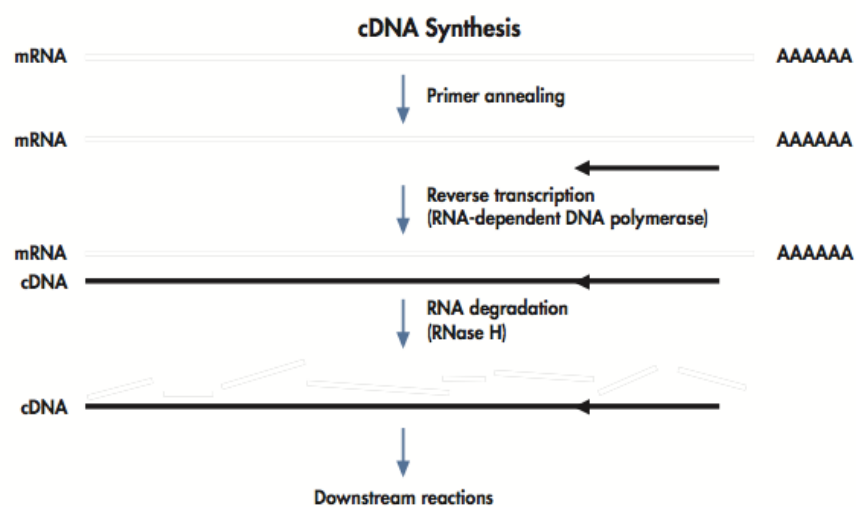


Figure 7: cDNA synthesis of the first strand with Omniscript Revers Transcriptase (Source: Qiagen).

Primers for cDNA synthesis were not included in this kit; a set of random primer hexamers, (primers with six nucleotides in random order (Fisher Scientific, Oslo, Fermentes)) was used to include as many sequences as possible. RNA template and all reaction components (Table III) needed for the procedure was thawed on ice. To avoid secondary structures in the RNA before cDNA synthesis, the RNA was heated for 5 min at 65°C and transferred to ice immediately after. The content of the cDNA synthesis is listed in Table IV below. The amounts of double-distilled water (Qiagen) and RNA template are added according to the estimated RNA amount based on the RNA gel electrophoresis image. Water instead of enzyme was used as a negative control.

Table IV: Components in cDNA synthesis

Component	Volume per sample (µL)
-----------	------------------------

10x RT Buffer	2.0
dNTP Mix	2.0
Omniscript Revers Transcriptase	1.0
Random Primer hexamer	2.0
H ₂ O	Variable
Template RNA	Variable
Total volume (ul) per sample:	20.0

In case of weak RNA products, more template is used in the cDNA synthesis. The PCR machine is set on 37°C for 1 hour and then cooled to 4°C. Samples were then stored in -20°C or directly used as template in 16S rRNA gene amplifications.

3.6.4 Amplification of microbial 16S rRNA gene using PCR

The 16S rRNA gene is the most studied and used for taxonomical analysis and identification. It encodes the 16S ribosomal RNA in the small subunit of the ribosome. As explained before, RNA can be a measurement of activity of microorganisms, and by performing quantification and identification of the 16S rRNA molecules, we can know more about who is active (454 pyrosequencing) and how many (quantification PCR) they are in an environmental sample. 16S rRNA genes were amplified using Universal prokaryotic primers. These primers will bind to specific locations of the 16S rDNA genes in both archaeal and bacterial species, and include as many prokaryotes as possible. The primers used were Uni787F (5'-ATTAGATACCCNGGTAG-3', where N can be all four bases) (Roeh et al, 2007) and Uni1391R (5'-GACGGGCGGTGWGTRCA-3', where W=weak (A or T), and R= purine (A or G)) (Lane et al, 1991). This created a strand of 604 base pairs (bp) that was amplified by Polymerase Chain Reaction (PCR). For the amplification the polymerase Phusion® High-Fidelity DNA Polymerase (New England Biolabs) was used. This is an effective enzyme and performs at a very high fidelity, speed, specificity and yield. The cDNA samples and components of the PCR mixture were thawed on ice before use. The PCR mixture was then prepared as described in Table V below, and the cDNA was diluted with distilled water, 1:10.

Table V: Master mixture reaction components in 16S rRNA amplification.

Component	Volume per sample (µL)
Primer 787F (100 µM stock)	1.0

Primer 1391R (100 μ M stock)	1.0
Phusion	10.0
H ₂ O	6.0
Template (1:10)	2.0
Total volume	20.0

During a PCR run the following three steps are repeated: the denaturation, the annealing and the elongation steps. The denaturation step lasts 30 seconds at 98 °C and makes the DNA strands separate. The annealing step is where the specific primers bind to the template, this was at 57°C for 15 seconds and here the temperature is too low for the polymerase to function. The elongation step at 72°C and lasts for 20 seconds, and is where polymerase adds nucleotides to the single stranded DNA, making it double stranded, and ready for a new denaturation. This cycling is repeated 30 times. After the 30 cycles there is a step of 7 minutes at 72 °C, to make sure all DNA synthesis is complete. The last step in the PCR is cooling down the samples to 4 °C until the samples are collected. The resulting DNA product, amplicons (a piece of DNA/RNA created by amplification techniques), was analyzed using gel electrophoresis using a 1% agarose gel matrix made with 1xTAE buffer and added Gel Red dye (Biotium). This nucleic fluorescent dye is environmentally safe, stable, sensitive and binds to dsDNA, ssDNA and RNA. The electrophoresis settings were 50 V for 30 minutes. Images were obtained as described in Section 3.5.1. Positive (Cave biofilm sample) and negative (water instead of template) controls were included in all PCR runs. The negative control can test for contamination in the samples and enzyme solution, by running a sample without template or without the polymerase. A positive control tests the primers and the rest of the PCR mixture to see if the DNA/RNA isolations have been successful. During the PCR run a number of biases can occur and alter the result (e.g. like chimeric sequences (where two wrong DNA strands are coupled), deletion of partial sequences and point mutations (Lanzén et al., 2013)).

3.7 Quantification of 16S rRNA genes using qPCR

Quantitative Real-time Polymerase Chain Reaction (qPCR) is used to simultaneously amplify and quantify a chosen gene. This method was used on cDNA to measure the number of 16S rRNA (cDNA) from all the four lander dives and selected sediment depths. A qPCR (StepOne™ Real-Time PCR Systems from Applied Biosystems) is like a classical PCR reaction, but additionally the amount of amplified product is measured every cycle. A special

polymerase called SYBR Green 2x was used, which is a premix of SYBR GREEN I dye, nucleotides, AmpliTaqGold®DNA polymerase, and optimized buffer components. In the thermal cycle, the SYBR Green I dye becomes fluorescent when binding non-specifically to double stranded PCR products and a camera inside the machine detects this. The number of light signals will be proportional to amplified product detected in every cycle (elongation step), and the machine creates a graph over the fluorescence accumulation. There are three phases in the Real-time qPCR, which are exponential, linear and plateau. In the exponential phase the reagents are in excess and the product doubles in each cycle. The reagents become short in the linear phase, and in the plateau phase they are all used up and the PCR reactions stops. The exponential phase is where the number of PCR products is calculated, by finding when the threshold line (which is where the fluorescent light is detected) is above background intensity and at what cycle this occurs (Ct value) (see Fig. 8). The technique also provides a melting curve after the PCR for quality control, to detect non-specific amplicons, which can indicate contaminations.

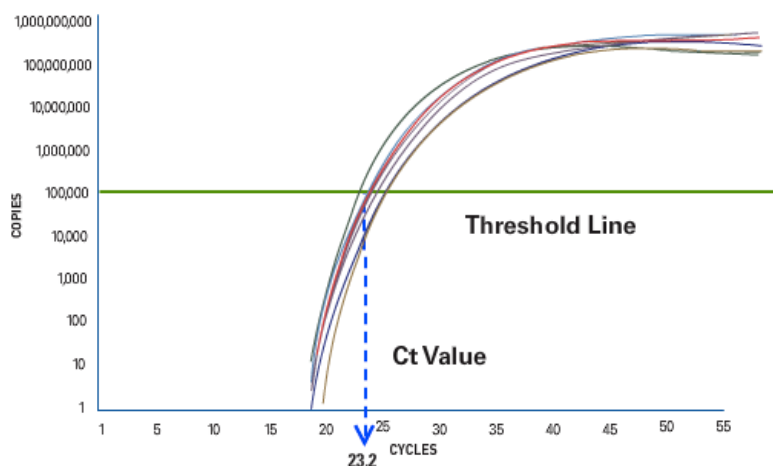


Figure 8: Real-time qPCR graph. Showing example of threshold line and Ct Value during the exponential phase.

The SYBR Green emits a green fluorescent light and is detected by a spike in a graph (melting curve) and indicates the melting point of the amplicons. Contaminated samples will have weak or no peaks (Applied Biosystems protocol, 2007). The primer pair for bacteria and archaea was used in separate reactions. For amplification of bacterial 16S rRNA genes the primer 341f (5'-CCTACGGGWWGGCWGCA-3' W=weak) and 518r (5'-ATTACCGCGGCTGCTGG-3', Muyzer et al, 1993) were used. For archaeal 16S rRNA gene amplification the primers Uni515F (5'-CAGCMGCCGCGGTAA-3', where M= amino (A or T), Lane et al, 1991) and A908R (5'-CCCGCCAATTCCTTTAAGTT-3' Jurgens et al, 1997)

were used. The PCR setups are different for bacteria and archaea. A standard is needed for the program to design a proper standard curve for the reaction; these are solutions with a known number of amplicons. The standard for bacteria 16S rRNA genes is from $15.9-1.59 \times 10^7$ copies of the target gene (7 different). The standard used for archaeal 16S rRNA gene is from $10-10^7$ numbers of copies of the target gene (7 different). All samples (standard and samples with template) will have three replicates in case of error in the PCR reaction. All cDNA templates were diluted 1:5 in double distilled water (Qiagen). Here it is also important to include negative (water instead of template and water instead of enzyme) controls. The components of the qPCR mixture are given in the Table VI below:

Table VI: Overview of components in qPCR master mixture

Component:	Volume per sample (μL):
SYBR Green 2x mix	10.0
Primer 341f (100 μ M stock)	0.1
Primer Un518r (100 μ M stock)	0.1
H ₂ O	8.8
Template (1:5)	1.0

All samples had three parallels, in case some qPCR reactions did not perform properly. If one of the triplets failed in the qPCR, these were removed so that they could not impact the result. There was separate qPCR runs for bacterial 16S rRNA genes and archaeal 16S rRNA genes, because different primers were used. The PCR program for bacteria was initiated with a hot start denaturation step for 15 minutes at 95°C, followed by 35 cycles of denaturation for 15 seconds at 95°C, annealing for 30 seconds at 58°C and elongation for 30 seconds at 72°C. The melting curve started with 15 second denaturation at 95°C, followed by 60°C for 1 minute. This was increased to 95°C (reading every 0,5°C gradient between 60°C and 95°C), and finished with 95°C for 15 seconds. The PCR program for archaea was initiated with a denaturation step for 15 seconds at 95°C, followed by 40 cycles of denaturation for 30 seconds at 95°C, annealing for 30 seconds at 60°C and elongation for 45 seconds at 72°C. The melting curve measurement/calculation is the same as for bacteria (see above). The qPCR data has to be checked that all samples are within the standard curve. This is by adjusting the threshold, R² value (as close as possible to 1.00) and Efficiency % (as close as possible to 100%). The result, number of copies of 16S rRNA in the original sediment sample, needs to be calibrated to the number of 16S rRNA per gram sediment, by integrating all elutions, μ L

sample used in cDNA synthesis and qPCR, and weight of the original sediment sample. By filling in numbers in Equation 1 to get the answer in number of 16S rRNA genes per gram sediment (Equation 1).

(1)

$$\text{Number of 16S rRNA per gram sediment} = \frac{\text{qPCR mean value} \times \text{cDNA dilution} \times \text{RNA dilution}}{\text{ul used in cDNA synthesis} \times \text{weight of sediment}}$$

3.8 Statistical methods and analysis:

Statistics can be used to summarize results, and put a number to the confidence in the data and uncover patterns that are not obvious to the naked eye. The computer programs *SigmaPlot* (Systad Software) was used for t-tests and Spearman's rank correlation, Excel (Microsoft Office 2012) was used for making column-bar plots and regression plots, and Principal Component Analysis (PCA) was done in MatLab (MathWorks). The statistical analysis performed used data from the qPCR, pH measurements and sediment oxygen consumption rates. Principal Component Analysis (PCA) was also used on 454 sequencing data (Section 3.10.4).

These are the tests that were used in this thesis:

Column-bar plot is used to compare the mean number of 16S rRNA genes from the CO₂ Experiment, Control and Baseline treatment. In Excel (Microsoft Office 2012) Standard error (SE) was calculated for the CO₂ Experiment treatment, and standard deviation (SD) was calculated for the Control and Baseline treatment, because there were only two variables. And the 'typical' number of 16S rRNA genes (around 68%) would lie somewhere within this error range (spread) (Townend, 2002). The different treatments are plotted separately here, because they are kept separate in the qPCR plot and the 454 sequencing analysis. But for the t-test, the Control and Baseline are joined for a stronger statistical test. A *t-test* is used when we want to compare the means of two populations. The populations I compared were the mean number of 16S rRNA genes from the CO₂ Experiments against the mean number of 16S rRNA genes from the Control/Baseline (separate test for depths and archaea/bacteria) in a two-tailed unpaired t-test using the computer program *SigmaPlot*. All tests need a null-hypothesis (H₀), which is stated 'there is no difference between the populations', and the test will answer this. The answer is given in a P-value (probability), which tells us the probability of the null

hypothesis being true, that there is not a relationship between two types of measurements. Where a low P-value ($\leq 0,05$, 5%) indicates that there is less than 5% chance that the null hypothesis is correct, and a high P-value ($\geq 0,05$), indicates that the hypothesis can be true (John Townend, 2002). The number of archaeal and bacterial 16S rRNA per gram sediment from the CO₂ Experiment was compared to the number of 16S rRNA per gram sediment from the Control treatment and the Baseline treatment in a t-test to see if the H₀ stated below was supported or unsupported.

Hypothesis tested were:

H₀ = there is no difference between the number of bacterial 16S rRNA genes in the CO₂ experiment versus the number of bacterial 16S rRNA genes in the Control and Baseline treatment.

H₁ = there is no difference between the number of archaeal 16S rRNA genes in the CO₂ experiment versus the number of archaeal 16S rRNA genes in the Control and Baseline treatment.

Regression is used to study the relationship between two types of measurements if we think that one of the variables is dependent on the other. If the other variable responds linearly on average, then a linear test can be used. Regression can also be used if the relationship is not a straight line, but the dependent variable responds logarithmically or exponentially to the independent variable. Spearman's rank correlation can be used to test the relationship when the relationship between the variables is non-linear. The Spearman's rank coefficient, ρ or r_s , measures the strength of association between the variables or *correlation*, and can be between +1 and -1, where a number close to +1 or -1 is a strong correlation and a number close to 0 is no correlation (like R²). If the ρ coefficient is positive the dependant variable (number of 16S rRNA genes) increases when the independent variable (pH or SOC) increases, and if ρ is negative then the dependent variable decrease when the independent variable increases. For regression Excel can make an equation, which can be made to predict the values of one type of measurement and find the R² value (correlation between the variables).

Measurement of pH (H⁺ ions): the pH electrode mounted inside the chambers of the lander did not function correctly, therefore the pH used here is the average pH registered from the

seven syringes attached to each chamber. After the lander was recalled to the surface this pH was measured by Dr. Laila J. Reigstad.

Measurement of sediment oxygen consumption: The oxygen concentration was measured every minute inside the chamber by a very accurate electrode (Aanderaa oxygen optode 3975A with 5% accuracy). The sediment oxygen consumption was calculated by taking the first measured oxygen concentration and subtracting the last measured oxygen concentration and dividing by the time between the two measurements converting it to the flux of O₂ per m⁻² d⁻¹. The sediment oxygen consumption rate is directly linked to the respiration rates by the organisms in the sediment.

We want to investigate if there is a relationship between the number of 16S rRNA (for bacteria and archaea) and the parameters pH and sediment oxygen consumption (SOC, mmol O₂ m⁻² d⁻¹), and find the p-value to ‘support’ or ‘reject’ the null-hypothesis stated below. The pH was plotted against the number of archaeal/bacterial 16S rRNA genes and the number of 16S rRNA was plotted against SOC. Because the pH could have an effect on the number of 16S rRNA numbers, and the sediment oxygen consumption rely on the microbes respiration rate (activity).

H₂ = there is no relationship between pH and the number of bacterial 16S rRNA genes.

H₃ = there is no relationship between pH and the number of archaeal 16S rRNA genes.

H₄ = there is no relationship between the number of bacterial 16S rRNA genes and SOC.

H₅ = there is no relationship between the number of archaeal 16S rRNA genes and SOC.

Principal Component Analysis (PCA) is a mathematical tool, highlight changes/differences in the microbial community structure from the 454 sequencing data and find trends in this dataset that could not be seen otherwise. The PCA uses a covariance structure to transform the dataset onto a new set of independent axes (orthogonal transformation) oriented in the direction of the greatest variance. The first axis is called first principal component axis (PC1) and accounts for the largest variance of the data, the second principal component axis (PC2), is perpendicular and independent of PC1 and accounts for the second largest variance in the data. The statistical program MatLab (MathWorks) was used to find significant patterns in the qPCR data.

3.9 16S rRNA gene Amplicon 454 Sequencing:

The 454 pyrosequencing technology (Roche Diagnostics Corporation) was used to sequence the amplified 16S rRNA genes, by using a GS FLX+/Titanium instrument (Roche, emulsion PCR) which can do a massive parallel sequencing approach. In emPCR single DNA molecules are attached to beads in wells on a plate, bases (dNTP) are washed over the plate in turn, which emits a light upon binding. This is then read by a machine determining the sequence (Quince et al., 2009). First, the samples must be purified (remove primers, nucleotides and enzymes) and tagged before they are sent for analysis. The GS Junior Titanium Sequencing Kit (454 Sequencing, Roche) was used to prepare the samples and this procedure for tagging using a specific primer design is important in this analysis. A few requirements are essential for the function of the primer tags for the 454 Sequence System emulsion PCR (em PCR) at the Norwegian Sequencing Centre (NSC). These are; the primers (primer A and primer B) must start with a specific sequence (in blue) in the 5'- end and must end with the sequence 'TCAG' (in red) (Fig. 9) for the amplicons to bind to the Capture Beads in the emPCR. In the 3' end of the primers there is a chosen sequence, in this case 787f and 1391r (sequence in section 3.6). The mid-section of the primers, Multiplex Identifiers (MID), is used to 'barcode' the amplicons, where one sample is given one unique sequence so this can later be identified and we then know what sample the amplicon comes from (454 Sequencing System Guidelines for Amplicon Experimental Design (2011), Roche). This is important because all the different samples sent for analysis to NSC will be merged into one sample.

<p>Forward primer (Primer A, Lib-L): 5'-CCATCTCATCCCTGCGTGTCTCCGACTCAG-(MID)-(template-specific sequence)-3'</p> <p>Reverse primer (Primer B, Lib-L): 5'-CCTATCCCCTGTGTGCCTTGGCAGTCTCAG-(template-specific sequence)-3'</p>

Figure 9: Forward (primer A) and reverse (primer B) primer sequence designed for 454 sequence tagging (Source: www.my454.com, Guideline Protocol).

The product from 16S rRNA PCR amplification must be of high quality (view on gel image for a pure 16S rRNA gene amplicon bands and concentration determine by both gel image and UV spectrophotometry) to proceed with purification and tagging of the amplicons. The purification of the nine 16S rRNA amplicons in this study was done by adding 100 µL binding solution to the amplified 16S rRNA samples, followed by the whole volume (117 µL,

subtracted the volume used on gel electrophoresis) that was transferred to the filter tubes, and centrifuged at max speed (19 000 x g) for 1 minute. The catch tube was then emptied, and 0,5 mL ethanol was added to the filter tube WHY, this was again centrifuged at max speed for 1 minute and then again for 2 minutes to dry the filter. The filters were then transferred to new, labeled columns and 50 µL elution buffer was added, and centrifuged for 1 minute at max speed. 3 µL of the product was controlled by gel electrophoresis on a 1% agarose gel on 50 volt for 30 minutes.

Then the samples are ready to proceed with AMPure XP bead purification of amplicons (Protocol: Norwegian Sequencing Centre, 2011). The PCR samples and the Ampure XP magnetic beads was mixed (0,7:1 Ampure beads : DNA ratio) and vortexed for 20 seconds, and then transferred to a 96 well PCR plate and incubated on a magnet block for 5 minutes to separate beads from solution. The clear solution was discarded making sure to not disturb the beads. Afterwards, 500 µL 70% ethanol was added and let incubate for 1 min and then all the ethanol was removed carefully. This step was repeated twice, while the plate was still on a magnet to completely remove all residual compounds. The plate was then air-dried for 15 minutes to remove all ethanol. After, 25 µL elution buffer (PCR water) was added to the samples, then they was sealed, vortexed and centrifuged shortly, and then placed on magnet block for 5 minutes to separate beads from solution. Finally, the clear solution was transferred to PCR tubes. 3 µL of the solution from each of the nine samples was quality checked on gel and the concentration was measured by UV spectrophotometry. The samples can now be merged into one sample, because the amplicons from each sample has a unique tag, which will be recognized by the emPCR machine. The samples were then sent for 454 sequencing to the Norwegian High-Throughput Sequencing Centre (NSC) at the University of Oslo. The 454 technique can give hundred thousands of reads per run and sequence reads of around 500 base pairs in length with high accuracy and throughput.

3.6.1 Samples selected for 16S rRNA gene amplicon 454 sequencing

Altogether nine samples from three of the lander dives were selected for amplicon 454 sequencing. The samples were from RISCS2, both chambers (Table 1) and RISCS3, chamber 2. The RISCS2 samples were chosen because these were the most suitable to compare since this dive has both a control and a CO₂ Experimental chamber (only 60 centimeters between the chambers). Additionally, dive RISCS3 Chamber 2 was included as a Baseline, because it is the physically closest Baseline to RISCS2 dive. The depths 0-1 and 1-2 cm were combined

to reduce number of samples. This gave a total of nine samples for RNA. The sequenced output data from the NCS was analyzed by bioinformatics computer programs (see section 3.8) resulting in taxonomic profiles of the active prokaryotic community present.

3.10 Bioinformatic tools and procedures for the 454 sequencing data:

Sequenced amplicon datasets were retrieved from Norwegian Sequencing Centre (NSC) as Standard Flowgram Format (SFF) files. These files were very large (100-200 MB per sample) and the DNA sequences (referred to as “reads”) therein must be quality checked and treated for amplicon noise. This is a highly demanding procedure. *Linux Ubuntu* is a command-line terminal used to communicate with UIB server Glassvinger where the bioinformatic pipeline is located. (See Section 3.10.1 below) (Lanzen et al., 2012).

3.10.1 Removal of noise from 454 sequencing data

It is important to remove noise from the sequence data to give a true sequence diversity in the samples when using the 454 sequencing approach (Quince *et al.*, 2009). By calculating the probability of mistakes (mismatch of bases) in the 454-pyrosequencing procedure it is possible to remove false sequences from the data. An algorithm, called PyroNoise, created by Quince and his co-workers, can remove noise, PCR point errors from the sequence, and remove chimeric sequences (incorrect alignments) (Quince *et al.*, 2011). The flowgram (SFF) file from NSC is run through an in-house script named RunPreSplit.sh. The following steps are included in the script PyroNoise: PyroDist (calculating distances between flowgrams), PyroNoiseM (remove noise), SeqDist (calculate the PCR-error-corrected distances between sequences, SeqNoise (remove PCR error) and Perseus (remove chimeric sequences).

3.10.2 CREST

CREST (Classification Resources for Environmental Sequence Tags) is a web server at the University of Bergen with a flexible and reliable system for taxonomic classification of microorganisms from environmental samples and uses an alignment-based classification method with the lowest common ancestor (LCA) algorithm and explicit rank similarity criteria (Lanzen *et al.*, 2012). CREST uses the reference database SilvaMod, because it contains extensive information of phyla, orders, family and genera. The SilvaMod derives from SILVA Reference alignment and uses information from SILVA SSURef and NCBI Taxonomy. The output file (good.fa files) from the bioinformatical pipeline scripts (see section 3.7.1) is uploaded to on-line CREST (<http://apps.cbu.uib.no/crest>), and the taxonomic

classification results were sent to user by e-mail. The taxonomic classification result from CREST was 1) organized in sector diagrams to highlight diversity and the distribution of bacteria and archaea, 2) collected in separate tables for phylum, class and OTU (see Section 3.10.3) and the subjected to Principal Component analysis in order to find patterns in the 454 sequencing data that otherwise not be obvious to the naked eye.

3.10.3 Principal Component Analysis of the microbial community structure:

The statistical program MatLab (MathWorks) was used to do the ordination plots on phylum level, class level and OTU level of the 454 sequencing data obtained from the nine selected samples from RISCs dive 2 and 3. In order to discover potential community impacts of the CO₂ acidification it might not be enough to look only in changes at phylum and class levels. A third level to be considered is the operational taxonomic units (OTU), or species richness in the samples. Operational taxonomical units have different definitions after what it will be used for. But here it can be considered as the lowest taxonomic level, which a sequence can be identified. To do this all OTUs in all nine samples needed to be compared. The nine Good.fa files from the bioinformatical pipeline were joined into one file in the Glassvinger Terminal, and then run through the script *OTUDist.sh*. This result is send by e-mail with an overview of all OTUs and their sequence.

Relative abundance of the 454 sequencing data was used in the PCA, instead of absolute abundance. This is because the total number of cellular organisms identified in one sample varies from 2 507 to 14 521. Relative abundance data represent a type of compositional data that sum up to a constant value (e.g. 100%). This constant-sum limitation performs a forced correlation: if the proportion of one taxon increases, the proportion of all others have to decrease. This forced correlation can distort the covariance structure of the data, and compromise the interpretation of PCA results. The 454 sequencing data was therefore subjected to a centered log-ratio transformation with multiplicative zero replacement to "open up" the compositional data (Aitchison, 1986, Martín-Fernández *et al.*, 2003, Jørgensen *et al.*, 2012). The relative abundance tables for the Phylum and Class level were made by Dr Laila J. Reigstad at CGB and the PCA analysis were performed by Dr Bjarte Hannisdal also at CGB.

4.0 Results:

A benthic lander equipped with two chambers was used to conduct an *in situ* CO₂ experiment, in order to mimic a leakage from a sub-seafloor CO₂ storage site. The chambers were given one out of three treatments; 1) CO₂ acidified seawater (20 000 µatm pCO₂) and ¹³C labelled algae was injected to the chamber and is referred to as CO₂ Experiment, 2) ¹³C labelled algae was added to the chamber and is referred to as Control, and 3) in the last treatment nothing was added to the chamber and is referred to as Baseline (Fig. 4). The benthic lander was deployed to the seafloor in Byfjorden, Bergen four times and the incubation time for the CO₂ exposure was 40 hours each dive.

Sediment samples for RNA extractions were prepared from the chamber sediment when lander was back on ship deck. pH and sediment oxygen consumption was measured inside the chamber during the whole experimental life span, and this data were used in the statistical analysis. The selected sediment horizons from each chamber were 0-1 cm, 1-2 cm, 3-4 cm and 6-7 cm. These depths were chosen because the largest impact was expected to be on the top sediment layers. The work presented in this thesis is part of a larger study at CGB on how the environment might be affected by CO₂ leaking up from sub seafloor CO₂ storage sites. In this thesis the focus is on the archaeal and bacterial community and how they respond to the CO₂ acidification. By analysing RNA from the sediment, the focus is on who the active members of the microbial community are and which respond they have to the CO₂ acidification treatment.

pH observations in the CO₂ Experiment:

In the CO₂ Experiment 100 mL of CO₂ acidified seawater was injected into the chamber in RISC2 chamber 1 and RISC4 chamber 1 and 2. The water in the 100mL had a pH of 5.1, corresponding to 20 000 µatm pCO₂. Looking at the pH measurements in syringe 2, sampled 40 minutes after CO₂ injection (Table I), the pH in RISC2 chamber 1 was measured to 6.6, while the pH in both chambers of RISC4 was measured to 7.4. With the normal seawater pH in Byfjorden of 8.0, the pH of RISC2 chamber 1 corresponds to more than one pH unit drop, while for RISC4 the pH drop was about 0.5 pH unit. Using the CO₂calc this corresponds to 12 000 µatm pCO₂ in the RISC2 chamber 1 and 2 000 µatm pCO₂ in both chambers of the RISC4 dive. Why these different pH values occurred is unknown.

4.1 Numbers of bacterial and archaeal 16S rRNA gene copies per gram sediment (RNA level)

4.1.1 RNA isolation and cDNA synthesis

In order to evaluate if the CO₂-acidification experiment had any effect on the *active* microbial community composition in the seafloor sediment in Byfjorden, all analyses were carried out on complementary DNA (cDNA). The cDNA was made from total RNA isolated directly from the sediment, and both the 23S ribosomal RNA subunit (2900 base pairs) as well as the 16S ribosomal RNA subunits (1540 base pairs) was visible after the RNA isolation and following agarose gel electrophoresis (Fig. 10).

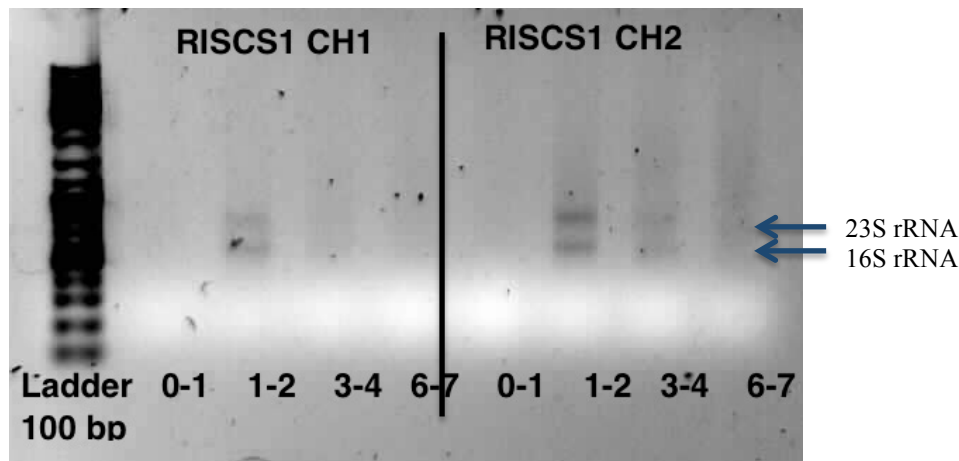


Figure 10: Examples of the total RNA isolated from sediment in the RISCS1 dive. Numbers at the bottom indicate the various sediment depths the RNA was isolated from. Left panel shows the total RNA from lander Chamber 1 in RISCS dive 1. Panel to the right shows the total RNA isolated from sediment in Chamber 2 of RISCS dive 1. Blue arrows indicate band of 23S and 16S rRNA. (Ladder 100 bp: MBI Fermentas).

The electrophoresis showed that RNA was successfully isolated, and the complementary DNA could then be synthesized from the 4 sediment depths from the 7 chambers. These cDNA samples were the basis for the whole master thesis, and were thereby used in the following analysis 16S Amplicon PCR, qPCR and 454 pyrosequencing.

4.1.2 Amplification of 16S rRNA genes using PCR

The 16S rRNA gene is the most studied and used for taxonomical analysis and identification. It encodes the 16S ribosomal RNA in the small subunit of the ribosome (a complex molecular machinery responsible for building proteins). To evaluate the quality of the synthesised

cDNA from 4 sediment depths per chamber, conventional PCR that amplified bacterial 16S rRNA genes was carried out using the primer set Uni787F/1391R. The 604 base pairs long DNA fragment of the bacterial 16S rRNA genes were successfully amplified from all samples, and an example of the amplified genes are given in Figure 11.



Figure 11: Example of PCR-amplified bacterial 16S rRNA genes (primers Uni787F/1391R) from the sediment cDNA, from sediments of RISCS2 and RISCS3. The numbers on the bottom is the depth RNA was isolated from. The left panel is from RISCS2 Chamber 2 (Control), the panel in the middle is from RISCS2 Chamber 1 (CO₂ Experiment), and the right panel is from RISCS3 Chamber 2 (Baseline). (Ladder 100 bp: MBI Fermentes)

4.1.3 Quantification of bacterial and archaeal 16S rRNA genes using quantitative PCR

Real-Time quantification PCR is an efficient method to quantify a targeted gene in the microbial genome. In this thesis the technique were used both the archaeal and bacterial small subunit 16S rRNA genes. By quantifying these genes, we can estimate the general microbial activity in a given sample, and compare the samples that were exposed to CO₂ acidified water to those that were not. The qPCR was performed on four different sediment layers from all of the eight chambers.

The bacterial 16S rRNA gene was successfully quantified in all samples using the qPCR... The R² value was calculated by the qPCR machine and was between 0.988 and 0.997 in all runs, which is close to the anticipated value of 1. The estimated amplification efficiency (Eff%) was between 59.4% and 79.87 %, which are a little low. The mean value of the 16S rRNA triplets from each sample (from the raw data of the quantitative qPCR run) was used to calculate the number of 16S rRNA per gram sediment (Equation 1) in all data points. The result from the calculations based by the qPCR was logarithmically plotted against depth (cm) (Fig.12). The qPCR data (numbers of 16S rRNA) from the different treatments was plotted separately, because we wanted to see if there was a trend between the treatments.

- Bacterial 16S rRNA copy numbers in sediment exposed to 2 000 or 12 000 $\mu\text{atm pCO}_2$:

The number of copies of the bacterial 16S rRNA in the CO_2 Experiment ranged from $2.0\text{E}7$ to $1.44\text{E}10$ number of 16S rRNA per gram sediment in the surface layer (0-1 cm) of the sediment (Fig. 12A). There was a large difference in 16S rRNA numbers between the treatment of 2 000 $\mu\text{atm pCO}_2$ (RISCS4) versus the 12 000 $\mu\text{atm pCO}_2$ (RISCS2 chamber 1). It was the RISCS2 Chamber 1 had had the highest number of 16S rRNA ($1.44\text{E}10$ bacterial 16S rRNA), while the number of 16S rRNA measured in RISCS4 chamber 1 and 2 was highly similar (Fig. 12A).

- Bacterial 16S rRNA copy numbers in Control sediment:

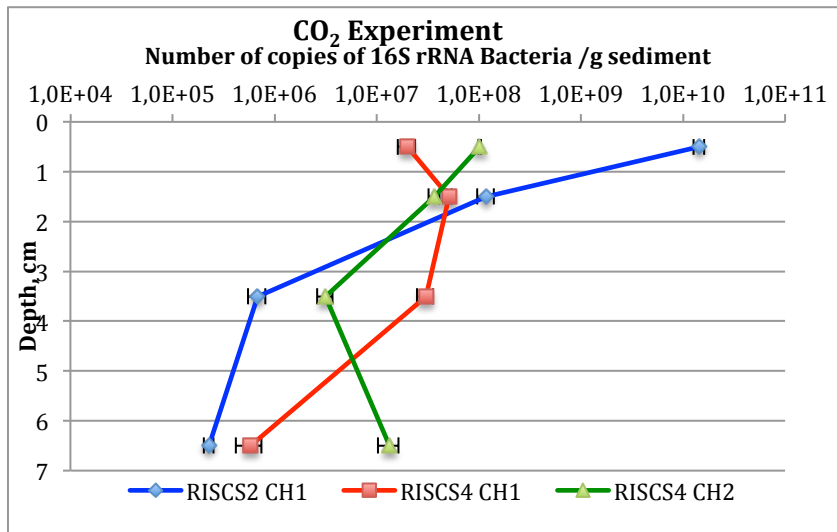
The number of copies of bacterial 16S rRNA from the two chambers, which received the Control treatment, was plotted together. The number of 16S rRNA was in RISCS1 Chamber2 $5.0\text{E}7$ and in RISCS2 Chamber2 $3.0\text{E}8$ number of 16S rRNA per gram sediment in the surface layer. There is also a great variability between the numbers of 16S rRNA from the Control treatment in depth 1-2 cm (Fig. 12B).

- Bacterial 16S rRNA copy numbers in Baseline sediment:

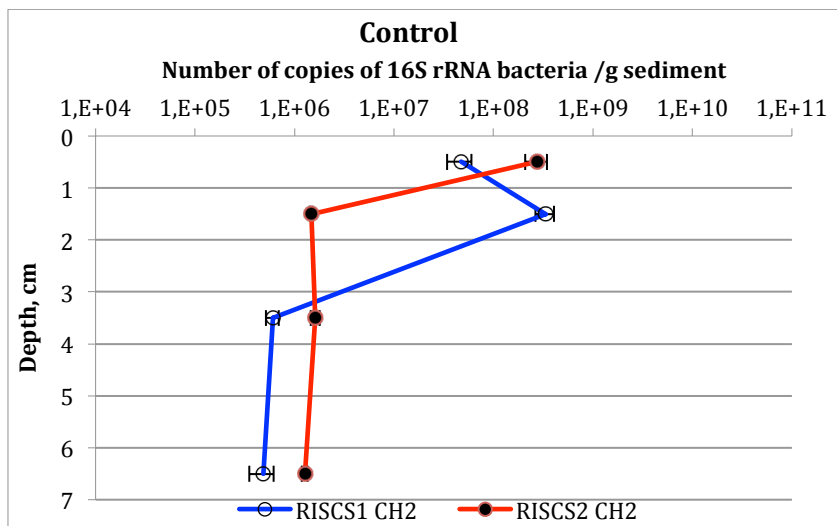
The number of 16S rRNA from the two chambers, which received the Baseline treatment, was plotted together. The number of copies of 16S rRNA genes was between $1.0\text{E}7$ and $2.3\text{E}9$ per gram sediment in the surface layer (Fig. 12 C).

A general trend in all chambers from all treatments (Fig.12A, B and C) is that there is a higher number of copies of the 16S rRNA gene in the surface layers (between $\text{E}7$ and $\text{E}10$ at depth 0-1 cm, between $\text{E}6$ and $4\text{E}8$ at depth 1-2 cm) than in the deeper sediment layers (from $5\text{E}5$ to $3\text{E}7$ at depth 3-4 cm and $\text{E}5$ to $\text{E}7$ at depth 6-7 cm), especially for RISCS2 Chamber 1 (CO_2 Experiment) and RISCS3 Chamber 2 (Baseline). But not all chambers have a steady decrease in number of 16S rRNA relative to depth, RISCS1 Chamber 1 (Baseline) and RISCS1 Chamber 2 (Control) have fewer copies of the 16S rRNA in the top layer than in 0-1 than in depth 1-2 cm (See discussion; Section 5.0).

A)



B)



C)

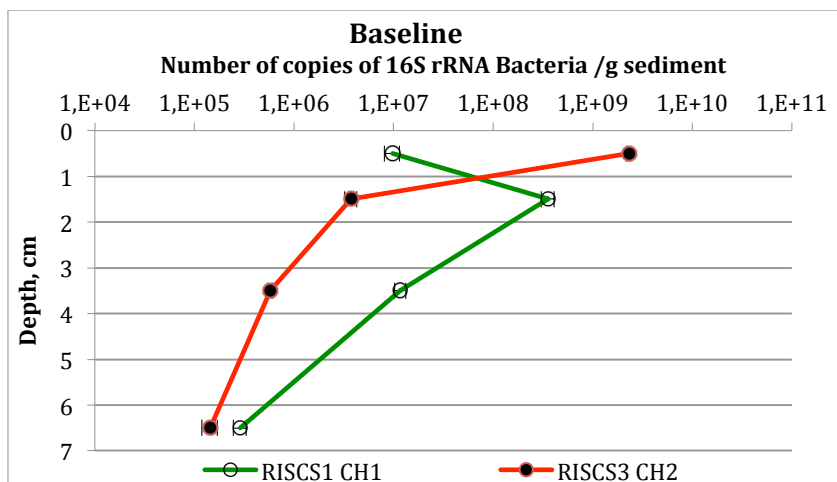


Figure 12: Number of bacterial 16S rRNA copies per gram sediment plotted logarithmically against sediment depth (cm). Each point represents triplicate qPCR analyses. A) Sediment exposed to 2 000 (RISC4) or 12 000 (RISC2 chamber1) uatm pCO₂ (dives: RISC2 Chamber 1, RISC4 Chamber 1 and

2), B) Control sediment exposed to ¹³C labelled algae (dives: RISC1 Chamber 2 and RISC2 chamber 2),
C) Untreated Baseline sediment (dives: RISC1 Chamber 1 and RISC3 Chamber 2).

With these differences in bacterial 16S rRNA numbers in mind, the same sediment cDNA were subjected to qPCR for amplification of the archaeal 16S rRNA gene. As for their bacterial counterpart, the archaeal 16S rRNA gene copy numbers per gram sediment were plotted logarithmically against depth (Fig.13). The archaeal number of copies of 16S rRNA genes follows a similar pattern as the bacterial number of 16S rRNA, but they are two to three magnitudes lower than for bacteria.

- Archaeal 16S rRNA copy numbers in sediment exposed to 2 000 or 12 000 $\mu\text{atm pCO}_2$:

In our lander experiment, the sediments of three chambers were exposed to CO₂ acidified seawater. In the two of the chambers (RISC 4 chamber 1 and 2 exposed to 2 000 $\mu\text{atm pCO}_2$) the calculated number of archaeal 16S rRNA copies per gram sediment was similar; both in the range of E5, but in the RISC2 Chamber 1 (exposed to 12 000 $\mu\text{atm pCO}_2$) the copy number was as high as 3.7E8 (Fig. 13A). Looking at the deeper sediment layers, two of the CO₂ exposed sediments show decrease in 16S rRNA copy numbers downwards in the sediment, while the RISC4 Chamber 1 actually increases the copy numbers from top layer to the 1-2 cm layer.

- Archaeal 16S rRNA copy numbers in Control sediment:

During the lander experiment, sediment in two chambers was treated as controls, meaning only the ¹³C labeled freeze-dried algae were added. The number of archaeal 16S rRNA genes in these two chambers was different throughout the analyzed sediment depth (Fig. 13B). There were differences in the top layer copy numbers ranging from E5 (RISC1 Chamber 2) to E6 (RISC2 Chamber 2), but it is at 1-2 cm depth that we find the largest difference with 4,3E4 versus 6,6E6, respectively.

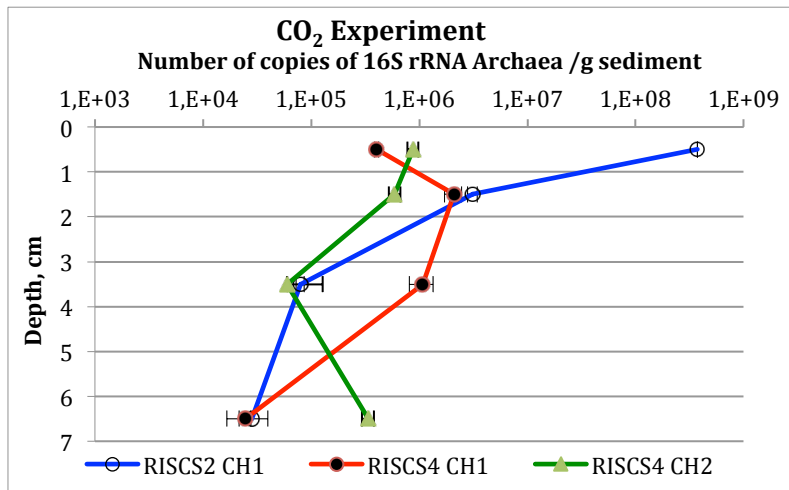
- Archaeal 16S rRNA copy numbers in Baseline sediment:

The number of copies of 16S rRNA genes from the Baseline treatment was 1.5E+5 (RISC1 Chamber 1) and 6.6E7 (RISC3 Chamber 2) number of copies of 16S rRNA genes (Fig. 13C) in the surface layer. There is also a large variability between the numbers of copies of 16S rRNA from the same depth, for both the Control and the Baseline treatment.

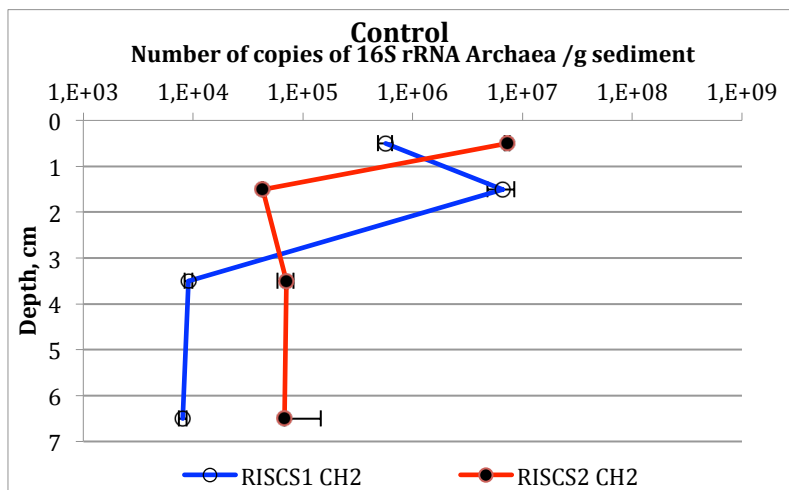
Like for bacteria, the number of archaeal 16S rRNA copies per gram sediment is higher in the

top layers (0-1 cm depth and 1-2 cm depth) than in the deeper layers (3-4 cm depth and 6-7 cm depth) in all chambers. Also similar to bacterial 16S rRNA copy numbers is it that in RISC1 chamber 1 (Baseline) and 2 (Control) and in RISC4 Chamber 1 (CO₂ Experiment) have a higher number of archaeal 16S rRNA at depth 1-2 cm than in the surface layer (Fig 13).

A)



B)



C)

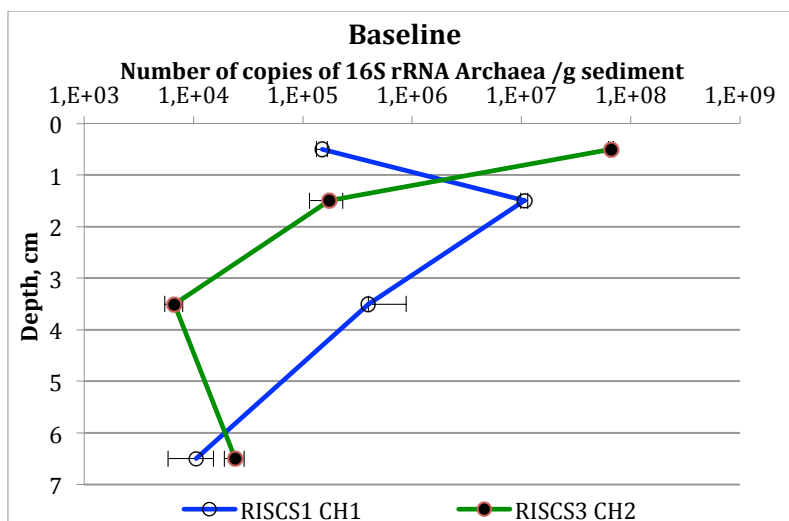


Figure 13: Number of archaeal 16S rRNA copies per gram sediment plotted logarithmically against sediment depth (cm). Each point represents triplicate qPCR analyses. A) Sediment exposed to 2 000 (RISC4) or 12 000 (RISC2 chamber1) uatm pCO₂ (dives: RISC2 Chamber 1, RISC4 Chamber 1 and

2), B) Control sediment exposed to ^{13}C labelled algae (dives: RISC1 Chamber 2 and RISC2 chamber 2), C) Untreated Baseline sediment (dives: RISC1 Chamber 1 and RISC3 Chamber 2).

Even though qPCR runs were done separate for bacteria and archaea, the pattern between the numbers of 16S rRNA genes from the same sample are quite similar (only being a few magnitudes lower for archaea than bacteria) (Fig.14). The PCA plot below (Fig. 14) clearly demonstrates that the number of copies of bacterial and archaeal 16S rRNA in the top layer (0.5 cm depth is average number of 16S rRNA of depth 0-1 cm and 1-2 cm) is significantly higher than in the two lower layers (3-4 cm and 6-7 cm depth).

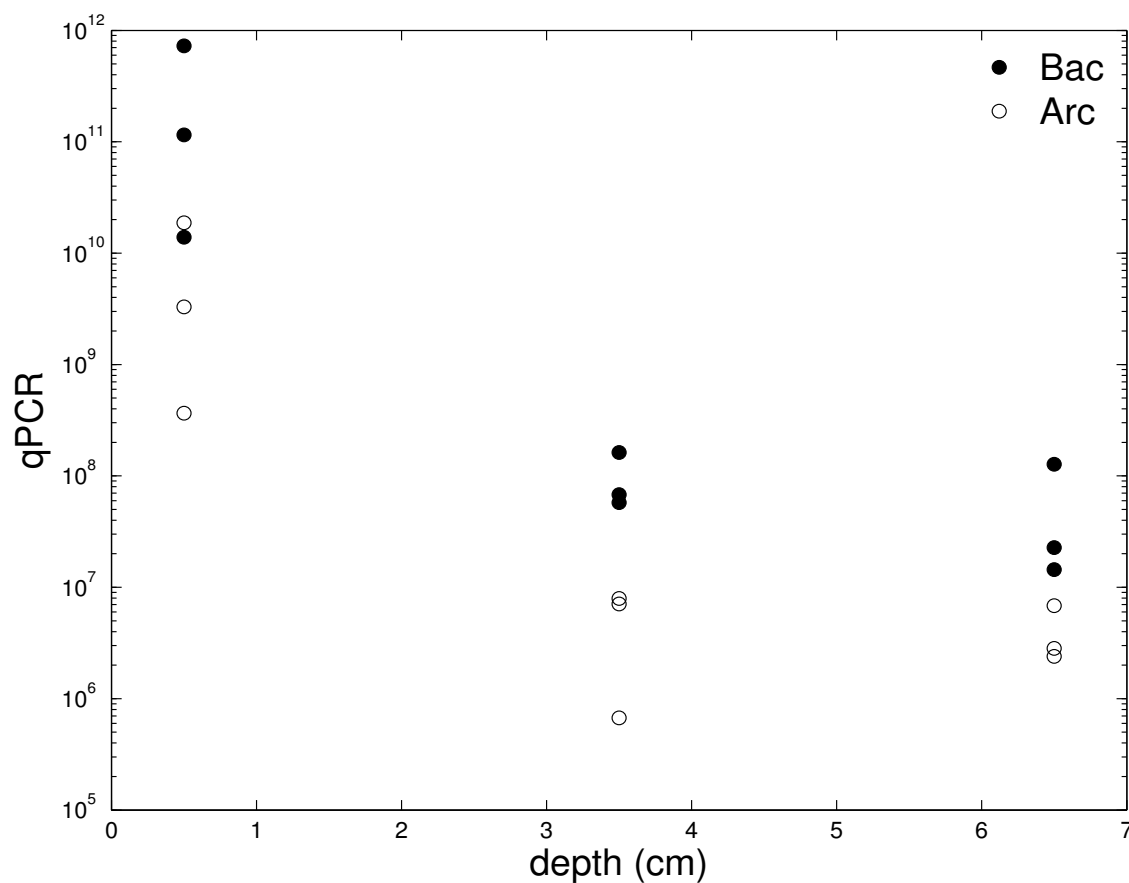


Figure 14: Principal Component Analysis of number of bacterial and archaeal 16S rRNA plotted against sediment depth. The data clustering at 0.5 cm depth is average number of 16S rRNA of depth 0-1 cm and 1-2 cm.

4.2 Statistical analyses on number of 16S rRNA per gram sediment:

In order to evaluate if there was a significant difference between the number of bacterial and archaeal 16S rRNA copy numbers per gram sediment due to the separate treatments, t-test were carried out. Regression tests were done on number of copies of 16S rRNA for both bacteria and archaea (separately) had any statistical correlations to other measured parameters in the *in situ* set-up.

4.2.3 T-test analyses for significant difference between the three treatments:

The t-test calculates if there is a significant difference between two populations. In this case the number of 16S rRNA genes from the CO₂ Experiment is tested against the number of 16S rRNA genes from the Control and Baseline treatments. The number of copies of 16S rRNA genes are shown in column-bar diagrams (separate plots for bacteria and archaea), and are divided into the different treatments; CO₂ Experiment treatment (Blue bar), Control treatment (red bar) and Baseline conditions (green bar) in an exponential scale (Fig.15), where the mean from each treatment is used. For CO₂ Experiment treatment \pm standard error (SE) is used and for Control and Baseline \pm standard deviation (SD) is used.

The plots in Figure 15 shows that the mean numbers of bacterial 16S rRNA copies per gram sediment decrease with increased depth, but that there is no a significant difference between the three treatments. The error bars in the three treatments are large, indicating a high degree of variability in the parameters measured. The error bars also overlap between the treatments in all depths, which shows that the power of the test is too low to detect a difference between the mean number of 16S rRNA genes from the CO₂ Experiment and the mean number of 16S rRNA from Control/Baseline (Fig.15). The t-test gave P-values between 0.37 and 0.51, which is considerably higher than the desired P-value of ≤ 0.05 , concluding that there is no relationship between the number of copies of 16S rRNA in the sediment which received the CO₂ treatment and the sediment which did not (Control treatment and Baseline conditions).

Number of copies of Bacterial 16S rRNA /g sediment

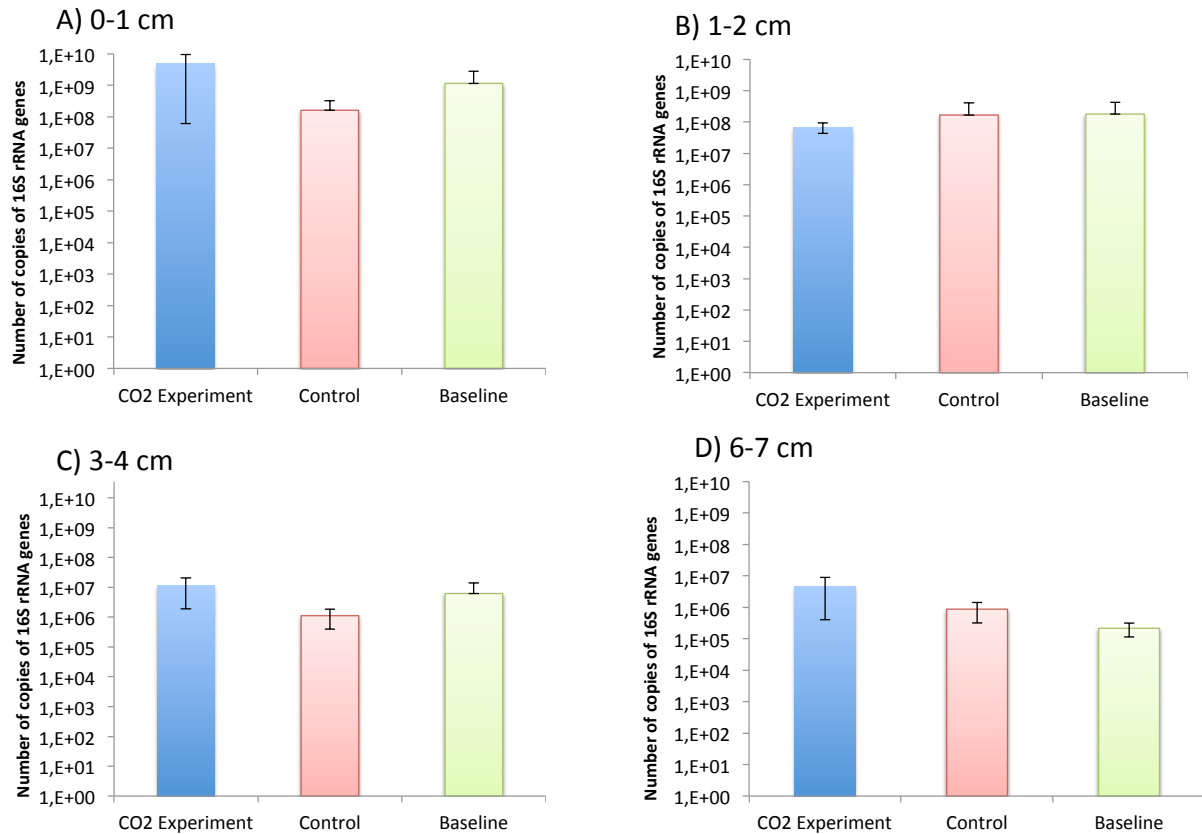


Figure 15: Mean bacterial 16S rRNA numbers from different treatments. 16.A) 0-1 cm sediment depth, B) 1-2 cm sediment depth, C) 3-4 cm sediment depth, D) 6-7 cm sediment depth. Error bars denote ± 1 SE for CO₂ Experiment, \pm SD for the Control and Baseline treatment (Note: exponential scale on y-axis).

The mean number of archaeal 16S rRNA per gram sediment from the CO₂ Experiment treatment was compared to the mean number of 16S rRNA from the Control treatment and the Baseline treatment, and this is shown in column-bar diagrams (Fig.16). The three treatments have an even distribution and there is no significant difference between them. The error bars also overlap in the different treatments in all depths for archaea (Fig.16). The t-test gave a P-value between 0.42 and 0.49. There is no data suggesting that there is a significant difference between the samples receiving the CO₂ treatment and those that did not, when comparing the number of copies of 16S rRNA genes per gram sediment.

Number of copies of Archaeal 16S rRNA /g sediment

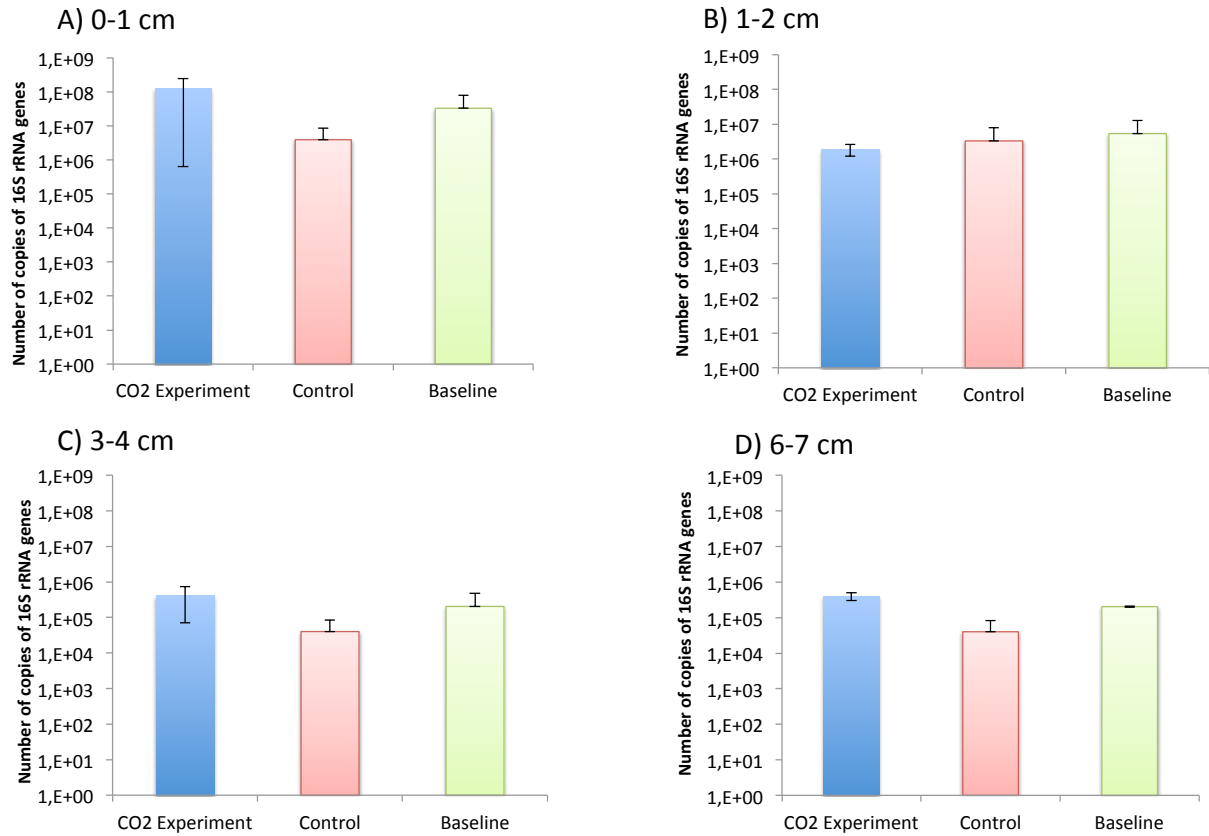


Figure 16: Mean Archaeal 16S rRNA numbers from different treatments. 16.A) 0-1 cm sediment depth, B) 1-2 cm sediment depth, C) 3-4 cm sediment depth, D) 6-7 cm sediment depth. Error bars denote ± 1 SE for CO₂ Experiment, \pm SD for the Control and Baseline treatment (Note: exponential scale on y-axis).

4.7.2 Interpreting pH and sediment oxygen consumption (SOC) data using regression analyses:

The regression analyses in our lander experiment were used to show if there were relationships between the pH measurements or sediment oxygen consumption and the number of copies of bacterial or archaeal 16S rRNA genes per gram sediment.

Chamber water pH: The pH values used here is the pH measured from syringe number 2-7 (Table I). Because of this the pH of the water inside the chambers in the CO₂ Experiment (40 minutes after injection, see Table 1) ranged between 6.98 and 7.36, with RISC2 Chamber 1 being the lowest at 6.98. This was also the dive/chamber with the highest copy numbers of 16S rRNA genes for both bacteria and archaea. The overall pH in the CO₂ Experiment chambers was lower than in the other chambers with the Control treatment and Baseline conditions, which ranged between 7.6 and 8.0 (Table VII).

Chamber sediment oxygen consumption (SOC): The oxygen level was obtained by oxygen electrode, and the first recorded oxygen level minus the last recorded oxygen level divided by time gives us the flux of $O_2 \text{ m}^{-2} \text{ d}^{-1}$. The SOC over 40 hours in our lander experiment were between 4.1 and 5.96 $O_2 \text{ m}^{-2} \text{ d}^{-1}$ in RISC4 chamber 2 and 1, respectively. And double in RISC2 chamber 1 at 10.9 $O_2 \text{ m}^{-2} \text{ d}^{-1}$. In the Control chambers the SOC was between 3.3 and 5.3 $O_2 \text{ m}^{-2} \text{ d}^{-1}$ (only two measured). As for the pH and microbial 16S rRNA copy numbers, a special notice is brought to RISC2 Chamber 1 here as well, which had a considerably higher sediment oxygen consumption (10.9 $\text{mmol } O_2 \text{ m}^{-2} \text{ d}^{-1}$). The pH, SOC and 16S rRNA data were further used in a regression analysis. The SOC was not measured in all dives because the sensors failed to measure (Table VII).

Table VII: Average pH in water overlaying sediment (syringe 2-7) and sediment oxygen consumption (SOC) with \pm SD

Dive_Chamber (treatment):	pH	SOC (mmol $O_2 \text{ m}^{-2} \text{ d}^{-1}$)
RISC1_CH1 (Baseline)	7.90 \pm 0.2	na
RISC1_CH2 (Control)	8.01 \pm 0.1	3,34 \pm 0.9
RISC2_CH1 (CO_2 Experiment)	6.98 \pm 0.2	10,94 \pm 1.0
RISC2_CH2 (Control)	7.61 \pm 0.02	5,31 \pm 0.7
RISC3_CH2 (Baseline)	7.90 \pm 0.02	na
RISC4_CH1 (CO_2 Experiment)	7.36 \pm 0.05	5,96 \pm 0.6
RISC4_CH2 (CO_2 Experiment)	7.36 \pm 0.05	4,13 \pm 0.2

Na: not analysed

Regression analyses were carried out for both bacterial and archaeal 16S rRNA numbers per gram sediment plotted against pH and SOC plotted against bacterial and archaeal 16S rRNA numbers. This was done because the pH could have an effect on the number of 16S rRNA numbers, and the sediment oxygen consumption rely on the microbes' respiration rate (activity).

The number of copies of bacterial 16S rRNA for bacteria was plotted against the pH value for the depths 0-1 cm, 1-2 cm, 3-4 cm and 6-7 cm (Fig.17). R^2 and the equation of an exponential line are calculated by Excel and placed in the upper right corner of the graph window. The R^2 value for depth 0-1 cm is 0.19, which means that 19% of the variability in number of bacterial 16S rRNA is explained by the pH. The R^2 in the other depths is between 5.8E-05 (1-2 cm depth), 0.02 (3-4 cm depth) and 0.06 (6-7 cm depth), these are very low values for correlation. When the R^2 is very close to 0, there is no correlation between the number of bacterial 16S

rRNA and pH. The relationship between the variables is hardly exponential at all, but R^2 is higher for an exponential fit than a linear relationship. R^2 is closer to 0 than to +1 and it is therefore no correlation between the number of bacterial 16S rRNA genes and pH in any depths. The point that stands out in Figure 17A at 0-1 cm depth is the RISC2 Chamber 1. This has a very high bacterial 16S rRNA copy number per gram sediment, being 1.44×10^{10} , and the lowest chamber water pH of 6,98. This single point is the cause of the higher R^2 correlation value at depth 0-1 cm. Figure 17 B, C and D also have points standing out, but these do not contribute to a higher correlation (R^2 value).

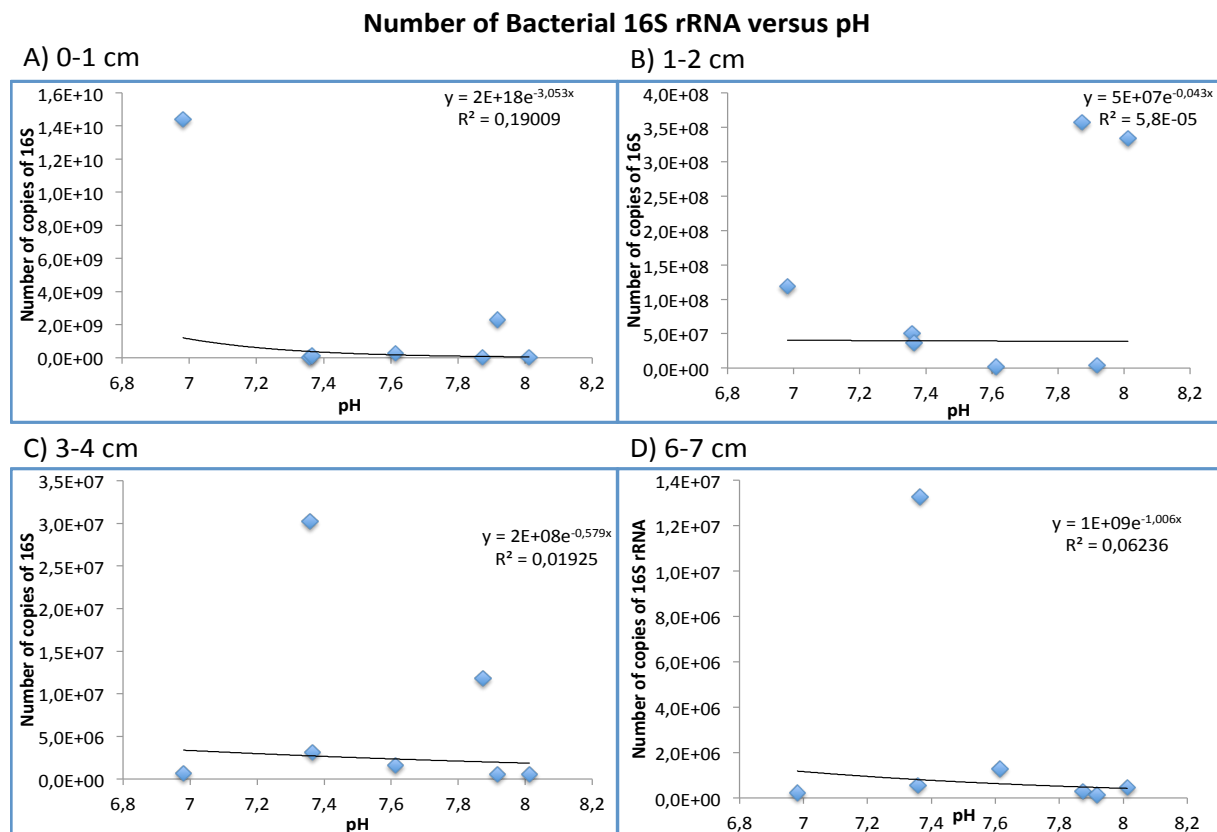


Figure 17: Regression of number of copies of bacterial 16S rRNA per gram sediment plotted against pH, A) 0-1 cm depth, B) 1-2 cm depth, C) 3-4 cm depth, D) 6-7 cm depth.

The same regression analyses were done between pH and archaeal 16S rRNA copy numbers per gram sediment (Fig.18). R^2 varied between the different sediment depths, from 0,17 in the top layer, 0,0003 at 1-2 cm and 0,23 at 6-7 cm, This means that 17% of the variability in number of archaeal 16S rRNA was explained by the pH in the surface layer, and 23% in the 6-7 cm depth. These R^2 values were very low, and this means that there is little to no correlation between the variables (Fig.18).

Number of Archaeal 16S rRNA versus pH

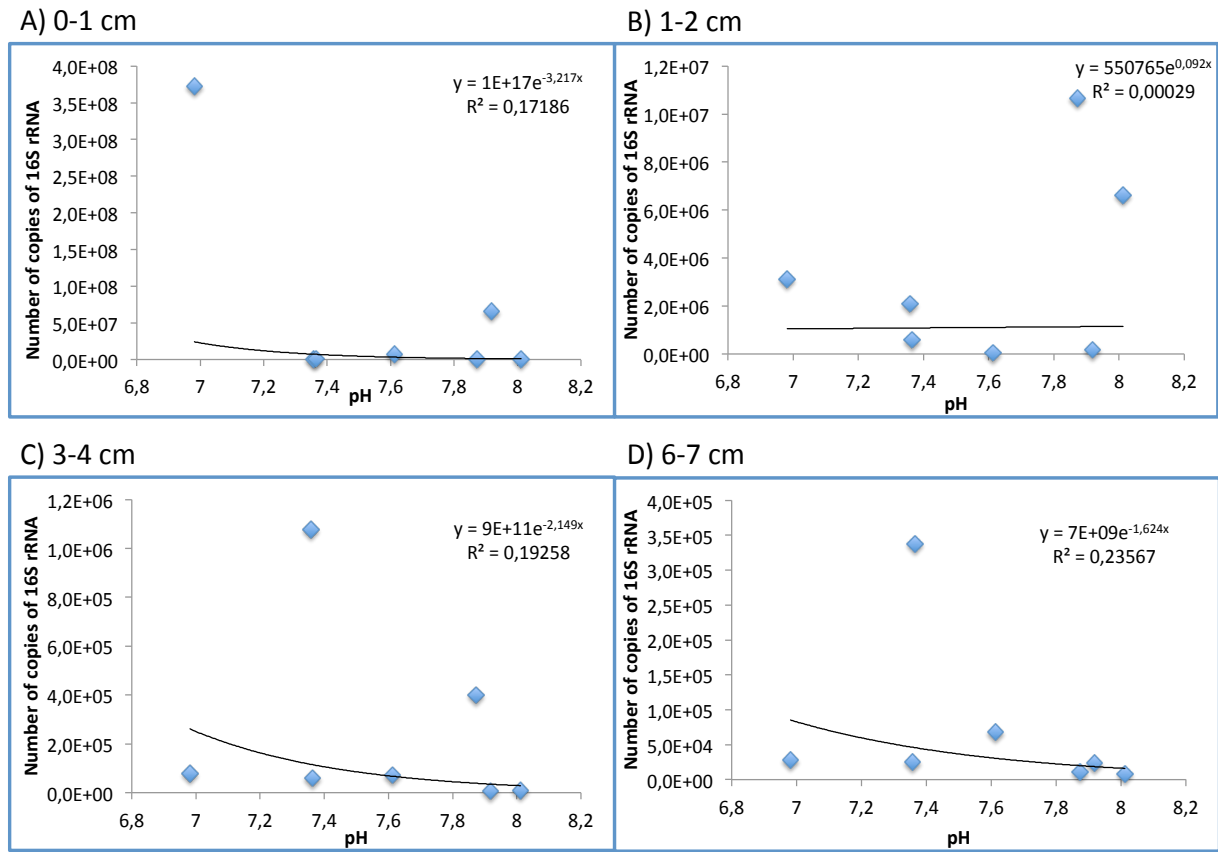


Figure 18: Regression of number of copies of archaeal 16S rRNA per gram sediment plotted against pH, A) 0-1 cm depth, B) 1-2 cm depth, C) 3-4 cm depth, D) 6-7 cm depth.

The sediment oxygen consumption (SOC) was plotted against the numbers of copies of 16S rRNA for bacteria in an exponential regression (Fig.19). There was a potential correlation between the number of bacterial 16S rRNA and oxygen consumption in the sediments at depth 0-1 cm, where there was an exponential line and R² was 0.64, which is closer to 1 (Fig. 19A). This means that 64% of the variability in SOC was explained by the number of bacterial 16S rRNA per gram sediment in RISC2 Chamber 1 in 0-1 cm depth. In the other depths the R² varies between 0,005 and 0.3, which are very low (Fig.19). Again, it is the RISC2 Chamber 1 at 0-1 cm depth that stands out. The Spearman's rank correlation was calculated for data in Fig. 19A to test the relationship between the number of copies of bacterial 16S rRNA and SOC, and this was $\rho = 0.2$, which is not very close to the anticipated value of +1 or -1. The Spearman's rank was also calculated for Fig. 19 B, C and D, but these were also low (-0.3 to +0.2).

Number of Bacterial 16S rRNA versus sediment oxygen consumption (SOC)

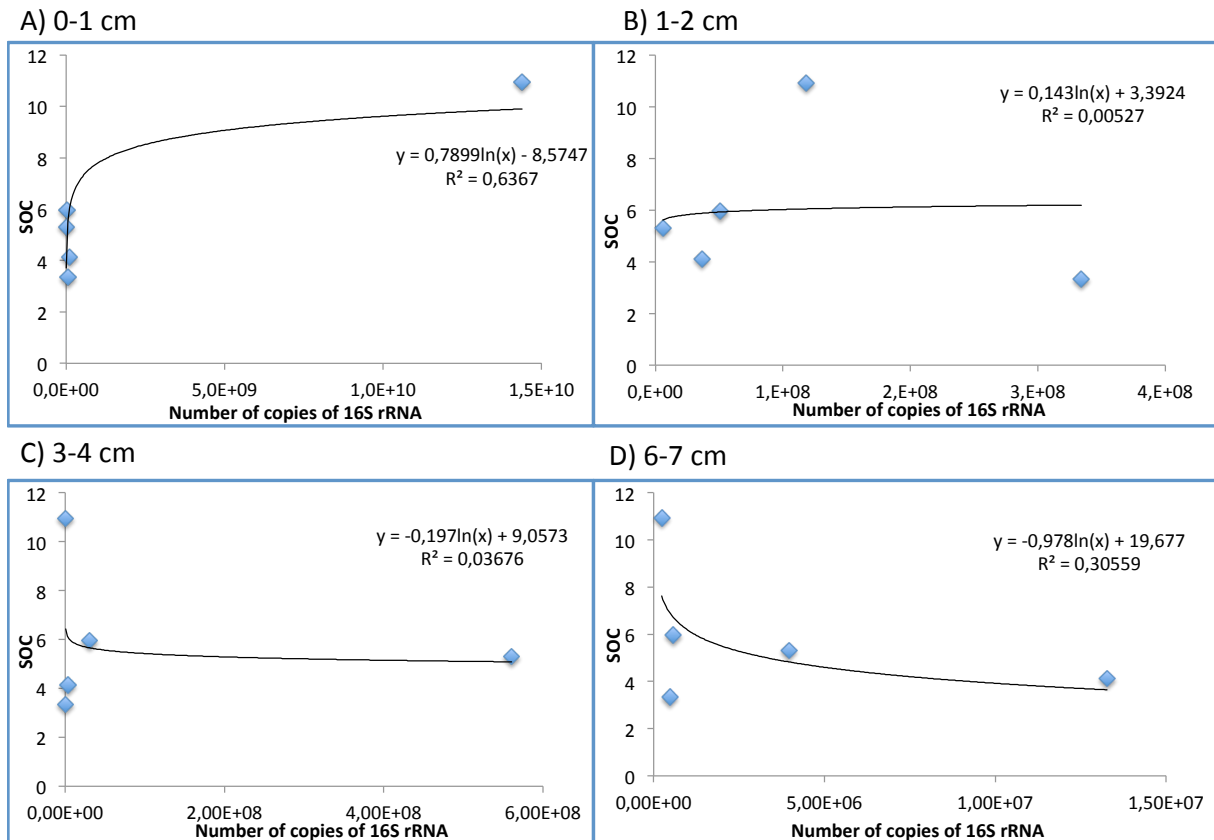


Figure 19: Regression of number of copies of bacterial 16S rRNA plotted against SOC, A) 0-1 cm depth, B) 1-2 cm depth, C) 3-4 cm depth, D) 6-7 cm depth

The SOC was also plotted against numbers of copies of archaeal 16S rRNA genes per gram sediment (Fig.20). There was a very strong correlation between the number of archaeal 16S rRNA per gram sediment and the SOC for 0-1 cm depth, with an R^2 value of 0.90. This is a very high value, showing than 90% of the variability in sediment oxygen consumption was explained by the number of archaeal 16S rRNA per gram sediment. In the depths 1-2 cm, 3-4 cm and 6-7 cm the R^2 varies between 0.03 and 0.01, which are very low values, and therefore there are no correlation between the SOC and the archaeal gene copy numbers. The Spearman's rank correlation was calculated for data in Fig. 20A to test the relationship between the number of copies of archaeal 16S rRNA and SOC, and this was $\rho = 0.6$, which is closer to the anticipated value of +1. The Spearman's rank correlation was also calculated for the other depths, but these were very low (-0.3 to +0.2).

Number of Archaeal 16S rRNA versus sediment oxygen consumption (SOC)

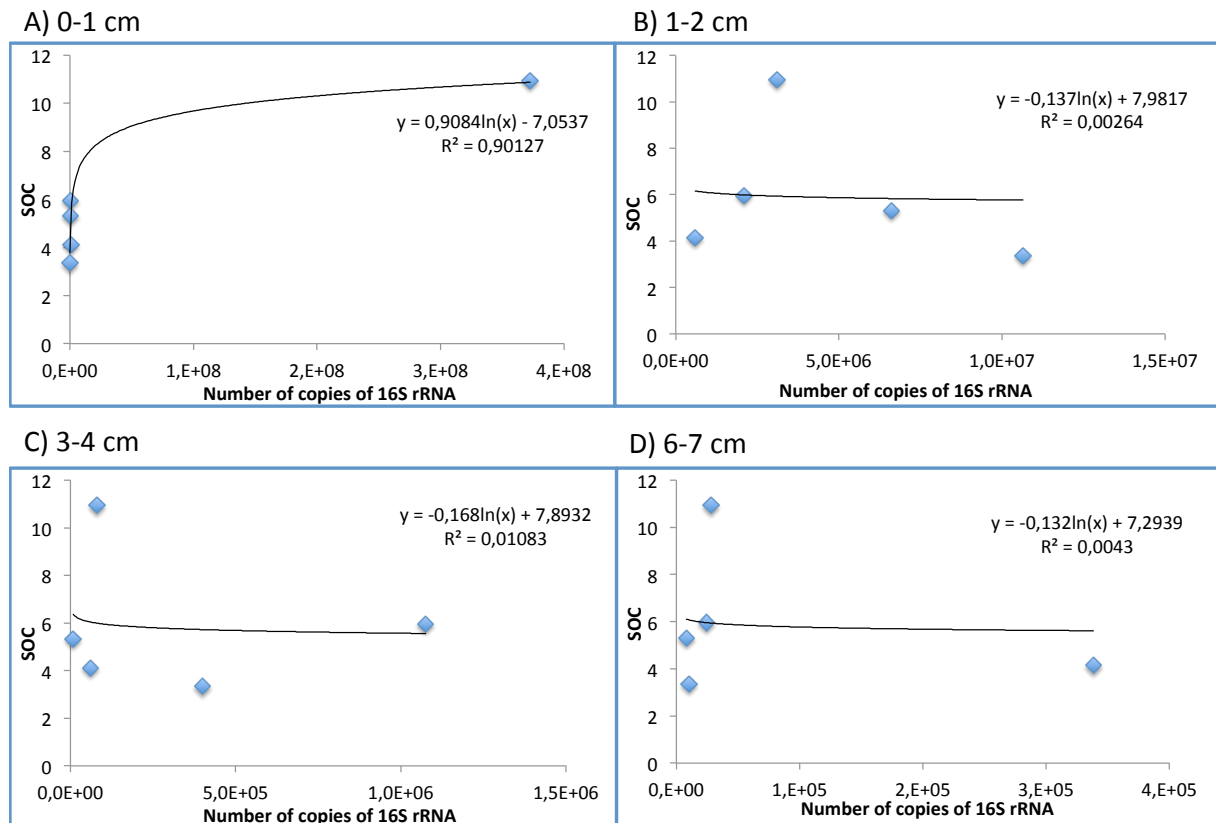


Figure 20: Regression of number of copies of archaeal 16S rRNA plotted against SOC, A) 0-1 cm depth, B) 1-2 cm depth, C) 3-4 cm depth, D) 6-7 cm depth

4.3 Microbial community composition

By sequencing the 16S ribosomal RNA in prokaryotic cells the organism can be identified and then classified according to its closest relatives. Taxonomic classification is an important step following sequencing, and is used to identify or predict the taxonomical location for an organism from a given ecosystem, by comparing its sequence to previously analysed and identified species (Lanzen *et al.*, 2013). These analyses can aid in understanding the environment and the function of the organisms living here. 454 pyrosequencing is a method that can identify thousands of nucleic acid fragments (“reads”) in one sample, and therefore we can get a deep understanding of the active microbial community in our samples. The nine samples included in this analysis were from the lander dives RISC2 Chamber 1 (CO₂ Experiment exposed to 12 000 $\mu\text{atm pCO}_2$) and 2 (Control), and RISC3 Chamber 2 (Baseline). The depth horizons chosen from each dive are 0-2 cm (depth 0-1 cm and 1-2 cm were combined), 3-4 cm and 6-7 cm. The PCR primers used were universal, so the 454 sequencing gave taxonomic information for archaea and bacteria, as well as the relation between them. The data received from Norwegian Sequencing Centre was treated for noise,

PCR point errors and removed chimeric sequences (incorrect alignments) using the CGB-developed AmpliconNoise software, and taxonomically classified using CREST.

4.3.1 Amplicon 454 Sequencing of 16S rRNA genes:

The amplicon 454 sequencing done in the lander experiment identified what taxonomic groups of archaea and bacteria that are active in the sediments of Byfjorden and if/how they reacted to the exposure of 12 000 $\mu\text{atm pCO}_2$. The differences between what groups are more active and what groups are less active were compared in the CO₂ Experiment to the Control treatment and Baseline conditions, as well as the three different sediment depths. In total between 3 000 and 12 000 reads were obtained per sample after the AmpliconNoise, and all these belong to either the domain Archaea or Bacteria. Altogether 65 832 reads were obtained from the nine samples. The results obtained from CREST are a systematic overview of the different taxonomic groups (Bacteria, Archaea) on different taxonomic levels (domain, phylum, order, family, genus) and the absolute number of these present in a specific sample community. This information was further organised into sector diagrams based on Phylum level (Fig. 21) and Class level (Fig. 22), which represent the distribution of these in the nine different microbial communities investigated. *Thaumarchaeota*, *Cloroflexi*, *Planctomycetes*, *Acidobacteria* and *Proteobacteria* were present in all samples, but there was a small variation in their overall presence to the community across treatments and baseline conditions. The phyla that constituted over 2% of the total community are presented in sector diagrams (Fig. 21 and 22).

The abundance of the domain archaea comprises 52% of the number of copies of 16S rRNA reads in the microbial community in the sample from the surface sediments from the CO₂ Experiment, and around 40% in the surface sediments from the Control treatment and Baseline conditions (Fig. 21, top panels). There was also a higher abundance of archaea in the sediment samples from the CO₂ Experiment (30%) at depth 3-4 cm, compared to the Control and Baseline sediments (hence 15% and 22%) (Fig. 21, middle panels). The relative abundance of reads of archaeal 16S rRNA decreased with increased sediment depth in all three treatments (CO₂ Experiment, Control and Baseline) to hence 15%, 14% and 22% at 6-7 cm depth (Fig. 21, lower panels).

Looking deeper into the CREST classification revealed that the dominating archaeal phyla belong to the *Thaumarchaeota* (Fig. 21). Comparing the taxonomy in the CO₂ Experiment,

the Control treatments and the baseline conditions there was a trend that the CO₂ Experiment sediment had a greater ratio of the *Thaumarchaeota* at 0-2 cm (52%) and 3-4 cm (30%) compared to Control (0-2 cm: 38% and 3-4 cm: 15%) and Baseline (0-2 cm: 41% and 3-4 cm: 22%). However, at 6-7 cm the relative abundance of *Thaumarchaeota* reads is very similar to the other samples (15%, 14% and 22%). The phyla *Cloroflexi*, *Planctomycetes*, *Acidobacteria* and *Proteobacteria* had a very similar distribution in the CO₂ Experiment, Control and Baseline samples.

Concerning the bacterial taxonomy in total, 55 bacterial phyla were identified in these marine sediments, and the largest ones were the *Cloroflexi*, *Planctomycetes*, *Acidobacteria*, *Bacteroidetes*, *Proteobacteria* and several candidate divisions.

Looking at phylum level differences in Control treatment versus Baseline conditions, which was only the adding of ¹³C labelled algae or not, the Control and Baseline taxonomic group distributions were very similar at all depths. This is an interesting finding as they are taken from different locations in the fjord, separated by a distance of 52 m (Fig. 3). The bacterial phylum *Planctomycetes* increase in number of copies of 16S rRNA with increased depth in the sediment, but there was not a difference between the CO₂ Experiment, Control and Baseline treatments (Fig. 21).

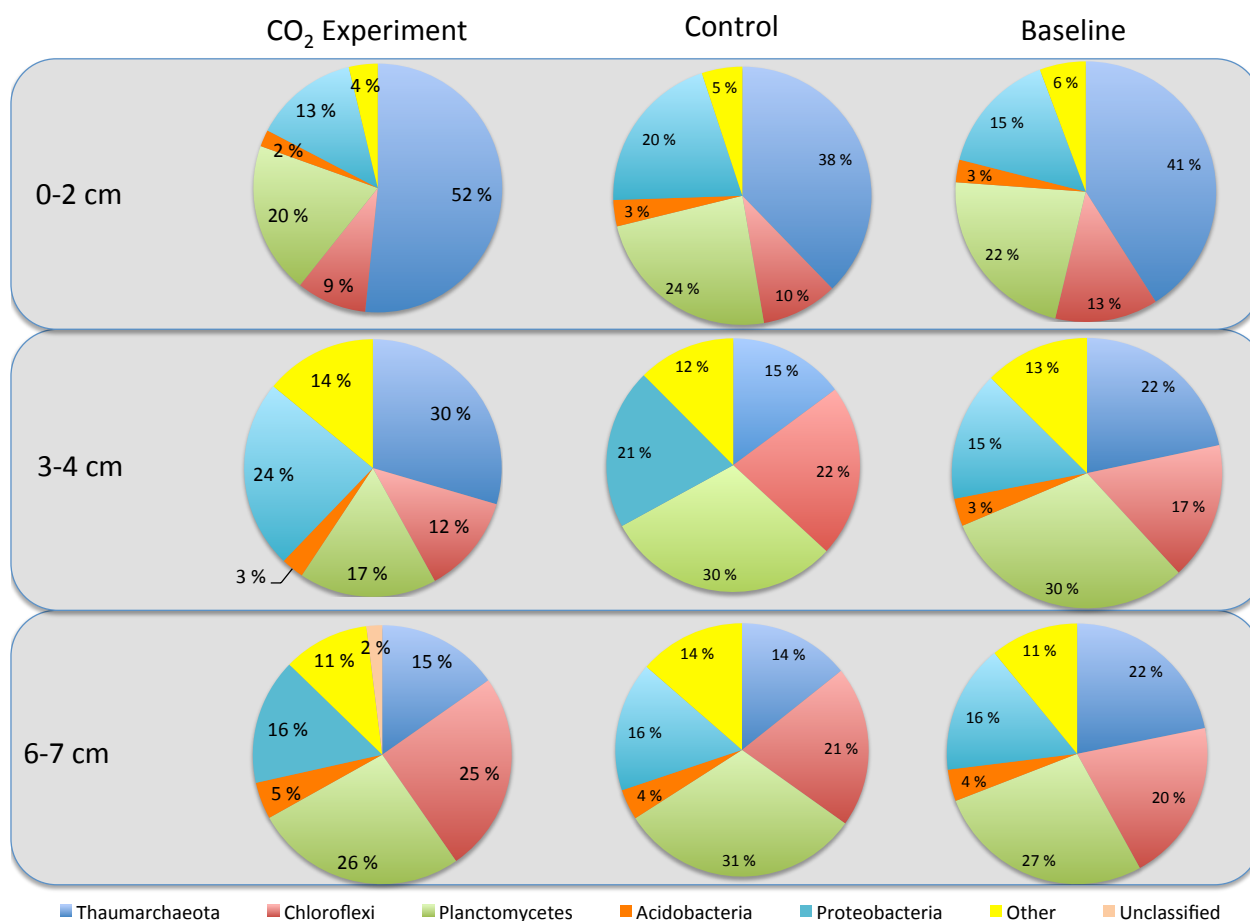


Figure 21: Overview of distributions of different phyla from 454 sequencing data that constitute more than 2% of total amplicon reads. The sediment depths are indicated to the left. From the top going down: the left row is the CO₂ Experiment (exposed to 12 000 μ atm pCO₂) community, middle row is Control community and right row is Baseline community structure of the active population. The sector group “Other” is a collection of phylum that constitutes less than 2% of the total number of amplicon reads. This group includes several candidate divisions, and known and unknown phyla of bacteria, which alone do not make up more than 2% of total number of amplicon reads. The group “Unclassified” is sequences that could not be classified by CREST to any deeper level than domain

Further relative abundance analyses were carried out on class level (Fig. 22). Concerning on the archaea, 12 different classes were represented. By far the most abundant was the Marine Group 1.1a that dominated the total active community in 0-2 cm horizon (51%) and 3-4 cm horizon (28%) in the CO₂ Experiment compared to Control and Baseline (38% in 0-2 cm and 14% in 3-4 cm depth in Control, and 41% in depth 0-2 cm and 21% in depth 3-4 cm in the Baseline treatment) (Fig.22). While at 6-7 cm the ratios between the CO₂ Experiment, Control and Baseline treatments were very similar for the Maring group 1.1a (15%, 14% and 21%, respectively).

Looking at the bacterial classes present in the microbial communities a total number of 107 classes were identified. And the most relative abundant bacterial classes were Caldilineae

(Cloroflexi), Anaerolineae (Cloroflexi), Physisphaerae (Planctomycetes), Planctomycetacia (Planctomycetes), Acidobacteria (class), Deltaproteobacteria (Proteobacteria), Gammaproteobacteria (Proteobacteria) (Fig. 22).

Sediments from the CO₂ Experiment treatment had fewer lineages from the phyla Cloroflexi, the classes Cadilineae and Anaerolineae, which were found in all samples, but samples from the Baseline treatment also had the classes Cloroflexi Subdivision 10 and 13 (Fig. 22). The classes Physisphaerae and Planctomycetacia, belonging to the phyla Planctomycetes, have similar distribution in the CO₂ Experiment, Control and Baseline (6% and 10% in the CO₂ Experiment treatment, 6% and 14% in the Control treatment, and 4% and 14% in the Baseline) in the top layer. Physisphaerae increase in activity with increasing depth (from 6%, 6% and 4% in the surface layer of all treatments to 13%, 15% and 12% in the bottom layer of all treatments) (Fig.22). Gammaproteobacteria has a steady ratio in all samples and in all depths (between 8% and 13%).

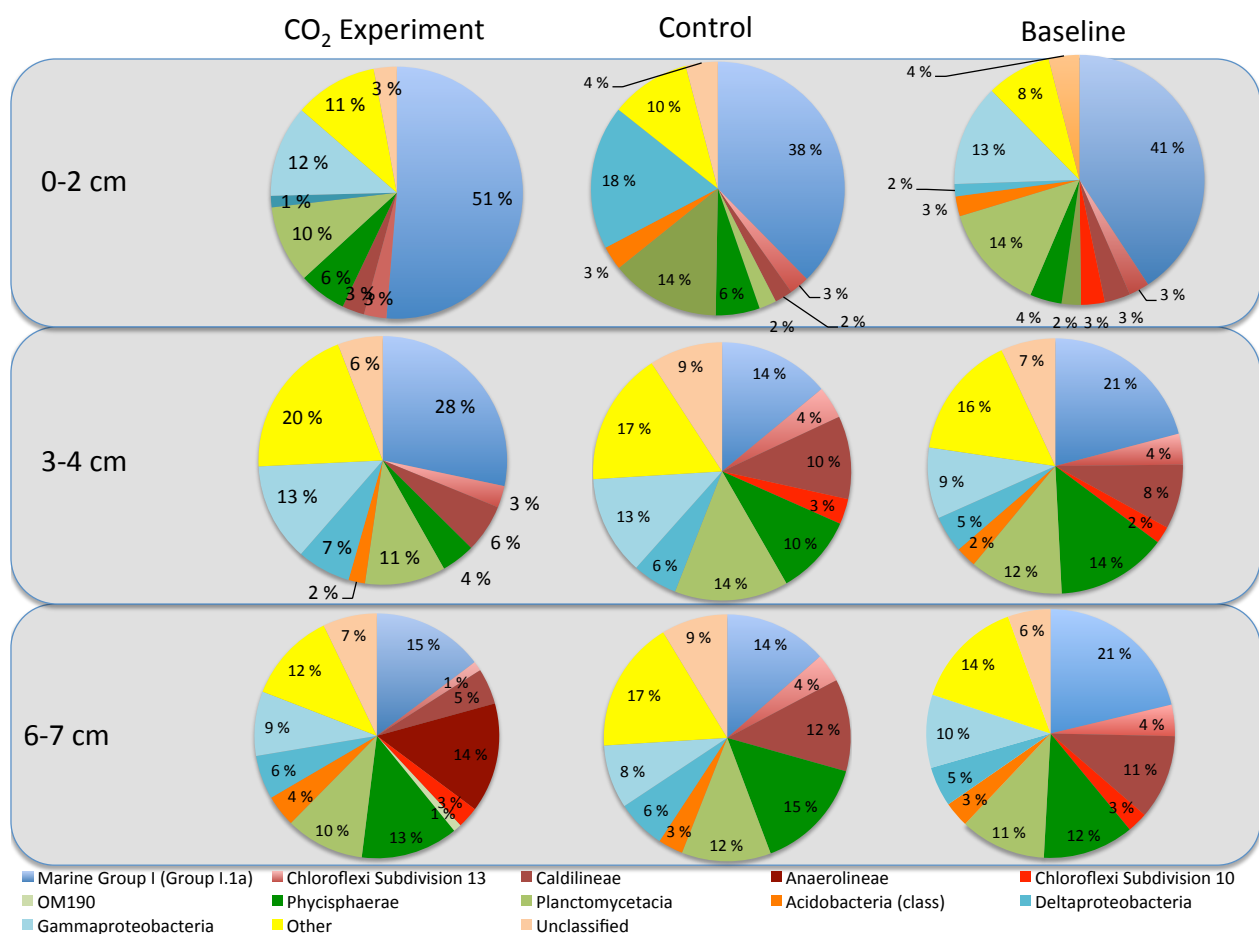


Figure 22: Overview of distributions of different classes from the 454 sequencing data. The sediment depths are indicated to the left. From the top going down: the left row is the CO₂ Experiment (exposed to

12 000 $\mu\text{atm pCO}_2$) community, middle row is Control community and right row is Baseline community structure of the active population. The sector group “Other” is a collection of classes that constitute less than 2% of the total number of amplicon reads. This group includes several candidate divisions, and known and unknown classes of bacteria, which alone do not make up more than 2% of total number of amplicon reads. The group “Unclassified” is sequences that could not be classified by CREST to a deeper level than domain.

It was not possible to proceed to lower taxonomic levels (order, family, genus), because in some lineages over half or all sequences are lost from class to order (can not be classified further than class), this would then give a wrong ratio of some orders if other orders were gone in the same sample because they could not be identified (Appendix Table IV).

Operational taxonomic units:

The richness or number of Operational Taxonomic Units (OTUs) demonstrates the lowest taxonomic level, which a sequence can be classified, and is the number of taxa in a given sample, or environment. These analyses can aid in understanding the environment and the function of the organisms living here. One file with all the sequencing data was created, and the list of OTUs was created by CREST. This is so we do not have to study all organisms present, because many of these are very little abundant, but rather focus on the organisms that dominate the active microbial community and therefore probably have a large impact on the environment. These OTUs will be further analysed by PCA.

4.3.2 Principal Component Analysis (PCA):

Principal Component Analysis (PCA) with centred log-ratio transformation was used to find potential patterns in the relative abundance 454 sequencing data. These are patterns not visible in the previous sector diagrams. In order to look for significant differences between the treatments and the baseline conditions, at all three sediment depths, separate PCA plots were made for phylum level, class level and OTU level. Five different principal components were analysed (PC1, -2, -3, -4, -5).

Interestingly, in the PC1/PC2 scatter plots of both phylum and class level, the samples belonging to the top layer, the 0-2 cm depth (points with blue colour), cluster together on the positive side of PC1, while the points representing different treatments at 3-4 and 6-7 cm depth cluster together on the negative side of PC1 (Fig. 23 and 24). It is therefore possible to assume that the PC1 is representing the depth gradient in the sediment and therefore the clustering is simply caused by the sediment horizons and are not related to the different

treatments. This gave indications that PC1/PC2 plots will not reveal changes due to the CO2 Experiment On phylum and class level.

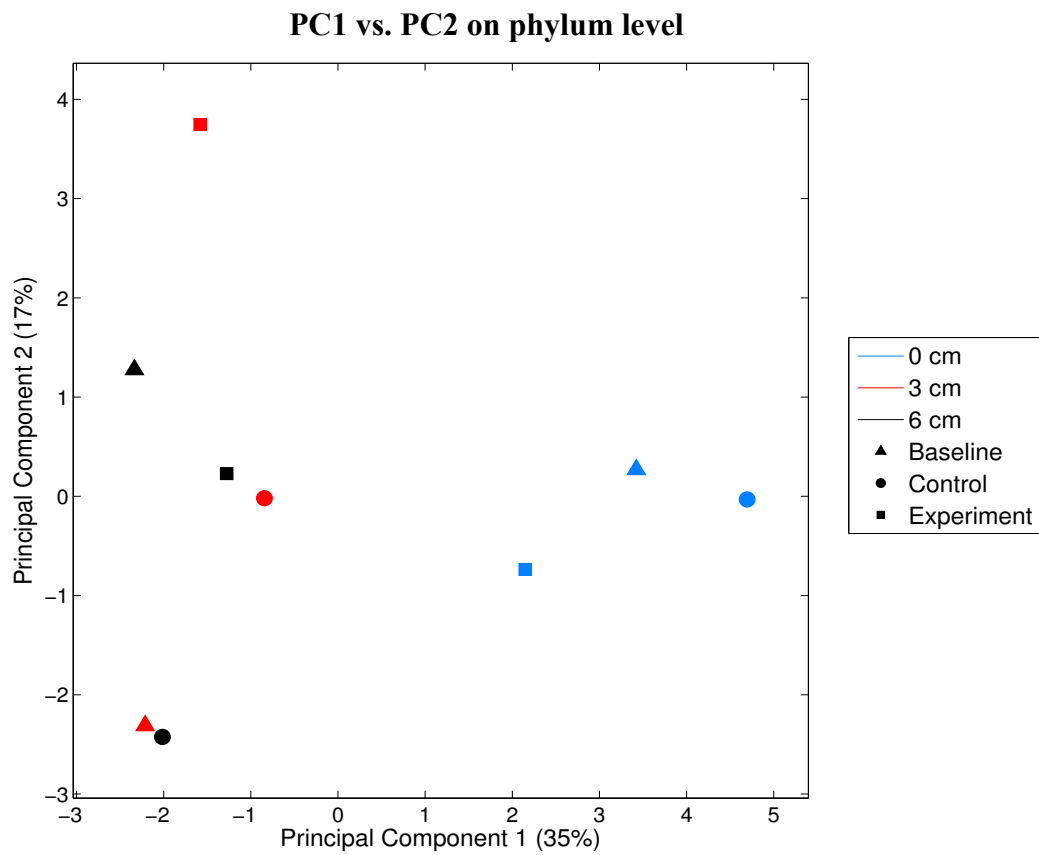


Figure 23: Scatter plot of the 454 sequencing samples on phylum level measured along the maximum variation axis, PC1 and PC2. The box on the right indicate the meaning of the colour and shape of the points in the plot.

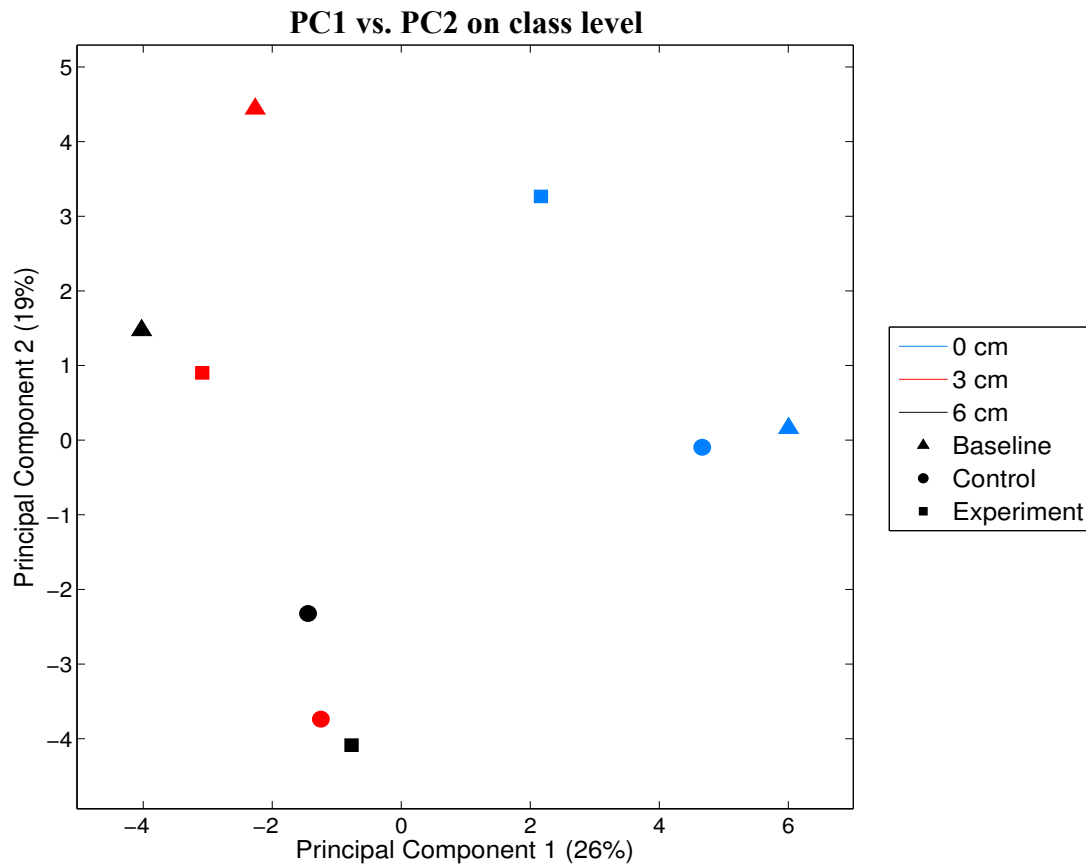


Figure 24: Scatter plot of the 454 sequencing samples on class level measured along the maximum variation axis, PC1 and PC2. The box on the right indicate the meaning of the colour and shape of the points in the plot.

Concentrating further on any potential impacts of the CO₂ Experiment at the phylum level, we did looked for specific pattern along any principal component axes (up to PC5) without finding any. However, on class level the data from the CO₂ Experiment samples cluster on the positive side of PC3, while the data from the Control and Baseline treatments cluster on the negative side of PC3 (Fig. 25).

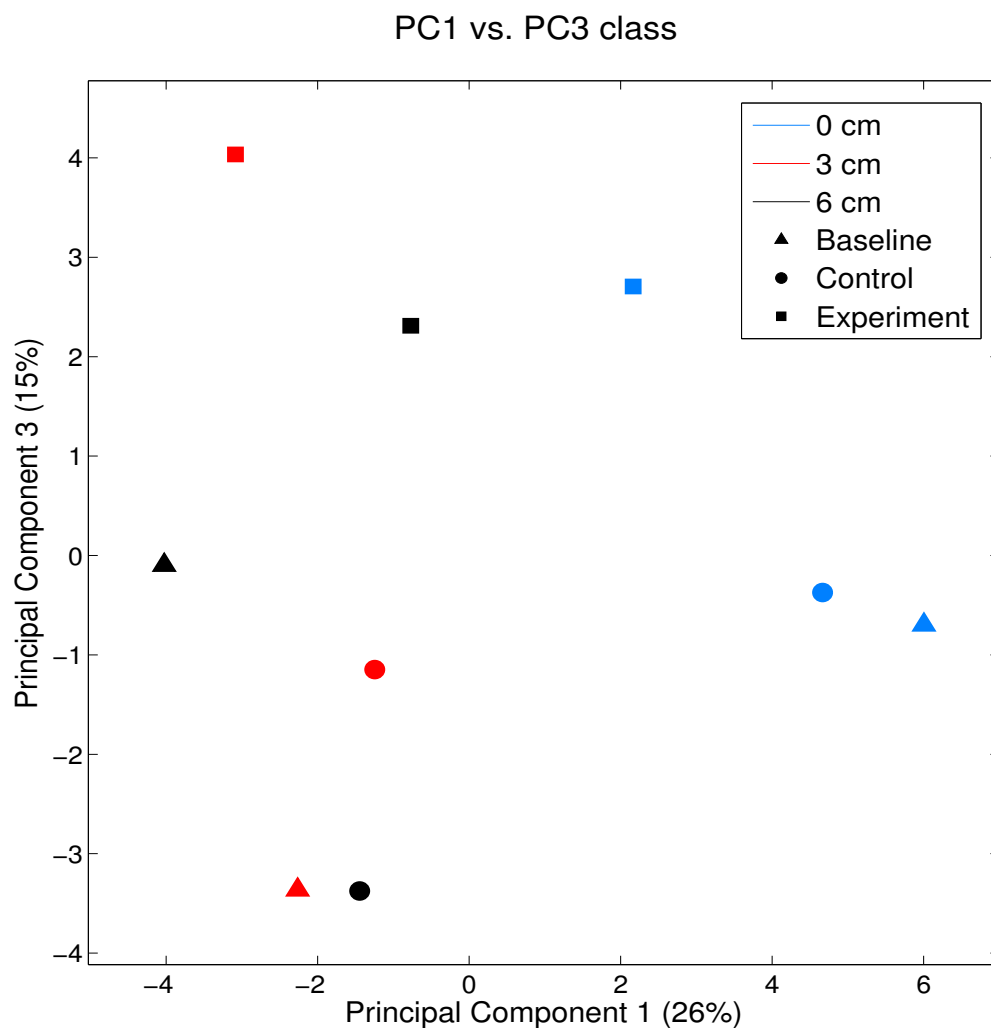


Figure 25: Scatter plot of the 454 sequencing samples on class level measured along the maximum variation axis, PC1 and PC3. The box in the upper right corner indicate the meaning of the colour and shape of the points in the plot.

Seeing that the class level relative abundance shows effect of all three sediment depths, made us look at plots on OTU level in order to find any distinct pattern between the treatments. The number of OTUs or richness demonstrates the number of taxa in a given sample or environment, which can be calculated in several different ways. There was in total 9279 OTUs detected in the 454 sequencing data, and the PCA plot was based on a <0.1% cut-off (excluded taxa that constitutes less than 0.1% of the total sequences). This resulted in a data set of 76 OTUs (Fig. 26). Plotting out the OTUs a new pattern along PC2 appeared, which is independent of depth (PC1). The samples from the CO₂ Experiment cluster separately from the Baseline/Control samples along the PC2. This pattern could occur because of the different treatments (CO₂ Experiment, Control and Baseline).

PC1 vs. PC2 on OTU level

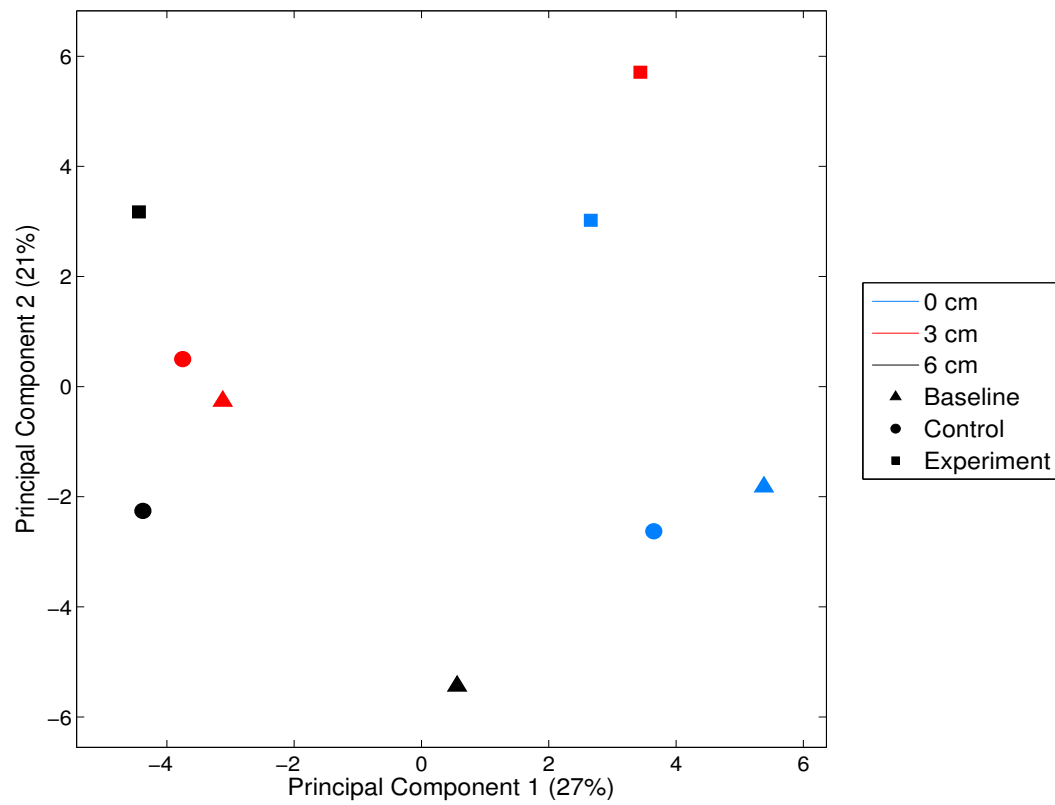


Figure 26: Scatter plot of the 454 sequencing samples on OTU level measured along the maximum variation axis, PC1 and PC2. The box on the right indicate the meaning of the colour and shape of the points in the plot.

5.0 Discussion:

5.1 Overview of Experiment

This thesis is a part of projects concerned with the safety around sub seafloor CO₂ storage and we wanted to see how a leakage from a CO₂ storage site would affect the microbial environment on the seafloor. In this experiment we used a benthic lander with two chambers to perform an *in situ* experiment where the sediment was exposed to CO₂ acidified seawater (2 000 or 12 000 µatm pCO₂) for 40 hours. The point was to give CO₂ acidified water to the sediment of chamber 1 and not to the chamber 2 and compare potential impacts on the microbial sediment community in the two. It was also the intention to give all CO₂ Experiments 12 000 µatm pCO₂, but in the last dive (RISCS4) both injections appeared to be incomplete for unknown reasons, although the injection was triggered. The result was that the sediment in RISCS4 chamber 1 and 2 was only exposed to 2 000 µatm pCO₂. The chambers was closed during the experiment so only the part of sediment and ocean water inside the chambers are affected. The focus of this thesis was to see how the bacteria and archaea are affected by the CO₂ acidification by using molecular methods giving data that could be used in statistical approaches. Several studies reveal that a higher CO₂ concentration/lowered pH has a significant impact on the living community in several habitats like soil (He *et al.*, 2010), deep ocean waters (Huesemann *et al.*, 2002) and marine sediments (Inagaki *et al.*, 2006, Widdicombe *et al.*, 2009).

The lander was lowered to the seafloor four times in the Byfjorden in Bergen in August/September 2011. The two lander chambers were equipped with sensors for temperature, pH and sediment oxygen consumption, which was registered and stored by the lander-attached computer unit. When the lander was back on deck the sediment and water samples for RNA extractions and other analyses were harvested (see section 3.0 Materials and Methods). Each of the lander dives lasted for 40 hours. The reason for using 40 hour elevated CO₂ exposure was that test runs had shown that during longer incubations, the oxygen levels inside the chambers became so low that the effect seen on the living community might come from lack of oxygen and not from the abrupt CO₂ acidification. Because of the short timeframe of the experiment RNA is a good parameter to study because it is rapidly produced and used in the cell, and is the best place to look for early changes. RNA can be a measurement of activity of microorganisms, because active cells produce RNA for growth

and metabolic activity and the 16S ribosomal RNA from the small subunit of the ribosome is heavily applied for taxonomic and phylogenetic classification and can be used for identification and quantification of microbial activity and community structure analyses (Poulsen *et al.*, 1993, Bremer *et al.*, 1996, Lanzen *et al.*, 2010). Altogether sediment of three chambers were exposed to CO₂ acidified seawater plus the ¹³C labeled dead algae, two chambers treated as Controls with only ¹³C dead algae added, and finally three chambers were nothing was added and thereby represents the Baseline conditions of the Byfjorden sediment. Because there is limited amount of parallels in the experimental setup, a challenge has been to avoid over interpret the statistical significance of the resulting microbial data. As described in Section 5.2 the marine sediment is a highly heterogeneous habitat, where there can be large natural variations in the sediment from different sites (Sebens, 1991).

5.2 Sediment as a habitat

The pH naturally decreases with sediment depth from around pH 8 in the sediment surface to pH 7 in deeper sediment horizons, but this can vary dependant on the grain size (Widdicomb *et al.*, 2009). This is due to biological residuals and geochemical species diffusing from below (Zhu *et al.*, 2006). A question is therefore if microorganisms deep in the sediment would be as much affected by a decrease in pH by the abrupt CO₂ acidification as the upper sediment cm would. Oxygen in sediments becomes depleted as you go deeper, therefore microorganisms living deeper in the sediments use alternative electron donors to survive, and therefore they may not be affected by the lowered pH. Factors in the sediment that can disturb potential changes following the CO₂ acidification are important to recognise; First, bottom dwelling macrofauna, bioturbation and bioirrigation can disturb the pattern of oxygen level and pH locally by stirring oxygen and other nutrients deeper into the sediments and this could give a higher microbial activity in these areas (Zhu *et al.*, 2006). Secondly, any decaying animal within the sediment or landing on the sediment could also give more food to the local bacteria and archaea in the sediments and could affect the microbial activity independently of CO₂ acidification or not. Third, the decomposing could also cause the pH to decrease significantly (Zhu *et al.*, 2006).

Another factor needing to be considered was an experimental issue with the lander chamber construction. When the lander was retrieved from the water and transferred to the boat deck, large amounts of seawater was running out of the chambers. This might have washed away or mixed/stirred the fine-grained top sediment resulting in sediment and microbes simply being

washed away with the water. There are unfortunately no methods we in retrospect could use to determine how much sediment was removed/stirred and what the effects this might have on our data (see discussions below).

5.3 Number of copies of 16S rRNA genes measured by qPCR

The 16S rRNA gene is the most used gene for taxonomical and phylogenetic analysis and identification, and for the work in this thesis, the 16S rRNA genes were used to determine if there were any differences between sediment samples exposed to abrupt CO₂ acidification and those not exposed. Classifying prokaryotes from environmental samples using their genome is more reliable than phenotypic methods (for example Gram staining and studying the microorganisms in a microscope), and the 16S rRNA gene is suitable as a molecular marker because of its properties (Case *et al.*, 2006). The number of copies of 16S rRNA in this thesis is referred to as the level of microbial activity because active cells produce RNA for growth and metabolic activity (Poulsen *et al.*, 1993, Bremer *et al.*, 1996). The basis for the whole study was therefore RNA extractions directly from the seafloor sediment, followed by synthesis of the complementary DNA strand (cDNA synthesis). In our study, the number of copies of 16S rRNA was measured by a qPCR approach, using separate set-ups for the bacterial (Fig. 12) and the archaeal analyses (Fig. 13). In addition to the top cm layer, three more sediment horizons were analysed in all sediments treated with CO₂-acidified sea water/¹³C algae (CO₂ Experiment), treated with the ¹³C algae only (Control), as well as the Baseline conditions.

Concerning the bacterial 16S rRNA copy numbers in the overall experiment, there was between 10⁷ (Baseline) and 10¹⁰ (CO₂ Experiment) number of copies of the 16S rRNA per gram sediment in the surface layer of the sediment (Fig. 12). Looking at the top layer in the three chambers receiving the pCO₂ treatment, there was a large spread in bacterial number of 16S rRNA, the chambers of RISC4 exposed to 2 000 µatm pCO₂ both being 10⁷, while the sediments of RISC2 chamber 1, exposed to 12 000 µatm pCO₂ was 10¹⁰ (Fig. 12A). For archaea the same trend was seen in the CO₂ Experiment, the number of 16S rRNA from RISC 2 chamber 1 was 10⁸ number of 16S rRNA, and RISC4 both chamber was 10⁵ number of 16S rRNA, which was not different from the 16S rRNA numbers from the Control/Baseline qPCR data (between 10⁵ and 10⁶ number of 16S rRNA). This shows that the exposure of 2 000 µatm pCO₂ had little impact on the microbial activity, while lowering the pH with over 1 unit gave a clear increase in activity.

The overall trend of the number of copies of 16S rRNA obtained from qPCR was that the number of 16S rRNA (bacteria and archaea) decreased with increased depth (Fig.14) to between 10^5 (Baseline) and 10^7 (CO_2 Experiment) number of bacterial 16S rRNA and at depth 6-7 cm (Fig 12). The same trend was observed for archaea, but the number of copies of 16S rRNA per gram sediment was a few magnitudes lower (between 10^4 - 10^5 number of archaeal 16S rRNA at depth 6-7 cm) (Fig. 13). This was expected, and normal for marine sediments (Jørgensen et al., 2012).

In some of the dives and in some depths there was a large spread within the data (Fig.12 and 13). And heterogeneity in the sediment can be a possible explanation for the wide spread in qPCR numbers in the samples. If the different dives are plotted together instead of the treatments (RISCS1 plotted together in one graph, and RISCS2 in a separate graph, and RISCS4 in one graph) then the 16S rRNA numbers follow a more similar pattern, within the same dive (Appendix Figure 1). But there is still quite some difference between some of the 16S rRNA copy numbers from the same depth. This could indicate that the number of 16S rRNA varies substantially from location to location on the seafloor, not only between the dives, but also between the two chambers on the same dive (60 cm apart). The high number of copies of the 16S rRNA gene for both bacteria (1.44×10^{10}) and archea (3.7×10^8) in the top layer of the sediment in RISCS2 Chamber 1 could be because the sediments in this chamber was exposed to lowest pH (12 000 $\mu\text{atm pCO}_2$), compared to both chambers of the RISCS4 dive, which was exposed to only 2 000 $\mu\text{atm pCO}_2$. The conditions in RISCS2 chamber 1 could have caused some microorganisms or animals to struggle and die off, and some other bacterial or archaeal lineages to benefit from this, and become increasingly active, which could have led to the high sediment oxygen consumption that was measured in this chamber (See section 5.4).

On the other hand, some of the chambers (RISCS1 Chamber 1 and 2 and RISCS4 Chamber 1 (CO_2 Experiment) had a lower number of copies of 16S rRNA in top layer (0-1 cm) than in second layer (1-2 cm), which was not expected (expected to be highest in the top layer). In these chambers it looks as if there has been a shift or displacement, where the second layer (depth 1-2 cm) is actually the top layer. Then the number of 16S rRNA would be more similar between the depths (Fig. 12 and 13).

5.4. pH and sediment oxygen consumption (SOC)

The pH used in this thesis was measured in all the seven water syringes (Table 1) immediately after the lander was on deck by Dr. Laila J. Reigstad. The sediment oxygen consumption (SOC) was measured by an electrode inside the chamber, and afterwards calculated to flux of O_2 $mmol\ m^{-2}\ d^{-1}$ (Table VII). The pH measured from the syringes was the lowest in the CO_2 Experiment of RISC2 Chamber 1, with pH measured to 6,98 (average of syringe 2-7 Table I) in RISC2 Chamber 1, and interestingly it was also here the sediment oxygen consumption (SOC) was the highest ($10,94\ mmol\ m^{-2}\ d^{-1}$), and the copy number of 16S rRNA is the highest for both archaea and bacteria in the top sediment layer (Fig. 12 and 13). The conditions were different in the two other chambers that received the CO_2 Experiment treatment (RISC4 chamber 1 and 2); the pH from the syringes were on average measured from syringe 2-7 to 7.36 in both chambers, the SOC was hence 3.3 and 5.3 $O_2\ mmol\ m^{-2}\ d^{-1}$, which is not different from the recorded SOC in the Control chambers (Table VII), and the number of bacterial and archaeal 16S rRNA in the surface layer did not stand out or was any different from the chambers which received the Control or the Baseline treatment (Fig. 12 and 13).

It would be in the top layer that the microorganisms would notice the decrease in pH the most because they are in direct contact with the overlaying seawater. Since large changes in number of bacterial and archaeal 16S rRNA were not detected in the CO_2 Experiments 0.5 pH unit below normal seawater (RISC4 Chamber 1 and 2 (both CO_2 Experiment), it appears that a small decrease in pH does not have a great impact on the number of bacterial and archaeal 16S rRNA. However, my results suggest that after approximately 1 pH unit drop (Table VII) it starts to have a greater impact on the microorganisms in the surface sediments (RISC2 chamber 1).

The high rate of SOC measured in RISC2 Chamber 1 (CO_2 Experiment exposed to $12\ 000\ \mu atm\ pCO_2$) could also be linked to the event of receiving CO_2 acidified water. In RISC4 Chamber 1 and 2 (both CO_2 Experiment, exposed to $2\ 000\ \mu atm\ pCO_2$) the sediment oxygen consumption (6.0 and $4.1\ O_2\ mmol\ m^{-2}\ d^{-1}$, respectively) was not different from the chambers that received the Control and Baseline treatment (3.3 and $5.3\ O_2\ mmol\ m^{-2}\ d^{-1}$, respectively) (Table VII). Since a high rate of SOC was not measured in any other chambers than RISC2 Chamber 1, it is likely that it is connected to the event of receiving CO_2 acidified water. Because a pH drop of 1 unit (like in this chamber, going from about 8,0 to 6,98) could be stressful on the microbes living in the sediment surface, this could be linked to the higher

activity of bacteria and archaea (qPCR data from RISC2 Chamber 1), which could come from a higher rate of respiration, which is measured by the increased sediment oxygen consumption in RISC2 Chamber 1.

5.5 T-test and regression

The purpose of the t-test was to test if there was a significant difference between the qPCR data from the CO₂ Experiment treatments and the qPCR data from the Control/Baseline treatment. Separate tests were done for the different depths, and for bacterial and archaeal 16S rRNA data. The qPCR data from the three CO₂ Experiments was joined into one group to make the t-test more solid. The same was done for the qPCR data from Control and Baseline. The t-test results showed no significant relationship between the number of bacterial and archaeal 16S rRNA from the CO₂ treatments and the Control treatment and Baseline conditions at any depths (P-values ≥ 0.05). The regression analysis of the number of copies of bacterial and archaeal 16S rRNA from all chambers plotted against pH (separate for all depths) also showed no statistical correlation (R^2 is closer to 0).

The regression of SOC plotted against number of copies of 16S rRNA show a strong relationship in top layer (0-1 cm) (Fig. 19 and 20). 64% of the variation in SOC is explained by the number of bacterial 16S rRNA genes and 90% of the variation in the sediment oxygen consumption is explained by the number of archaeal 16S rRNA genes. This indicates that an increase in microbial activity caused an increase in the SOC. There is no correlation between SOC and number of microbial 16S rRNA genes in deeper sediment layers, so it appears that acidification did not modify microbial processes dependant of oxygen below the surface layer layers (Fig. 19B-D and 20 B-D). It is the number of copies of 16S rRNA from RISC2 Chamber 1 in the surface sediment that contributes to the correlation in Figure 19 and 20, without it, the R^2 would be significantly lower.

5.6 Microbial communities

The 454 pyrosequencing method and bioinformatical approach identified the 16S rRNA pool in the samples, i.e. who is active in the sediment at time of analysis. For the 454 analyses, a universal primer set (detecting both archaea and bacteria 16S rRNA) were used on three different sediment horizons in three selected chambers: CO₂ Experiment (RISC2 Chamber 1, exposed to 12 000 $\mu\text{atm pCO}_2$), Control treatment (RISC2 Chamber 2) and Baseline conditions (RISC3 Chamber 2), altogether nine samples. The data set consisted of a total of

65 832 reads in all the nine samples, and the number of reads ranged between 3 000 and 14 500 reads in the separate samples. This is a very large variation between number of reads in each sample, and this is why we work on *relative* abundance data (instead of *absolute* abundance). Principal Component Analysis (PCA) was used to find other trends in the 454 sequencing data (see section 1.6.3), that otherwise could not be seen in the sector diagrams (Fig. 21 and 22).

When looking at all the treatments and all three sediment horizons investigated, the most abundant phyla identified by the 454 pyrosequencing data of the 16S rRNA amplicon, were *Thaumarchaeota*, *Cloroflexi*, *Planctomycetes*, *Acidobacteria* and *Proteobacteria* (Fig. 21). When looking at the seafloor community, these phyla are those that are expected in deep-sea sediments (Jørgensen et al., 2013). This means that the CO₂ Experiment did not change the fundamental community partners after 40 hours of 20 000 µatm pCO₂. Despite these very diverse phyla with representatives in many habitats both on land and in the ocean (Garrity *et al.*, 2001, Quaiser *et al.*, 2003), very few deep-sea prokaryotes have been cultured and identified and therefore their metabolisms are not known, and we do not know how they impact their environment.

Moving from the more overall community parameters, to the effects of the CO₂ Experiment treatment, a trend in the relative abundance of the *Thaumarchaeota* phylum was seen (Fig. 21). Focusing on the top sediment layer, the *Thaumarchaeota* relative abundance was 52% in the CO₂ Experiment treatment, and 38% and 41% in the Control treatment and Baseline conditions (Fig. 21, top panels). In the middle sediment layer (3-4 cm) The relative abundance of *Thaumarchaeota* decreased to 30% in the CO₂ Experiment and 15% and 22% in the Control treatment and the Baseline conditions. In the deepest analyzed sediment layer (6-7 cm) the relative abundance of *Thaumarchaeota* was 15% in the CO₂ Experiment and 14% and 22% in the Control and Baseline treatment. The relative abundance of *Thaumarchaeota* decreases with increased depth, this could be because they are ammonia-oxidizing archaea, which means that they use O₂ in their metabolic pathway (will be further explained below). As the oxygen level decreases downwards in the sediment, fewer *Thaumarchaeota* can be sustained.

Concerning the 454 relative abundance data on class level (Fig 22), the number 16S rRNA genes of the class *Marine group I(1a)* belonging to the phylum *Thaumarchaeota* in the CO₂

Experiment treatment was higher in the top layer (52%) compared to the top layer of the Control and the Baseline treatments (Hence 38% and 41%), and decreased in abundance to 6-7 cm depth (Fig. 22). The relative abundance of *Marine group 1(1a)* decreases with increased sediment depth from 28% at depth 3-4 cm to 15% at depth 6-7 cm in the CO₂ Experiment, and 14% at depth 3-4 cm and 6-7 cm in the Control treatment, and 21% at depth 3-4 cm and 6-7 cm in the Baseline conditions. None of the reads belonging to the domain Archaea could be identified on genus level in the 454 pyrosequencing method. Thus, the only cultured and characterized archaea is the *Nitrosopumilus maritimus* from Marine Group 1a collected from a marine aquarium tank, which is an ammonium oxidizing archaea (Walker *et al.*, 2010).

The *Thaumarchaeota* is a newly established, deep-branched phylum and is one of the most abundant Archaea on Earth (Walker *et al.*, 2010). This archaeal phylum is the only one known to have aerobic ammonia-oxidizing metabolisms, which convert reduced inorganic nitrogen, like ammonium to oxidized inorganic nitrogen, like nitrite, in a process called nitrification. Their extremely low oxygen and ammonium demands can be the reason for why they are so dominant in the open ocean sediments, and therefore also important for the global nitrification (Pester *et al.* 2011). But what could be the reason for the increase in activity of this archaeal lineage? One explanation could be that some microorganisms/animals in the sediment may have not been able to handle the decrease in pH caused by the injection of CO₂ acidified water and started dying and/or decomposing. Bacteria and fungi are mainly responsible for decomposing dead organic material to ammonium (NH₄⁺), by aerobic or anaerobic processes known from the nitrogen cycle (Konhauser, 2007). If there was a rise in ammonium from dead and decaying animals thus may have then been beneficial for the *Thaumarchaeota*, which gain energy from transforming ammonium (NH₄⁺) to nitrate (NO₂⁻) (Fig. 23), a process called ammonium-oxidation, and can therefore be the probable cause of the increase in activity of this archaeal lineage when exposed to lowered pH due to CO₂ acidification. The rise in *Thaumarchaeotal* activity is in contrast to the results of Huesemann *et al.*, (2002) who showed that the nitrification rate decreased by 50% with decreasing pH in association with mimicking deposition of CO₂ directly into deep ocean basins. But it is important to bear in mind, however, that the 454 sequencing data was only carried out on one sample, which was exposed to high levels of CO₂. Thus, further sampling is required to understand if a rise in *Thaumarchaeotal* activity was enhanced by high CO₂ conditions or if this single observation is an outlier.

The second most abundant phylum in number of 16S rRNA belongs to the bacterial phylum *Planctomycetes* (Fig. 21). It was not a clear difference in number of reads in the CO₂ Experiment compared to the Control/Baseline treatment in any of the depths. The highest number of reads belonged to the Planctomycetes was found at 3-4 cm and 6-7 cm depth in the sediment and ranged from 30% in the Control and Baseline treatment and 17% in the CO₂ Experiment at 3-4 cm depth, and 26% (CO₂ Experiment) to 31% (Control) at depth 6-7 cm. In the surface sediments the relative abundance of Planctomycetes decreased to 20% (CO₂ Experiment), 24% (Control) and 22% (Baseline). *Planctomycetes* is a widespread and a deep-branched phylum within Bacteria. Characteristics of this phylum are aerobic and anaerobic, Gram-negative, chemoheterotrophic bacteria, which lack peptidoglycan in their cell walls. Their cell morphology can be coccoid, ovoid and pear-shaped and they can reproduce by budding (Neef *et al.* 1998, Freitag *et al.*, 2003). Since the *Planctomycetes* can be anerobic it is possible that it is these that increase in relative abundance with increased depth.

On class level there were two classes belonging to the domain *Planctomycetes* that dominated in number of reads, these were *Physiphaerae* and *Planctomycetacia* (Fig. 22). The number of reads belonging to the class *Planctomycetacia* was consistent in all the three different treatments and all the depths. While the number of reads belonging to the class *Physiphaerae* increased with increased depth. But a difference between the different treatments could not be identified in any depths. The other bacterial phyla (*Cloroflexi*, *Acidobacteria* and *Proteobacteria*) and bacterial classes (*Caldilineae*, *Anaerolineae*, *Physiphaerae*, *Planctomycetacia*, *Acidobacteria* (class), *Deltaproteobacteria*, *Gammaproteobacteria*) identified by the 454 pyro sequencing method did not stand out in connection with the different treatments.

To sum up so far, the rise in number of 16S rRNA within the *Thaumarchaeota* in the CO₂ Experiment compared to the Control and the Baseline treatment may have been caused by the addition of CO₂ acidified water. This is because the samples used for the 454 sequencing are from RISC2 Chamber 1, where the lowest pH (6,98 in the overlying seawater), highest SOC (10,94 O₂ mmol m⁻² d⁻¹) and highest number of both bacterial and archaeal 16S rRNA copy numbers were recorded (Fig. 12A and 13A). We could then assume that all these observations were connected. Comparing the 454 data to the qPCR in terms of relative abundance could have been useful, but since the data was analysed from RNA not DNA and different primers were used in the two analyses, it was not possible to compare these two data sets with each

other. The closest study to this thesis is the article published by Morozova *et al.*, (2011) on how the microbial community in a saline aquifer changes after injection of CO₂ (Ketzin, Germany). Their study was conducted on DNA level and they used FISH, Single-Strand-Conformation Polymorphism (PCR-SSCP) and Denaturing Gradient Gel Electrophoresis (DGGE) to characterize the microbial community, and found that the microbial community was significantly influenced by the CO₂ injection. The community changed from a chemoorganotrophic to a chemolithotrophic population and that sulphate reducing bacteria was replaced with methanogenic archaea (Morozova *et al.*, 2011). In the study by Huesemann *et al.*, (2002) they collected ocean water and conducted their experiment in tanks applying the physical properties of a deep ocean waters and monitored the nitrification rate when exposing the tank to lowered pH by CO₂ acidification. And they found that the nitrification rate was halved when the pH decreased to 7, and almost non-existent when the pH was 6, and below this the marine microbial growth was negatively affected (Huesemann *et al.*, 2002). This is though not directly comparable to our lander data because we look at sediment communities, and not the community of the water masses.

5.6.3 Principal Component Analysis (PCA):

The PCA plots on phylum and class level both appear to show a weak depth gradient along PC1 (Fig. 23 and 24), where the samples from the surface sediments cluster together on the positive side of PC1 and the samples from 3-4 cm and 6-7 cm depth gather on the negative side of PC1. But it is not that the microbial populations are different at different depths in marine sediments, which is the focus in this thesis; it is rather a confirmation that the 454 sequencing data corresponds with previous marine sediment research and makes the results more trustworthy. On the other hand, a PCA plot on class level of PC1 against PC3 detected a weak pattern suggesting that there is a difference between the treatments on class level; the data from CO₂ Experiment cluster separately from the other data (Control/Baseline) along PC3 (Fig. 25, squares). Interestingly, this community clustering of all three sediment depths indicate that the CO₂ Experiment had effect on class level on all depths.

On the other hand in the PCA plot on OTU level show that there was a difference between the samples that were exposed to CO₂ acidified water (CO₂ Experiment of exposure to 12 000 µatm pCO₂) and those that received the Control/Baseline treatment (Fig. 26). Unfortunately, what exactly the difference was remains to be unknown. Although, we did not anticipate that the sample from depth 6-7 cm from the CO₂ Experiment would clustered together with depth

0-2 cm and 3-4 cm along the PC2 axis, which is interpreted as the “treatment” gradient. Together with the PC1/PC3 plot on class level (Fig. 25), it looks like the effect of the CO₂ Experiment is spread all the way down to 6-7 cm depths. A reason for this could be macrofaunal burials.

6.0 Conclusion:

There were three chambers exposed to CO₂ acidified water during the lander experiment, and of these three a special notice is brought to RISC2 chamber 1, where the effect of the 40-hour exposure to CO₂ acidification of 12 000 µatm pCO₂ showed an impact. Here, we measured the lowest pH in the overlaying water (6.98), the highest level of microbial activity (number of bacterial and archaeal 16S rRNA), and the highest SOC (flux O₂ mmol m⁻² d⁻¹). This could indicate that a pH drop of 1 unit (from pH 8.0 to 7.0) has a greater effect on the microbial community in deep-sea sediments. In both chambers of the RISC4 dive (exposed to 2 000 µatm pCO₂) showed that a decrease in 0.5 pH unit from normal seawater had little impact on the measured parameters. The conditions in these two chambers were more similar to the Control and Baseline chambers.

The regression of number of 16S rRNA plotted against SOC showed that there was a correlation between these two variables; 64% of the variability in SOC can be explained by number of bacterial 16S rRNA, and 90% of the variability in SOC can be explained by number of archaeal 16S rRNA, in the surface sediment (0-1 cm depth) (Fig. 19 and 20). It is mainly the data from RISC2 Chamber 1, which contribute to the correlation.

However, there was not found a significant correlation between pH and number of copies of 16S rRNA (Fig 17 and 18). The PCA plot of qPCR data versus depth (Fig. 14) detected a depth gradient pattern in the number of copies of microbial 16S rRNA, where the top layers (average of 0-1 cm and 1-2 cm) clustered separately from the lower sediment depths (3-4 cm and 6-7 cm depth) (Fig 14).

The 454 sequencing data showed that the archaeal phylum *Thaumarchaeota* dominated the active microbial community in the sediments, and especially high 16S rRNA amplicon reads were detected in the samples from the CO₂ Experiment (52%) compared to the Control/Baseline treatments (38% and 41%, respectively) (Fig. 21). Looking on the class level of *Thaumarchaeota*, it was the *Marine Group 1(1a)* that dominated the active microbial community, in the surface layer of the sediment (0-2 cm). This was also especially in the samples from the CO₂ Experiment (51%), compared to Control treatment (38%) and the Baseline conditions (41%) in the surface layer (Fig. 22). This could be because the *Thaumarchaeota* are ammonia oxidisers, and ammonia is produced in the process of decaying

animals/microorganisms. Other CO₂ acidification experiments show an increased portion of mortalities among meio/macrofauna, and in present study we therefore expected a higher rate of decay and thereby a higher concentration of ammonia for *Thaumarchaeota* to use.

The PC1/PC2 PCA performed on the CREST output of the 454 data first of all showed a weak depth gradient along PC1 on phylum level and on class (Fig. 23 and 24). Second, there was also picked up a weak pattern where the data from the CO₂ Experiment clustered separately from the data from Control and Baseline treatment on class level (along PC3) and OTU level (along PC2) (Fig. 25 and 26), which could indicate that there is a difference between the microbial community from the CO₂ Experiment sediment compared to Control/Baseline sediments.

However, because of few replicates it can be difficult to draw conclusions out of this, especially for the 454 data, which there is only one replicate per depth of each treatment. It is difficult to tell if the observations summarized above are due to heterogeneity or “patchiness” in the sediment or that they are trends connected to exposure of CO₂ acidified water. This research is definitely one step further in understanding how the microbial communities responds to elevated CO₂ in marine environments, but there is still a lot remaining to understand the full picture on this relevant topic in today’s society.

7.0 Further Studies:

The study presented in this thesis was only conducted on RNA level. It could be interesting to compare the qPCR data at the RNA level to a study at the DNA level (cell count by qPCR). This would answer if the cells became more or if they just became more active in response to the CO₂ Experiment.

A study on functional genes in the habitat is important to investigate because it will allow us to know what metabolic pathways will be affected by a CO₂ leak from a CO₂ storage site. It would be interesting to look into the *DsrB* and *AprA* genes involved in sulphate reducing and sulphate oxidizing bacteria as well as genes involved in nitrification. This was supposed to be included in this thesis, but there was not enough time.

The limitation of this experiment was the few replicates. To improve the statistics of the experiment there are three different levels where number of replicates could be increased; first more of the lander dives, to obtain more than one site exposed to 12 000 µatm pCO₂. Second, more cores could be taken from each chamber, and the third could be to analyse more samples per depth. This would significantly improve the strength of the statistical tests. On the other hand, what would also be interesting to investigate is what happens when the sediments are exposed to elevated CO₂ levels for more than 40 hours. However, this would require a total different experimental setup than in this study.

A geochemical pore water analysis could also be interesting to include to gain insight into the chemical residuals in the sediment and exploring how these are linked to the microbial community structure and how these are change during a CO₂ leakage event. The pore water was extracted from the sediment by Dr Laila Reigstad, and >20 different geochemical components were measured by Professor Ingunn H. Thorseth, but these data were not a part of this Master work.

This study is only focussed on prokaryotes, but there are a lot of eukaryotes in marine sediments, like fungi and Protista, which could impact the sediment habitat, and also be affected by the CO₂ treatment. Additionally, it would be interesting to investigate the viral

community. In this project the viral numbers were determined by flow cytometry (Dr. Ruth Anne Sandaa), but these numbers are not a part of this master study.

If another similar experiment should be performed, it would be interesting to expose the environments inside the chambers to different amounts of CO₂ (different pH levels). It would be possible to investigate what amounts of CO₂ the microorganisms could not handle or cope with.

References:

- 454 Life Science Corporation, A Roche Company, Branford. 454 System Guidelines for Amplicon Experimental Design (2011). p.: 30-34.
- Ambion® RNA reagents and consumables, Life technology corporation (2012). <http://www.invitrogen.com/site/us/en/home/brands/ambion.html>
- Atsushi Ishimatsu, Takashi Kikkawa, Masahiro Hayashi, Kyoung-Seon Lee and Jun Kita (2004) Effects of CO₂ on Marine Fish: Larvae and Adults.
- Bjørlykke, Knut., Hellevang, Helge., Aagård, Per (2011) Konsekvensene av et surere hav. Institutt for Geofag, UIO.
- Bremer, H. and Dennis, P.P. (1996) Modulation of Chemical Composition and Other Parameters of the Cell by Growth Rate. *Escherichia coli* and *Salmonella*: Cellular and Molecular Biology, pp. 1553-1569.
- Case, R. J., Boucher, Y., Dahllöf, I., Holmström, C., Doolittle, WF., Kjelleberg, S. (2006) Use of 16S rRNA and *rpoB* Genes as Molecular Markers for Microbial Ecology Studies.
- Coffin, R.B., Montgomery, M.T., Boyd, T.J., Masutani, S.M. (2004) Influence of CO₂ sequestration on bacterial production. *ELSEVIER*, pp 1511- 1520
- D'Hondt, S. Jorgensen, B.B., Miller, D.J., Batzke, A., Blake, R., Gragg, B.A et al. (2004) Distributions of microbial activities in deep seafloor sediments. *Science* 306: 2216-2221.
- Eiken, O., Ringrose, P., Hermanrud, C., Nazarian, B., Torp, T.A., Høier, L. (2010) Lessons learned from 14 years of CCS operations: Sleipner In Salah and Snøhvit. Elsevier.
- He, z., Xu, M., Deng, Y., Kang, S., Kellogg., L. Wu, L., Van Nostrand, J.D., Hobbie, S.E., Reich, P.B., Zhou, J. (2010) Metagenomic analysis reveals a marked divergence in the structure of belowground microbial communities at elevated CO₂. *Ecology Letters* **13**:564-575
- Fischer, J.B., Matisoff, G. (1981) High resolution pH profiles in recent sediments. *Hydrobiologia* 79, 277-284.
- Freitag, T.E., Prosser, J.I. (2003) Community Structure of Ammonia-Oxidizing Bacteria within Anoxic Marine Sediments. *AEM*. Pp 1359-1371
- Fry, C.J., Parkes, R.J., Cragg, P.A., Weightman, A.J., Webster, G. (2008) Prokaryotic diversity and activity in deep seafloor biosphere. *FEMS Microbiol Ecol* 66: 181-196.
- Garrity, GM., Holt, JG. 2001, Phylum BVI. Chloroflexi *phy. Nov.* Bergey's Manual of Systematic Bacteriology: p. 427-446
- Grassle, J.F. (1989). Species diversity in Deep-sea Communities. *Trends in Ecology and Evolution*. Pp. 12-15.

- Glud, RN. (2008) Oxygen dynamics in marine sediments. *Marine Biology Research*.
- Gupta, R. (2000) The phylogeny of proteobacteria: relationships to other eubacterial phyla and eukaryotes. *FEMS Microbiology Reviews*.
- Handelsman, J., Rondon, M. R., Brady, S. F., Clardy, J., Goodman, R. M. (1998). Molecular biological access to the chemistry of unknown soil microbes: A new frontier for natural products. *Chemistry & Biology* **5** (10): R245–R249.
- He, Z., Xu, M., Deng, Y., Kang, S., Kellogg, L., Wu, L., Van Nostrand, J.D., Hobbie, S.E., Reich, P.B. and Zhou, J. (2010) Metagenomic analysis reveals a marked divergence in the structure of belowground microbial communities at elevated CO₂. *Ecology Letters*, **13**: 564-575
- Hofman, G., Cleemput, O.V. (2004) Soil and Plan Nitrogen. *IFA*. Pp. 1-20
- Huesemann, MH., Skillmann, AD and Crecelius, EA. (2002) The inhibition of marine nitrification by ocean disposal of carbon dioxide.
- Inagaki, F. , Kuypers, M. , Tsunogai, U. , Ishibashi, J. , Nakamura, K. , Treude, T. , Ohkubo, S. , Nakaseama, M. , Gena, K. , Chiba, H. , Hirayama, H. , Nunoura, T. , Takai, K. , Jørgensen, B. B. , Horikoshi, K. and Boetius, A. (2006): Microbial community in a sediment-hosted CO₂ lake of the southern Okinawa Trough hydrothermal system. , *PNAS*, 103 (38), pp. 13899-13900
- Ishii, K., Fuki, M. (2001) Optimization of annealing temperature to reduce bias caused by primer mismatch in multitemplate PCR. *Appl Environmental Microbiol* **67**: 3753-3755.
- Jonathan G. Kramer, and Fred L. (1993) Singleton. Measurement of rRNA Variations in Natural Communities of Microorganisms on the Southeastern U.S Continental Shelf.
- Jorgensen, B.B., Boetius, A. (2007) Feast and famine – microbial life in deep sea bed. *Nat Rev Microbiol* **5**: 770-781
- Jorgensen, B.B. (2011) deep seafloor microbial cells on physiological standby. *Proceedings of the National Academy of Sciences* **108**: 18193-18194.
- Jørgensen, SL., Hannisdal, B., Lanzén, A., Baumberger, T., Flesland, K., Fonseca, R., Øvreås, L., Steen, IH., Thorseth, IH., Pedersen, RB., Schelper, C. (2012) Correlating microbial community profiles with geochemical data in highly stratified sediments from the Arctic Mid-Ocean Ridge. *PNAS*, **109** (42).
- Journal of the European Union: Directive 2009/31/EC of the European Parliament and of the Council of 23 April 2009. <http://eur-lex.europa.eu/LexUriServ/LexUriServ.do?uri=OJ:L:2009:140:0114:0135:EN:PDF>
- Jurgens, G., K. Lindstrom, and A. Saano, Novel group within the kingdom Grenarchaeota from boreal forest soil. *Appl. Environ. Microbiol.*, 1997. 63(2): p. 803-805.
- Kallmeyer, J., Pockalny, R., Adhikari, R.R., Smith, D.C., D'Hondt, S. (2012) Global distribution of microbial abundance and biomass in seafloor sediment. *Proc Natl Acad Sci USA* 109: 16213-16216.

Kongsjorden, H., Kårstad, O., Torp, T.A. (1998) Saline aquifer storage of carbon dioxide in the Sleipner project. *Waste management*. Pp 303-308.

Konhauser, K. (2007) Introduction to Geomicrobiology. Blackwell Science Ltd. **6**: 235-292

Lane, D.J., 16s/23S rRNA sequencing. In E. Stackebrandt and M Goodfellow (ed). *Nucleic acid techniques in bacterial systematics*, 1991. John Wiley & Sons Ltd., West Sussex, United Kingdom: p. 115-175.

Lanzén, A., Jørgensen, S., Bengtson, M.M., Jonassen, I., Øvreås, L., Urich, T. (2011) Exploring the composition and diversity of microbial communities at the Jan Mayen hydrothermal vent field using RNA and DNA. *FEMS*. **77**: 577-589.

Lanzén, A., Jørgensen, S., Huson, D., Gorfer, M., Grindhaug, SH., Jonassen, I., Øvreås, L., Urich, T. (2012). CREST – Classification Resources for Environmental Sequence Tags.

Lesaulnier, C., Papamichail, D., McCorkle, S., Ollivier, B., Skiena, S. (2007) Elevated atmospheric CO₂ affects soil microbial diversity associated with trembling aspen. *Environmental Microbiology*, **10**(4):926-41

Madsen, E.L. (2011) Microorganisms and their roles in fundamental biogeochemical cycles. *Biotechnology* **22**: 456-464. *Energy Procetia* pp. 4362–4370

Morozova, D., Wandrey, M., Alawi, M., Zimmer, M., Vieth, A., Zettlitzer, M., Würdemann. (2010) Monitoring of the microbial community composition in saline aquifers during CO₂ storage by fluorescence in situ hybridization. *International Journal of Greenhouse Gas Control*. Pp. 981-989

Morozova, D., Zettlitzer, M., Let, D., Würdemann, H. (2011) Monitoring of the microbial community composition in deep subsurface saline aquifers during CO₂ storage in Ketzin, Germany.

Muyzer, G., E.C. Dewaal, and A.G. Uitterlinden, Profiling of Complex Microbial Populations by Denaturing Gradient Gel-Electrophoresis Analysis of Polymerase Chain-Reaction-Amplified Genes-Coding for 16S Ribosomal RNA. *Applied and Environmental Microbiology*, 1993. **59**(3): p. 283-290.

Nanoura, T., Takaki, Y., Kazama, H., Hirai, M., Ashi, J., Imchi, H., Takai, K. (2012). Microbial diversity in deep-sea methane seep sediments presented by SSU rRNA gene tag sequencing.

Neef, A., Amann, R., Schlezner, H., Schleifer, KH. (1998). Monitoring a widespread bacterial group: *in situ* detection of planctomycetes with 16S rRNA-targeted probes.

Nealson, K. (2006) Lakes of liquid CO₂ in the deep sea. *PNAS*. Pp. 13903–13904

Nelson, David R.; Lehninger, Albert L; Cox, Michael (2005). *Lehninger principles of biochemistry*. New York: W.H. Freeman. p. 148.

Orcutt, BN., Sylvan, JB., Knab, NB., Edwards, KJ. (2011) Microbial Ecology of the Dark Ocean above, at, and below the Seafloor. *Microbiol. Mol. Biol. Rev.* **June 2011** vol. 75 no. 2 **361-422**

Parkes, JR., Cragg, BA., Wellsbury, P. (2000) Recent studies on bacterial populations and processes in subseafloor sediments: A review. *Hydrogeology Journal*, pp. 11-28

Pester, M., Schleper, C., Wagner, M. (2011) The Thaumarchaeota: an emerging view of their phylogeny and ecophysiology.

Plattner GK., Joos, F., Stocker, TF and Marchal, O (2001) Feedback mechanisms and sensitivities of ocean carbon uptake under global warming. *Tellus*, 53B, 564–592
Official

Poulsen, L.K., Ballard, G. and Stahl, D.A. (1993) Use of rRNA fluorescence in situ hybridization for measuring the activity of single cells in young and established biofilms. *Applied Environmental Microbiology*, **59**: 1354-1360.

Quaiser, A., Ochsenreiter, T., Lanz, C., Shauster, S., Treusch, AH., Ech, J., Schleper, C. 2003. Acidobacteria form a coherent but highly diverse group within the bacterial domain: evidence from environmental genomics. *Mol. Microbiol.* Pp. 563-575.

Quince, C., Lanzén, A., Curtis, TP., Davenport, RJ., Hall, N., Head, IM., Read, LF., Sloan, WT. (2009), Accurate determination of microbial diversity from 454 pyrosequencing data. *Nature America*.

Quince, C., Lanzén, A. (2011) Removing noise from pyrosequenced amplicons. *BMC Bioinformatics* **12**, 38.

Robbins, L.L., Hansen, M.E., Kleypas, J.A., and Meylan, S.C., 2010, CO2calc—A user-friendly seawater carbon calculator for Windows, Max OS X, and iOS (iPhone): U.S. Geological Survey Open-File Report 2010–1280, 17 p.

Roche Diagnostics Corporations (1996-2012). 454 sequencing, Target:
<http://my454.com/applications/targeted-resequencing/index.asp>

Roech, L.F.W., et al., Pyrosequencing enumerates and contrasts soil microbial diversity. *ISME J*, 2007. 1(4): p. 283-290.

Rutgers Van Der Loeff, M.M., Meadows P.S., and Allen, J.A. (1990) Oxygen in Pore Waters of Deep-Sea Sediments. *The Royal Society*, pp. 69-84

Sebens, K.P. (1991) Habitat structure and community dynamics in marine benthic systems. *Population and Community Biology*. Pp. 211-234.

Song, Y., Chen, B., Nishio, M., Akai, M. (2005) The study on density change of carbon dioxide seawater solution t high pressure and low temperature. *Energy*. Pp. 2298-2307.

STATOIL Brochure. Underground Storage of Carbon Dioxide: Emission Mitigation which counts (Nov.2009).

<https://docs.google.com/viewer?a=v&pid=gmail&attid=0.1&thid=135e26755735ac1d&mt=application/pdf&url=https://mail.google.com/mail/u/0/?ui%3D2%26ik%3D3fc870d9ee%26view%3Datt%26th%3D135e26755735ac1d%26attid%3D0.1%26disp%3Dsafe%26zw&sig=AHIEtbS4uZNgyDWFTZCBAcdmOQz0fEjHoQ>

Sweetman, AK., Witte, U. (2008) Microfaunal Response to Phytodetritus in a Bathyal Norwegian Fjord.

Sweetman, AK., and Witte, U. (2008) Response of an Abyssal Macrofaunal Community to a Phytodetrital Pulse.

Townend, J. (2002) Practical statistics for Environmental and biological Scientists. Pp 3-152

University of Bergen, CGB:

<http://www.uib.no/geobio/en/research/research-at-cgb/deep-sea-hydrothermal-systems-and-geodynamics/insights-into-the-seabed-in-byfjorden-bergen>

University of Bergen, CGB:

<http://www.uib.no/geobio/en/artikler/2011/09/sub-seabed-co2-storage-impact-on-marine-ecosystems>

Walker, C. B., de la Torre, J.R., Klotz, M.G., Urakawa, H., Pinel, N., Arp, D.J., Brochier-Armanet, C., Chain, P.S.G., Chain, P.P., Gollabgir, A., Hemp, J., *et al.* (2010) *Nitrosopumilus maritimus* genome reveals unique mechanisms for nitrification and autotrophy in globally distributed marine crenarchaea. PNAS pp. 8818-8823

Widdicombe, S., Dashfield, S.L., McNeill, C.L., Needham, H.R., Beesley, A., McEvoy, A., Øxnevad, S., Clarke, K.R., Berge, J.A. (2009) Effects of CO₂ induced seawater acidification on infaunal diversity and sediment nutrient fluxes.

Whitman, W.B., Coleman, D.C., Wiebe, W.J. (1998). Prokaryotes: the Unseen Majority.

Yanagawa, K., Morono, Y., Beer, D., Haeckel, M., Sunamura, M., Futagami, T., Hoshino, T., Terada, T., Nakamura, K., Urabe, T., Rehder, G., Boetius, A., Inagaki, F. (2012), Metabolically active microbial communities in marine sediment under high-CO₂ and low-pH extremes. ISME Journal.

Zhu, Q., Aller, R.C., Fan, Y. (2006) Two-dimensional pH distributions and dynamics in bioturbated marine sediments.

APPENDIX:

RNA isolation: Protocol: Qaigen RNAEasy PLUS Kit

Table I: Gram sediment used in each isolation

	RISCS1 CH1	RISCS1 CH2	RISCS2 CH1	RISCS2 CH2	RISCS3 CH2	RISCS4 CH1	RISCS4 CH2
0-1 cm	0.410	0.220	0.11	0.670	0.100	0.700	0.576
1-2 cm	0.290	0.210	0.72	0.850	0.710	0.360	0.640
3-4 cm	0.476	0.410	0.72	0.767	0.850	0.330	0.350
6-7 cm	0.750	0.675	0.84	0.950	0.820	0.660	0.680

Table II: qPCR raw data for Bacteria

Navn:	Quantity	Quantity Mean	Quantity SD
RISCS2 CH1 0-1	7764031,5	7911332	917789,375
RISCS2 CH1 0-1	7076101,5	7911332	917789,375
RISCS2 CH1 0-1	8893863	7911332	917789,375
RISCS2 CH1 1-2	738709,4375	853316,75	162079,2188
RISCS2 CH1 1-2	967924,0625	853316,75	162079,2188
RISCS2 CH1 1-2			
RISCS2 CH1 3-4	10551,74023	9782,639648	1890,986084
RISCS2 CH1 3-4	11167,88867	9782,639648	1890,986084
RISCS2 CH1 3-4	7628,289063	9782,639648	1890,986084
RISCS2 CH1 6-7	1068,396606	954,2660522	104,7754135
RISCS2 CH1 6-7	931,9649048	954,2660522	104,7754135
RISCS2 CH1 6-7	862,4365845	954,2660522	104,7754135
RISCS2 CH2 0-1			
RISCS2 CH2 0-1	1526310,375	1855628,25	465725,9063
RISCS2 CH2 0-1	2184946,25	1855628,25	465725,9063
RISCS2 CH2 1-2	24473,3457	25067,18555	514,5629272
RISCS2 CH2 1-2	25347,07422	25067,18555	514,5629272
RISCS2 CH2 1-2	25381,13867	25067,18555	514,5629272
RISCS2 CH2 3-4	13908,61035	12455,5752	1266,575439
RISCS2 CH2 3-4	11585,07617	12455,5752	1266,575439
RISCS2 CH2 3-4	11873,04004	12455,5752	1266,575439
RISCS2 CH2 6-7	22406,58203	24169,07031	1693,516846
RISCS2 CH2 6-7	24316,67578	24169,07031	1693,516846
RISCS2 CH2 6-7	25783,95313	24169,07031	1693,516846
RISCS3 CH2 0-1	1178269,75	1149247,75	37936,03516
RISCS3 CH2 0-1	1106321,375	1149247,75	37936,03516
RISCS3 CH2 0-1	1163152,25	1149247,75	37936,03516
RISCS3 CH2 1-2	24083,06641	26661,56836	3646,55249
RISCS3 CH2 1-2	29240,07031	26661,56836	3646,55249

RISCS3 CH2 1-2			
RISCS3 CH2 3-4	10182,78125	9787,460938	559,0673218
RISCS3 CH2 3-4	9392,140625	9787,460938	559,0673218
RISCS3 CH2 3-4			
RISCS3 CH2 6-7	2309,76416	2369,248291	425,5816345
RISCS3 CH2 6-7	1976,537964	2369,248291	425,5816345
RISCS3 CH2 6-7	2821,442627	2369,248291	425,5816345
Navn:	Quantity	Quantity Mean	Quantity SD
RISCS1 CH1 0-1	167684,2031	140332,5156	24107,33008
RISCS1 CH1 0-1	131137,4688	140332,5156	24107,33008
RISCS1 CH1 0-1	122175,8906	140332,5156	24107,33008
RISCS1 CH1 1-2	1771167,625	2067219,5	308694,25
RISCS1 CH1 1-2	2387167,25	2067219,5	308694,25
RISCS1 CH1 1-2	2043324	2067219,5	308694,25
RISCS1 CH1 3-4	127084,2344	139920,3438	18153
RISCS1 CH1 3-4			
RISCS1 CH1 3-4	152756,4531	139920,3438	18153
RISCS1 CH1 6-7			
RISCS1 CH1 6-7	8375,665039	7590,007324	1111,087769
RISCS1 CH1 6-7	6804,349609	7590,007324	1111,087769
RISCS1 CH2 0-1	249057,25	208467,0313	57403,25
RISCS1 CH2 0-1			
RISCS1 CH2 0-1	167876,7969	208467,0313	57403,25
RISCS1 CH2 1-2	1720385	1754202,875	375428,6563
RISCS1 CH2 1-2	2145396,25	1754202,875	375428,6563
RISCS1 CH2 1-2	1396827,125	1754202,875	375428,6563
RISCS1 CH2 3-4	9945,535156	8718,735352	1303,039063
RISCS1 CH2 3-4	8859,743164	8718,735352	1303,039063
RISCS1 CH2 3-4	7350,926758	8718,735352	1303,039063
RISCS1 CH2 6-7	6460,431152	6518,429688	1798,500366
RISCS1 CH2 6-7	8345,227539	6518,429688	1798,500366
RISCS1 CH2 6-7	4749,629883	6518,429688	1798,500366
RISCS4 CH1 0-1			
RISCS4 CH1 0-1	397336,2188	348816	68617,97656
RISCS4 CH1 0-1	300295,75	348816	68617,97656
RISCS4 CH1 1-2	618975,6875	646039,625	38274,14453
RISCS4 CH1 1-2			
RISCS4 CH1 1-2	673103,5	646039,625	38274,14453
RISCS4 CH1 3-4	180268,8594	149601,4844	27395,60352
RISCS4 CH1 3-4	140987,3594	149601,4844	27395,60352
RISCS4 CH1 3-4	127548,2031	149601,4844	27395,60352
RISCS4 CH1 6-7	12629,24023	9550,459961	2687,99292
RISCS4 CH1 6-7	8351,867188	9550,459961	2687,99292
RISCS4 CH1 6-7	7670,273926	9550,459961	2687,99292

RISCS4 CH2 0-1	2374432,5	2347699,75	66272,55469
RISCS4 CH2 0-1	2396430,5	2347699,75	66272,55469
RISCS4 CH2 0-1	2272236	2347699,75	66272,55469
RISCS4 CH2 1-2			
RISCS4 CH2 1-2	427052,5313	468420,875	58503,69531
RISCS4 CH2 1-2	509789,25	468420,875	58503,69531
RISCS4 CH2 3-4	32911,22656	27559,68164	4672,172363
RISCS4 CH2 3-4	24292,37109	27559,68164	4672,172363
RISCS4 CH2 3-4	25475,44531	27559,68164	4672,172363
RISCS4 CH2 6-7	378072,0625	315835,75	72157,27344
RISCS4 CH2 6-7	332693,125	315835,75	72157,27344

Table III: qPCR raw data for Archaea:

Navn:	Quantity	Quantity Mean	Quantity SD
RISCS2 CH1 0-1	204307	204841,2188	755,4993896
RISCS2 CH1 0-1	205375,4375	204841,2188	755,4993896
RISCS2 CH1 0-1			
RISCS2 CH1 1-2	23312,19727	22400,9707	2321,449951
RISCS2 CH1 1-2	24128,5625	22400,9707	2321,449951
RISCS2 CH1 1-2	19762,1543	22400,9707	2321,449951
RISCS2 CH1 3-4	1252,635254	1141,980347	96,52571106
RISCS2 CH1 3-4	1075,084595	1141,980347	96,52571106
RISCS2 CH1 3-4	1098,221069	1141,980347	96,52571106
RISCS2 CH1 6-7	174,9908295	118,6915054	49,09298325
RISCS2 CH1 6-7	84,80503845	118,6915054	49,09298325
RISCS2 CH1 6-7	96,27867126	118,6915054	49,09298325
RISCS2 CH2 0-1	49413,28125	48659,79688	1286,544556
RISCS2 CH2 0-1	47174,27344	48659,79688	1286,544556
RISCS2 CH2 0-1	49391,83203	48659,79688	1286,544556
RISCS2 CH2 1-2			
RISCS2 CH2 1-2			
RISCS2 CH2 1-2	729,1870117	729,1870117	
RISCS2 CH2 3-4	344,4210205	543,249939	181,3341522
RISCS2 CH2 3-4	699,5183105	543,249939	181,3341522
RISCS2 CH2 3-4	585,8105469	543,249939	181,3341522
RISCS2 CH2 6-7	1271,199585	1300,545532	733,3135376
RISCS2 CH2 6-7	582,34552	1300,545532	733,3135376
RISCS2 CH2 6-7	2048,091553	1300,545532	733,3135376
RISCS3 CH2 0-1	37710,58203	32876,63281	6836,233887
RISCS3 CH2 0-1	28042,6875	32876,63281	6836,233887
RISCS3 CH2 0-1			
RISCS3 CH2 1-2	1247,443848	1236,138184	208,410965
RISCS3 CH2 1-2	1438,666138	1236,138184	208,410965

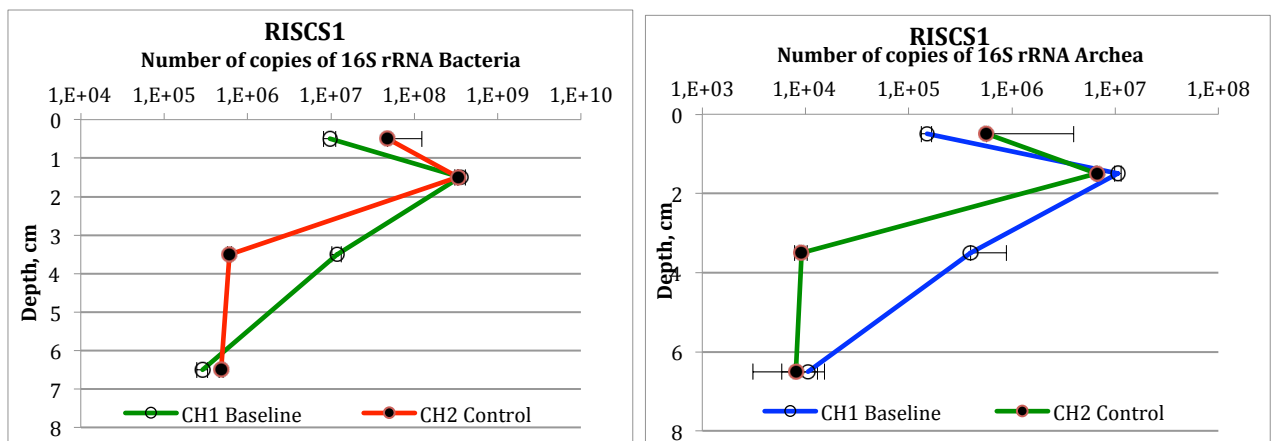
RISCS3 CH2 1-2	1022,304443	1236,138184	208,410965
RISCS3 CH2 3-4	114,8614197	114,0371933	10,7558279
RISCS3 CH2 3-4	124,357193	114,0371933	10,7558279
RISCS3 CH2 3-4	102,8929596	114,0371933	10,7558279
RISCS3 CH2 6-7	335,9718018	393,7410889	81,69811249
RISCS3 CH2 6-7	451,510376	393,7410889	81,69811249
RISCS3 CH2 6-7			
Navn:	Quantity	Quantity Mean	Quantity SD
RISCS1 CH1 0-1	2331,948242	2157,794434	246,2905121
RISCS1 CH1 0-1	1983,640869	2157,794434	246,2905121
RISCS1 CH1 0-1			
RISCS1 CH1 1-2	66157,02344	61754,44922	4695,926758
RISCS1 CH1 1-2	56811,85938	61754,44922	4695,926758
RISCS1 CH1 1-2	62294,44922	61754,44922	4695,926758
RISCS1 CH1 3-4	8825,475586	4760,119141	5749,282227
RISCS1 CH1 3-4	694,7629395	4760,119141	5749,282227
RISCS1 CH1 3-4			
RISCS1 CH1 6-7	190,2792969	277,5185547	123,374939
RISCS1 CH1 6-7	364,7578125	277,5185547	123,374939
RISCS1 CH1 6-7			
RISCS1 CH2 0-1	2508,806641	2499,843994	373,6589966
RISCS1 CH2 0-1	2868,941162	2499,843994	373,6589966
RISCS1 CH2 0-1	2121,784424	2499,843994	373,6589966
RISCS1 CH2 1-2	27992,24414	34735,67969	9536,65625
RISCS1 CH2 1-2	41479,11328	34735,67969	9536,65625
RISCS1 CH2 1-2			
RISCS1 CH2 3-4			
RISCS1 CH2 3-4	138,4270935	130,7297821	10,88563633
RISCS1 CH2 3-4	123,0324783	130,7297821	10,88563633
RISCS1 CH2 6-7	102,6869812	109,0584259	9,010583878
RISCS1 CH2 6-7	115,4298706	109,0584259	9,010583878
RISCS1 CH2 6-7			
Navn:	Quantity	Quantity Mean	Quantity SD
RISCS4 CH1 0-1	7277,519043	7087,495605	312,8283691
RISCS4 CH1 0-1	6726,438477	7087,495605	312,8283691
RISCS4 CH1 0-1	7258,527832	7087,495605	312,8283691
RISCS4 CH1 1-2			
RISCS4 CH1 1-2	23051,76563	26340,47656	4650,940918
RISCS4 CH1 1-2	29629,18945	26340,47656	4650,940918
RISCS4 CH1 3-4	3806,942871	5324,450684	1332,588745
RISCS4 CH1 3-4	5862,59082	5324,450684	1332,588745
RISCS4 CH1 3-4	6303,818359	5324,450684	1332,588745
RISCS4 CH1 6-7	464,8919983	406,5970459	50,49851608

RISCS4 CH1 6-7	378,6224976	406,5970459	50,49851608
RISCS4 CH1 6-7	376,2767029	406,5970459	50,49851608
RISCS4 CH2 0-1	22356,01563	20199,53125	2396,370605
RISCS4 CH2 0-1	17619,69922	20199,53125	2396,370605
RISCS4 CH2 0-1	20622,88086	20199,53125	2396,370605
RISCS4 CH2 1-2	8547,495117	7605,049316	951,8265991
RISCS4 CH2 1-2	6644,111328	7605,049316	951,8265991
RISCS4 CH2 1-2	7623,541016	7605,049316	951,8265991
RISCS4 CH2 3-4			
RISCS4 CH2 3-4	101,6494675	522,2765503	594,8565674
RISCS4 CH2 3-4	942,9036865	522,2765503	594,8565674
RISCS4 CH2 6-7	8758,958008	8054,208984	996,6652832
RISCS4 CH2 6-7			
RISCS4 CH2 6-7	7349,460449	8054,208984	996,6652832

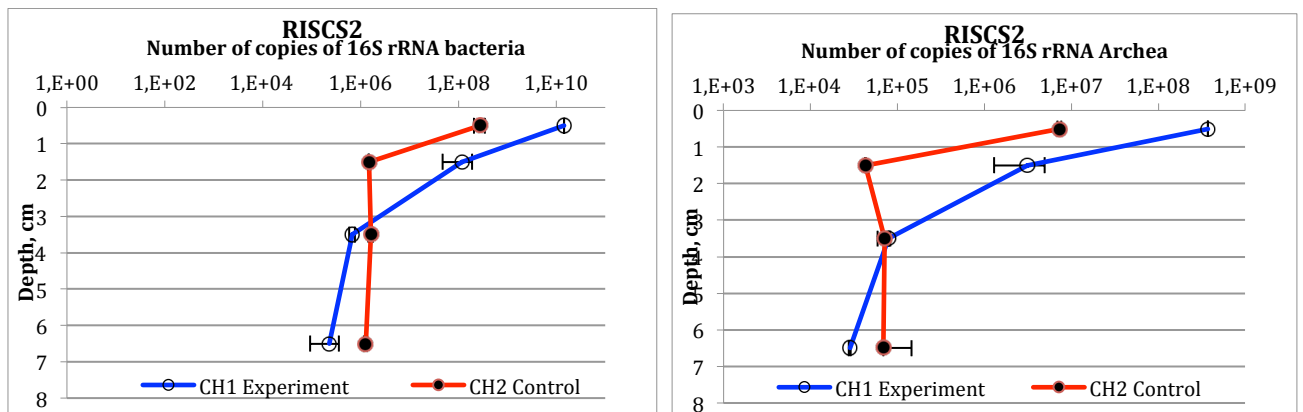
qPCR data after calculation arranged after dives:

Figure 1: Bacterial and archaeal numbers of 16S rRNA logarithmically plotted against depth.

A)



B)



C)

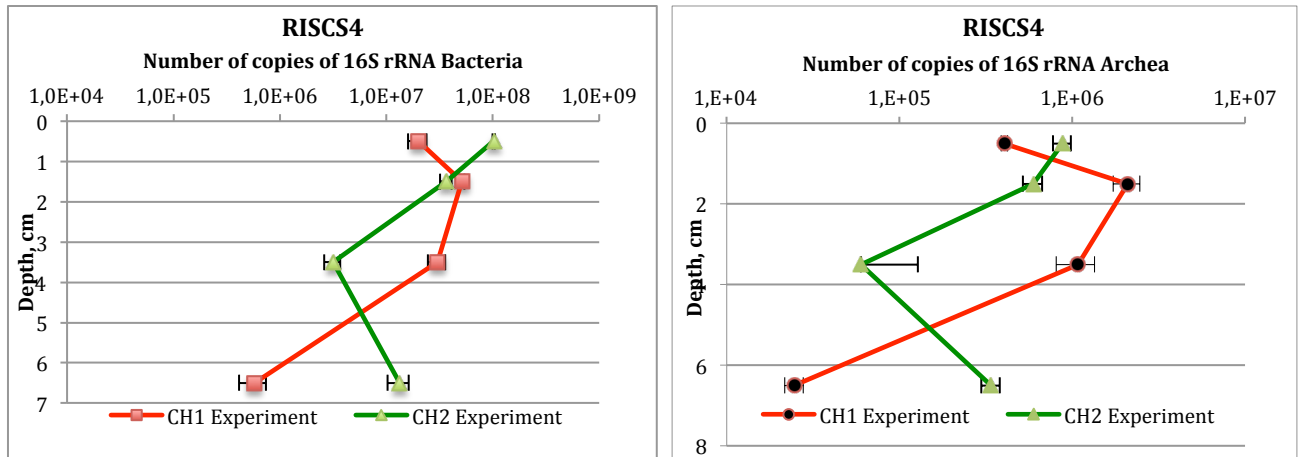


Figure 1: Bacterial and archaeal numbers of 16S rRNA logarithmically plotted against depth.

454 sequencing data:

Table IV: number of reads from the 454 sequencing analysis down to order level

	27	28	29	30	31	32	33	34	35
Total Amplicon reads:	3123	2507	14521	4653	5827	6868	8072	8671	11590
Sequences classified to:									
Phylum level	3113	2475	14434	4643	5793	6825	8053	8608	11517
Class level	3031	2360	13484	4463	5469	6429	7751	8072	10946
Order level	1898	1564	8910	3038	3744	4385	4987	5492	7095
% loss from tot. to order	39 %	38 %	39 %	35 %	36 %	36 %	38 %	37 %	39 %

Table V: Phylum present in the 454 data and their total numbers of reads in all 9 samples

Phylum:	Tot. No. of reads from all samples
Crenarchaeota (Archaea)	530
Thaumarchaeota (Archaea)	15792
Euryarchaeota (Archaea)	936
PAUC34f	113
LD1-PA38	25
Candidate division WS3	915
BHI80-139	20
Candidate division BRC1	272
Gemmatimonadetes	164
Candidate division TM7	293
Candidate division TM6	24
Halanaerobiales phylum incertae sedis	43
Candidate Division OP8	136
Candidate Division OP3	507

Candidate division OP9	18
BD1-5	149
Verrucomicrobia	96
Candidate division OD1	123
Candidate division SR1	1
Fusobacteria	81
Firmicutes	270
Fibrobacteres	16
Actinobacteria	785
Bacteroidetes	763
Chloroflexi	12088
Planctomycetes	17360
Acidobacteria	2394
Proteobacteria	10932
Chlorobi	63
Tenericutes	5
Chlamydiae	50
Cyanobacteria	67
Caldithrix	70
GN04	6
Spirochaetes	119
SAR406 Clade (Marine group A)	4
Lentisphaerae	25
Nitrospirae	59
Spring Alpine Meadow (SPAM)	5
Elusimicrobia	6
Armatimonadetes	22
WCHB1-60	9
LD1-PA38	7
RF3	4
Synergistetes	2
Candidate division AC1 (TA06)	4
Deinococcus-Thermus	4
Thermotogae	1
EM19	8
NC10	1
OC31	2
MVP-21	1

Table VI: Classes present in the 454 data and their total numbers of reads in all 9 samples

Classes:	Tot. No. of reads from all samples
Thaumarchaeota;Group 1A - pSL12	13
Thaumarchaeota;Group C3 - Group 1.2	209
Thaumarchaeota;Soil Crenarchaeotic Group (SCG) Group I.1b	37
Thaumarchaeota;Marine Group I (Group I.1a)	15514
Euryarchaeota;Methanomicrobia	24
Euryarchaeota;Methanobacteria	126
Euryarchaeota;Halobacteria	310
Euryarchaeota;Thermoplasmata	394
Crenarchaeota;Marine Benthic Group B - Deep Sea Archaeal Group (DSAG)	269
Crenarchaeota;Miscellaneous Crenarchaeotic Group	261
Cyanobacteria;Cyanobacteria (class)	57
Gemmatimonadetes;Gemmatimonadetes (class)	164
Spirochaetes;Spirochaetes (class)	32
Halanaerobiales class incertae sedis	9
Verrucomicrobia;Spartobacteria	8
Verrucomicrobia;Verrucomicrobiae	76
Verrucomicrobia;S-BQ2-57 soil group	5
Verrucomicrobia;OPB35 soil group	5
Fibrobacteres; Fibrobacteria	16
Fusobacteria;Fusobacteria (class)	82
Firmicutes;Clostridia	187
Firmicutes;Erysipelotrichi	21
Firmicutes;Bacilli	58
Actinobacteria;Acidimicrobiia	680
Actinobacteria;Actinobacteria (base/class)	31
Actinobacteria;Thermoleophilia	112
Actinobacteria;OPB41	6
Actinobacteria;Coriobacteriia	5
Bacteroidetes;VC2.1 Bac22	19
Bacteroidetes;BD2-2	235
Bacteroidetes;Cytophagia	265
Sphingobacteria	34
Bacteroidia	29
Bacteroidetes;Flavobacteria	125
Bacteroidetes;Rhodothermaceae incertae sedis	16
Bacteroidetes;SB-1	7
Bacteroidetes;Prolixibacter incertae sedis	4
Bacteroidetes;SB-5	6
Chloroflexi;Thermomicrobia	350
Chloroflexi;Ktedonobacteria	159

Chloroflexi;Chloroflexi Subdivision 13	612
Chloroflexi;Chloroflexi Subdivision 8 - TK10	62
Chloroflexi;Caldilineae	2486
Chloroflexi;Chloroflexi Subdivision 6	86
Chloroflexi;Chloroflexi Subdivision 2	42
Chloroflexi;Anaerolineae	6147
Chloroflexi;Chloroflexi Subdivision 5 - SAR202 clade	150
Chloroflexi;Chloroflexi Subdivision 10	1631
Chloroflexi;MSB-5B2	7
Chloroflexi;Chloroflexi Subdivision 10;KD4-96	248
Planctomycetes;MD2896-B258	54
Planctomycetes;Pla3 lineage	191
Planctomycetes;OM190	1010
Planctomycetes;vadinHA49	531
Planctomycetes;Pla4 lineage	459
Planctomycetes;BD7-11	133
Planctomycetes;Phycisphaerae	2888
Planctomycetes;Phycisphaerae	4069
Planctomycetes;Planctomycetacia	7813
Planctomycetes;028H05-P-BN-P5	6
Acidobacteria;RB25	144
Acidobacteria;Acidobacteria (class)	2090
Acidobacteria;Holophagae	150
Proteobacteria;TA18	40
Proteobacteria;Deltaproteobacteria	3041
Proteobacteria;Alphaproteobacteria	565
Proteobacteria;Epsilonproteobacteria	87
Proteobacteria;Betaproteobacteria	52
Proteobacteria;Gammaproteobacteria	6985
Proteobacteria;SPOTSOCT00	2
Proteobacteria;JTB23	25
Proteobacteria;Milano-WF1B-44	3
Proteobacteria;Zetaproteobacteria	2
Proteobacteria;CF2	1
Proteobacteria;SC3-20	1
Caldithrix;LCP-89	6
Candidate Division Caldithrix;Caldithrix	43
Candidate Division Caldithrix;LCP-89	3
Lentisphaerae;Lentisphaerae (class)	25
Nitrospirae;4-29	6
Nitrospirae;Nitrospira	53
Candidate division OP3;OP3 subdivision I (NPL-UPA2)	471
Chlamydiae;Chlamydiae (class)	50
Chlorobi;Ignavibacteria	63
Synergistetes;Synergistia	2

Armatimonadetes;Armatimonadetes Group 3	9
Spirochaetes;Spirochaetes (class)	87
Tenericutes;Mollicutes	5
Halanaerobiales phylum incertae sedis	34
Elusimicrobia;Elusimicrobia (class)	5
Thermotogae;Thermotogae (class)	1
Deinococcus-Thermus;Deinococci	4